Chair of Casting Research

Master's Thesis

Microstructure evolution of Al-Cu-Mg based alloy during rolling and annealing

Arman Moradizadeh

September 2024

Statutory declaration

MONTANUNIVERSITÄT LEOBEN
www.unileoben.ac.at

AFFIDAVIT

I declare on oath that I wrote this thesis independently, did not use any sources and aids other than those specified, have fully and truthfully reported the use of generative methods and models of artificial intelligence, and did not otherwise use any other unauthorized aids.

I declare that I have read, understood and complied with the "Good Scientific Practice" of the Montanuniversität Leoben.

Furthermore, I declare that the electronic and printed versions of the submitted thesis are identical in form and content.

Date 09.08.2024

Signature Author
Arman Moradizadeh

Acknowledgement

I would like to express my sincere gratitude to my supervisor, Priv.-Doz. MSc PhD Jiehua Li, for his invaluable time and dedication over the past few months. I would also like to acknowledge the support of my colleagues at the Chair of Casting Research. I would also like to thank the Chair of Metal Forming and ÖGI Leoben.

In addition, I would like to thank my father and my mother to get this opportunity to study at the Montanuniversität Leoben.

Kurzfassung

Die Al-Cu-Mg-basierte Legierungen sind aufgrund ihrer hohen Festigkeit in verschiedenen Industriezweigen, insbesondere in der Luftfahrt, weit verbreitet. Allerdings weisen diese Legierungen bei erhöhten Temperaturen, Fließfähigkeit, Heißrissbildung und Korrosionsbeständigkeit gewisse Nachteile auf. Ziel dieser Studie war es, den Einfluss von Kupfer (Cu), Silber (Ag) und SiC (SiC) auf die Mikrostruktur, Textur und Härte von Al-Cu-Mg-basierten Legierungen zu untersuchen. Anschließend wurde der Einfluss von 4 Gew.-% Cu, 0,7 Gew.-% Ag und 1 Gew.-% SiC, einzeln oder in Kombination, auf die genannten Parameter untersucht. Die Legierungen (Al-4Cu-0,3Mg, Al-4Cu-0,3Mg-0,7Ag und Al-4Cu-0,3Mg-0,7Ag-1SiC) wurden unter folgenden Bedingungen analysiert: (i) nach Lösungsbehandlung (T4) bei 540 °C für 6 Stunden; (ii) nach Warmwalzen bei 340 °C zu zwei unterschiedlichen Plattendicken im walzgehärteten Zustand; (iii) nach Warmwalzen und anschließender Alterung bei 180 °C für 32 Stunden; und (iv) nach Warmwalzen und anschließender Glühbehandlung bei 350 °C für 4 Stunden. Die Mikrostruktur wurde mittels optischer Mikroskopie nach Barker-Ätzung und Rasterelektronenmikroskopie (REM) für die Legierungen Al-4Cu-0,3Mg, Al-4Cu-0,3Mg-0,7Ag und Al-4Cu-0,3Mg-0,7Ag-1SiC sowie die entsprechenden gewalzten Proben untersucht. Die Vickers-Härte der T4-behandelten Proben wurde nach sieben Tagen natürlicher Alterung bestimmt.

Bei dieser Untersuchung wurde festgestellt, dass das Induktionsschmelzen aufgrund der Rührgeschwindigkeit nicht ausreicht, um SiC-Nanopartikel zuzusetzen. Daher wurde das mechanische Rühren während des Widerstandsschmelzens in einem Nabertherm-Tiegelofen verwendet, um SiC-Nanopartikel zuzusetzen und die Al-Verbundwerkstoffe herzustellen. Die Probe mit weniger Cu wies eine größere Korngröße und eine geringe Härte auf, was auf das Fehlen der Al_2Cu-Phase (Auscheidungshärtungsphase) zurückzuführen ist, was die Bedeutung dieser Phase für die Verbesserung der mechanischen Eigenschaften zeigt. Der Zusatz von 4 Gew.-% Cu führte zu einer Erhöhung der Härte, hauptsächlich aufgrund der Bildung einer erheblichen Menge an Ausscheidungen (Al_2Cu). Die Zugabe einer kleinen Menge (0,3 Gew.-%) Mg zu einer Al-Cu-Legierung mit 4 Gew.-% Cu erhöht die Härte der Legierung. Außerdem verzögert es die Bildung einer bestimmten Mikrostrukturart (sogenannte Guinier-Preston (GP)-Zonen) bei einer Temperatur von 180 °C. Die Zugabe eines dritten Legierungselements (wie Ag) zu Al-Cu-Mg-Legierungen erhöht ihre Härte durch Mischkristallhärtung. Dies geschieht, wenn Versetzungen, also Fehler im Kristallgitter, durch die Verzerrung des Kristallgitters des Hauptelements (Lösungsatom) durch das zusätzliche Element (Lösungsatom) bei der Verformung behindert werden. Die plastische Verformungsrate eines Materials wird durch seine Versetzungen bestimmt; eine höhere Härte resultiert aus einem größeren Widerstand gegen ihre Bewegung. Da Ag die mechanischen Eigenschaften verbessern kann, führt jedoch in diesem Fall die Zugabe von 0,7 Gew.-% Ag zu einer Al-4Cu-0,3Mg-Legierung zu einer erhöhten Korngröße und einer verringerten Härte, was darauf zurückzuführen sein kann, dass (i) Ag nicht als wirksam für die Verstärkung angesehen werden kann, wenn es sich sehr gut im Material löst und eine homogene feste Lösung mit geringer Gitterverzerrung bildet, und (ii) Ag die Rekristallisation bei hohen Temperaturen beeinflusst, was nach der Wärmebehandlung zu größeren Körnern führt, oder Ag-Atome können während der Verarbeitung an Korngrenzen segregieren, wodurch das Korn geschwächt und seine Anfälligkeit für Kornwachstum erhöht wird.

Nach der T4-Behandlung (540 °C für 6 Stunden) wurde die Korngröße reduziert. Dennoch zeigte die Legierung mit Ag eine größere Korngröße im Vergleich zur Legierung ohne Ag. Die Zugabe von 0,667 Gew.-% und 1 Gew.-% SiC zu einer Al-4Cu-0,3Mg-0,7Ag-Legierung führt zu einer feineren Struktur und einer erhöhten Härte der Legierung. Darüber hinaus wurde die T6-Behandlung durchgeführt. Die Legierung Al-4Cu-0,3Mg-0,7Ag-1SiC weist die höchsten Härtewerte auf, und die Ω-Phase zeigt eine außergewöhnliche Wärmebeständigkeit über einen Zeitraum von bis zu 32 Stunden.

Die Legierungen (Al-4Cu-0,3Mg, Al-4Cu-0,3Mg-0,7Ag und Al-4Cu-0,3Mg-0,7Ag-1SiC) wurden bei einer Temperatur von 340 °C warmgewalzt, wobei Dicken von 1 mm und 5 mm erzielt wurden. Nach dem Walzprozess war die Mikrostruktur zu klein, um mit einem optischen Mikroskop analysiert werden zu können. Daher wurde die Rasterelektronenmikroskopie (REM) mit Elektronenrückstreubeugung (EBSD) zur Untersuchung der Mikrostruktur und Textur verwendet. Die Härte der Proben verringerte sich nach dem Walzen unabhängig von den nachfolgenden Behandlungen im Vergleich zur ursprünglichen Legierung.

Die drei gewalzten Proben wurden bei einer Temperatur von 350 °C für 1, 2, 3 bzw. 4 Stunden geglüht. Nach einer Dauer von 4 Stunden weist die Legierung mit SiC im Vergleich zu den anderen Legierungen ohne SiC eine höhere Härte auf.

Diese Studie bietet eine umfassende Analyse des Einflusses von Legierungselementen (Cu, Mg, Ag, SiC) und des Warmwalzens auf die Mikrostruktur und Härte von Al-Cu-Mg-basierten Legierungen. Die erhaltenen Ergebnisse dieser Studie sind für die Weiterentwicklung von Al-Cu-Mg-basierten Legierungen von Bedeutung.

Abstract

Al-Cu-Mg based alloys are renowned for their high strength and are extensively utilized in several industries, particularly aerospace. However, Al-Cu-Mg based alloys have certain drawbacks when it comes to its suitability for usage at increased temperatures, fluidity, hot tearing and resistance to corrosion. To address and prevent these issues, this study primarily aims to investigate the impact of copper (Cu), silver (Ag), and silicon carbide (SiC) concentrations on the microstructure, texture, and hardness of Al-Cu-Mg based alloys. Subsequently, the impact of adding 4 wt.% Cu, 0.7 wt.% Ag, and 1 wt.% SiC, either alone or in combination, on the aforementioned parameters was investigated. The alloys (Al-4Cu-0.3Mg, Al-4Cu-0.3Mg-0.7Ag, and Al-4Cu-0.3Mg-0.7Ag-1SiC) were analyzed under the given conditions: (i) after solution treatment (T4) at a temperature of 540 °C for 6 hours; (ii) after hot rolling at a temperature of 340 °C to achieve two different plate thicknesses while in the rolled state; (iii) after hot rolling and then ageing at a temperature of 180 °C for 32 hours; and (IV) after hot rolling and annealing at a temperature of 350 °C for 4 hours. The microstructure was examined using an optical microscope after Barker etching and scanning electron microscopy (SEM) for the Al-4Cu-0.3Mg, Al-4Cu-0.3Mg-0.7Ag, and Al-4Cu-0.3Mg-0.7Ag-1SiC alloys, as well as the corresponding rolled samples. The Vickers hardness of the T4-treated samples was assessed following a seven-day period of natural ageing.

In this investigation, it was found that the stirring during induction melting is not enough for adding SiC nanoparticles. Mechanically stirring during electrical resistance melting within a Nabertherm crucible furnace is therefore used to add SiC nanoparticle and achieve the Al composites. The sample with less Cu was discovered to have a large grain size and a low level of hardness, which can be attributed to the absence of the Al_2Cu phase (precipitation hardening phase), indicating the importance of this phase in improving mechanical properties. The addition of 4 wt.% Cu resulted in an increase in hardness, mostly attributed to the development of a substantial quantity of precipitates (Al_2Cu). Adding a small amount (0.3 wt.%) of Mg to an Al-Cu alloy containing 4wt.% Cu makes the alloy harder. It also delays the formation of a particular type of microstructure (so-called Guinier-Preston (GP) zones) at a temperature of 180 °C. The addition of a third alloying element (such as Ag) to Al-Cu-Mg alloys increases their hardness through solid solution strengthening. This occurs when dislocations, or flaws in the crystal structure, are prevented from moving during deformation by the additional element's (solute atoms) distortion of the primary element's (solvent atoms) crystal lattice. A material's plastic deformation rate is determined by its dislocations; higher hardness results from greater resistance to their movement. As the Ag is able to improve the mechanical properties but in this case the addition of 0.7 wt.% Ag to an Al-4Cu-0.3Mg alloy results in an increased grain size and a decreased hardness, which can be attributed to the fact that (i) Ag may not be regarded to be effective for strengthening if it is very soluble in the material and forms a homogenous solid solution with a little lattice deformation, and (ii) Ag influences recrystallization at high temperatures, which causes bigger grains to develop after heat treatment or Ag atoms may segregate to grain boundaries during processing, weakening the grain and increasing its susceptibility to grain growth.

After undergoing T4 treatment (540 °C for 6 hours), the grain size was reduced. Nevertheless, the alloy with Ag displayed a greater grain size in comparison to the alloy without Ag. The addition of 0.667 wt.% and 1 wt.% SiC to an Al-4Cu-0.3Mg-0.7Ag alloy results in the alloy having a more refined structure and increased hardness. In addition, the T6 treatment

was also performed. The Al-4Cu-0.3Mg-0.7Ag-1SiC alloy exhibits the highest hardness values, and the Ω phase demonstrates an exceptional thermal stability during a period up to 32 hours.

The alloys (Al-4Cu-0.3Mg, Al-4Cu-0.3Mg-0.7Ag, and Al-4Cu-0.3Mg-0.7Ag-1SiC) were subjected to hot rolling at a temperature of 340 °C, with thicknesses of 1 mm and 5 mm, respectively. After the rolling process, the microstructure becomes too small to be analyzed using optical microscopy. Therefore, scanning electron microscopy (SEM) with electron backscatter diffraction (EBSD) was used to investigate the microstructure and texture. The specimens' hardness reduces after rolling, irrespective of subsequent treatments, in comparison to the initial alloy.

The three rolled samples were annealed at a temperature of 350 °C for durations of 1, 2, 3, and 4 hours, respectively. After a duration of 4 hours, the experimental findings indicate that the alloy with SiC exhibits a higher level of hardness compared to the other alloys without SiC.

This study provides a thorough analysis of how the addition of alloying elements (Cu, Mg, Ag, SiC) and the process of hot rolling affect the microstructure and hardness of Al-Cu-Mg based alloy. The obtained results of this study are significant for the further development of Al-Cu-Mg based alloys.

Table of Contents

1 Introduction

Aluminum (Al) and its alloys are crucial in modern lightweight construction, not only in the automotive industry but also in aircraft. There is a constant search for materials that are ever lighter yet provide improved mechanical and thermal characteristics. Due to their comparatively low density, extensive availability, and economic benefits, Al alloys have a considerable influence in these industries. Even little additions of alloying elements can have a significant impact on the formation of phases and precipitation, which in turn affects the characteristics of the components. Gaining a comprehensive understanding of both the physical components and the fundamental principles that cause these alterations is of utmost importance. With this understanding and expertise in how particular alloying elements impact characteristics, it is possible to create customized materials that precisely fulfill desired specifications. This entails the optimization of operations and the improvement of production efficiency. Nevertheless, comprehending the intricate atomic-level mechanisms occurring within a substance is not always attainable. Therefore, conclusions and assumptions regarding the behavior of alloys throughout the process of solidification and precipitation are frequently made based on previously solidified material. Furthermore, continuous technology developments bring about novel investigating procedures, facilitating the attainment of more profound findings throughout time.

Al is an essential element found in many inorganic noncarbonate soil minerals. The chemical reactivity of Al in soil can manifest in different forms, mostly determined by the pH levels and mineral composition of the surrounding environment. High quantities of Al in acidic soils can be detrimental to numerous plant species. However, this problem can be alleviated by employing a liming agent or opting for plant kinds that exhibit tolerance to Al. In the first stage of comprehensive Al analysis, especially when measuring Al using spectrometry, it is necessary to fuse and fully dissolve the sample in order to transform Al into a soluble state. Researchers in the domains of soil chemistry, mineralogy, and fertility have extensively studied the role of Al in soil exchange and acidic reactions. [1]

In addition, Al is a relatively new metal, as the first pure Al ingot was showcased by Henri Sainte-Claire Deville at the Paris World's Fair in 1855. The Bayer process, which involves the digestion of bauxite with caustic soda and the subsequent electrolytic decomposition of Al oxide in cryolite smelting, was successfully developed in 1886 by Bayer, Heroult, and Hall. [2] Although the production of Al has been constantly expanding, it has faced higher production costs as a result of more rigorous environmental laws. [3]

In order to get Al, we can utilize bauxite, a substance containing Al minerals that are hydroxidic and oxihydroxidic in nature, as well as iron and titanium oxides, silica (SiO_2), chromium (Cr), phosphorus (P), fluorine (F), and organic compounds. Bauxite generally has an alumina (Al_2O_3) content ranging from 40% to 60%, and around 20% of the Al can be recovered. Table 1-1 presents three mineral forms, with hydrargillite being the most soluble in sodium hydroxide (NaOH). [3]

Al alloys are commonly categorized into three groups: heat-treatable wrought alloys, non-heat-treatable wrought alloys, and casting alloys. Non-heat treatable wrought Al alloys encompass pure aluminum as well as alloys classified under the 1xxx, 3xxx, and 5xxx categories. The primary method employed to enhance the strength of these alloys is cold work. Heat-treatable wrought Al alloys, found in the 2xxx, 6xxx, and 7xxx series, the principal alloying

elements of these materials are Cu, Mg, Si, or Zn. These alloys have the ability to undergo precipitation hardening, which is a process that results in the attainment of high levels of strength. Al alloys that are appropriate for casting also include both non-heat-treatable and heat-treatable choices. The predominant cast Al alloys are categorized into the 2xxx, 3xxx, 4xxx, 7xxx, and 8xxx classes. It is important to mention that the strength characteristics achieved through casting are generally lower than those obtained in heat-treatable wrought alloys. [4] Heat-treatable cast Al alloys, particularly those belonging to the 2xxx and 7xxx series, are frequently employed in industries such as aerospace. One noteworthy feature of these alloy groups is their ongoing ageing process over the entire operational lifespan of aircraft. Although significant research has been carried out on the 2xxx series alloys, there are still fascinating phenomena that can impact mechanical properties that have yet to be uncovered in different heat treatments and deformation procedures. Comprehensive comprehension of these phenomena is essential for the advancement of next-generation Al alloys. [5],[6]

The Aluminum Association has devised a numbering system, outlined in Tables 1–2, for the classification of cast Al alloys based on their composition. [7]

Table 1-1:Three forms of minerals.

Type	Digestion temperature in ^{O}C	Concentration of NaOH in g/l	Concentration of Al_2O_3 in g/l
Hydrargillit y-$Al(OH)_3$	100-140	105-260	90-165
Boehmite y-AlOOH	200-240	105-250	90-180
Diaspore α-AlOOH	260	150-250	100-150

Table 1-2: Alloy composition designations. [7]

Designation	Major alloying element
1XX.X	Unalloyed Al
2XX.X	Cu
3XX.X	Si with Cu or Mg
4XX.X	Si
5XX.X	Mg
7XX.X	Zn with Cu, Mg, Cr, Mn
8XX.X	Sn

Al-Cu-Mg alloys, despite their favorable combination of strength and ductility, have certain limitations. As the temperature increases, the precipitates in the alloys can become larger, which results in a reduction in their strength. This occurs because the reinforcing precipitates, which are intermetallic compounds, progressively increase in size, thereby diminishing their ability to impede the movement of dislocations. A precise control of temperature during artificial ageing can facilitate the production of small precipitates. Nevertheless, the efficacy of this procedure is constrained by a limited range of ideal ageing duration and temperature. Deviations from this window can lead to under-aged or over-aged situations, which can impair desirable qualities. [8]

Welding Al-Cu-Mg alloys can be challenging since they are prone to hot cracking. Cracks emerge when the weld zone undergoes a simultaneous occurrence of elevated temperature and solidification shrinkage. To address this issue, one can alleviate it by carefully choosing welding procedures and filler materials. [9]

Al-Cu-Mg alloys are susceptible to localized corrosion, particularly intergranular corrosion, resulting in a damage to grain boundaries. This has the capacity to diminish the strength of the material and undermine its overall quality. The presence of Cu can exacerbate this issue. An enhanced corrosion resistance can be attained by meticulously choosing alloy compositions and suitable surface treatments. [10]

The principal alloying element in the 2xxx family of heat-treatable alloys is largely Cu, although other elements like Mg can also be used. The 2xxx series Al alloys are widely used in structural applications due to their advantageous mechanical properties when subjected to heat treatment. [11]

The objective of this master thesis is to examine the changes in microstructure and texture, as well as the formation of precipitates and the resulting hardness in Al-Cu-Mg based alloys.

A particular emphasis is placed on the impact of the supplementary components (Ag and SiC), resulting in a notable alteration of the microstructure and grain size. This analysis specifically focuses on the hardness under different conditions, including casting, T4, T6, rolling, and annealing. To achieve this objective, the alloy was initially synthesized in a sequential manner, commencing with high-purity Al and culminating in the desired composition of the final alloy. A total of seven samples for each material were fabricated and exposed to different heat treatments. In addition, the specified alloy was subjected to hot rolling and assessed in both its original rolled state and after undergoing annealing treatment. Various methods were employed to analyze intermetallic phases and precipitates. In addition to Barker etching and optical microscopy for grain size determination, more comprehensive microstructure analyses were conducted utilizing the scanning electron microscope (SEM).

The present study is organized into four chapters. The first chapter presents a comprehensive examination of the theoretical ideas related to the alloy system. It also discusses the current state of this alloy system, prospective solidification processes, grain refinement, heat treatment, and hardness. Furthermore, it explores the importance of age hardening, specifically focusing on the examined Al-Cu-Mg alloy. Subsequently, the second chapter, which focuses on experimental methodologies, provides a succinct elucidation of the employed apparatus, evaluation techniques, and the fabrication and conditioning of specimens. The third chapter gives the results and includes a concise commentary that is divided into two parts: analyzing the impact of alloying elements and evaluating the degree of rolling deformation. The summary in the fourth chapter condenses the data into a succinct format, providing a glimpse into potential directions for future research.

2 Theoretical principles

2.1 Al-Cu alloy

The addition of Cu in an Al-Cu alloy has a substantial influence on both the microstructure and the growth orientation of crystals. As the Cu content increases, the microstructure of α-Al changes from columnar to columnar dendritic. At greater concentrations of Cu, it further converts to equiaxed dendritic. This microstructure evolution is accompanied by a commensurate augmentation in the distance between primary dendrite arms. The changes in microstructure can be attributed to the increase in constitutional supercooling. [12]

Figure 2-1 [13] depicts the binary phase diagram of Al-Cu alloy. In this diagram, the two components combine to create several compounds. However, when the concentration of Cu is less than 10 wt.%, a phase called Al_2Cu (θ) appears in addition to the presence of α-Al. When observed under a microscope, this θ-phase displays a structure that is structured like a diamond. The θ-phase is highly brittle, which is why technical Al-Cu alloys are mainly found on the left side of the eutectic region. As a result, these alloys mostly contain the α-Al phase with different levels of eutectic content. [14]

In addition, the binary Al-Cu alloy system has a limited ability of the Cu atoms to dissolve in the Al matrix at normal room temperature, and it is also marked by the presence of many intermetallic phases**. Figure 2a)** demonstrates that there is a eutectic relationship between Al and the θ-phase (Al_2Cu) when the Cu concentration is around 17.5 atomic percent (at. %) and the temperature is 821 K (equivalent to approximately 548 °C). At this temperature, the Al matrix can dissolve up to around 2.5 at. % (equivalent to roughly 5.7 wt. %) of Cu. When an Al-Cu alloy containing less than 5.7 wt. %Cu is cooled slowly and close to equilibrium from the single-phase Al region, stable θ precipitates occur mostly at the borders between grains after surpassing the solubility line. Because of their large size and scattered distribution, these precipitates have a negligible impact on the overall strength enhancement.

In order to achieve an efficient precipitation hardening process, it is necessary to prevent the production of large precipitates that are controlled by diffusion. This can be accomplished by rapidly chilling the homogeneous Al region, for example, by immersing it in water. Following the quenching process, there is an initial presence of a solid solution containing an excess of Cu atoms and vacancies, both in double the expected amount. However, above absolute zero, this condition is disrupted by space exchange processes, specifically diffusion.

According to the Arrhenius equation, the rate of diffusion exhibits an exponential growth as the temperature rises in thermally triggered processes. The production of a measurable precipitate can be temporarily prevented for a few hours or days by subjecting it to deep-freezing. At a temperature of 20 °C, there is a noticeable increase in the 0.2% proof stress and tensile strength, together with a decrease in elongation at break, within a short span of time.

This phenomenon is referred to as natural ageing at room temperature or slightly higher temperatures. Information on this phenomenon has been in existence for more than a century. [15]

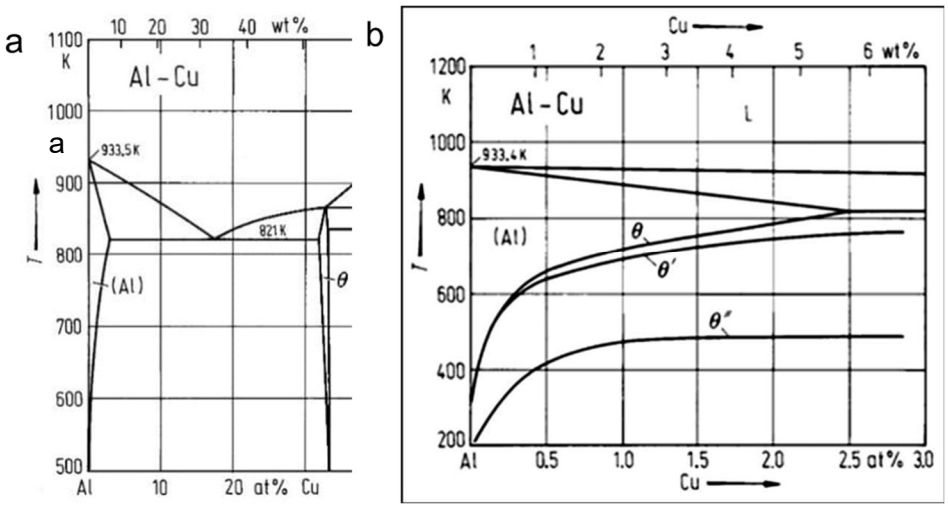

Figure 2-1: Binary phase diagram Al-Cu alloy, a) enlargement of the eutectic system Al-Al_2Cu, b) solubility range of Cu in Al and nucleation lines of the θ-, θ'- and θ'' precipitates. [15]

The phenomenon of strengthening by precipitation during ageing was initially elucidated in further detail by Guinier and Preston, who independently described it in 1938 using radiographic techniques. According to their statement, they are circular collections of Cu atoms that have a thickness of fewer than 5 atomic layers and a diameter of less than 100 atoms. Moreover, it was postulated that these precipitates are not in the θ-phase but rather exist as metastable and coherent structures. The Guinier-Preston I zones (GPI zones) are the name given to these precipitates in honor of their discoverers. Currently, there are a limited number of studies that accurately characterize the atomic structure, chemical makeup, and dimensions of GPI zones. [15]

The primary factors contributing to this are the diminutive dimensions and the challenging nature of experimental detection. Recent articles detail the separation of Cu atoms at vacancies and the creation of Cu clusters along the {111} plane with the highest packing density. The Curich clusters have a thickness of just one atomic layer and a diameter of a few nanometers. Fallah et al. determined that the clusters start off as circular discs and then gradually transform into elliptical shapes. There is a significant variation in the chemical makeup among the different clusters. Fallah et al. determined that the highest saturation value of Cu is approximately 30 at. %. [15]

2.2 Al-Cu-Mg alloys

Al alloys are widely used in the automotive industry because of their low weight and favorable fluidity. Due to their decreased weight, the automotive industry is progressively replacing numerous steel parts with Al alloys. Nevertheless, steel alloys are still utilized for the production of crucial components that require both high strength and flexibility. Various methods have been investigated to improve the mechanical characteristics of Al alloys, enabling them to compete with high-strength steel alloys. The techniques involved in this process include alloy modification, incorporation of nanoparticles, heat treatment, and semi-solid processing. The addition of Cu to Al alloys is a successful method for increasing their strength. However, the 2xxx series Al-Cu alloys are mostly used for forging rather than casting. Considering the superior cost-effectiveness and time efficiency of cast products compared to forged ones, it is advantageous to develop a casting procedure for Al-Cu-based alloys in order to inexpensively manufacture sophisticated objects. However, achieving a successful casting of these alloys requires an improved fluidity, reduced hot cracking tendency, and mechanical performance that is similar to forged products. [16]

Al-Cu alloys that include Mg, such as EN AW-2017 (AlCu4Mg) and EN AW-2024 (AlCu4Mg1), are highly significant in terms of their enhanced mechanical strength. Alfred Wilm successfully demonstrated the phenomenon of precipitation hardening in 1906 using the AlCu4Mg0.6 alloy. [15] Currently, there is an ongoing debate on the process of precipitate formation and the specific categories of precipitates in Al-Cu-Mg alloys. Wyss et al. found that the addition of Mg results in a higher void density and the creation of precipitates.

Figure 2-3 [17] demonstrates the occurrence by presenting a segment of the ternary state diagram of Al-Cu-Mg, specifically with small amounts of Cu and Mg alloying elements. Cu is crucial in attaining the ideal level of strength, usually falling within the range of 4.0 to 4.8 wt. %. Mg can increase the ability of a material to harden at normal temperatures and counteracts the impact of Fe, which is often found in pure Al in technical alloys. In addition, Mg expedites the solidification process inside the alloy system. [17]

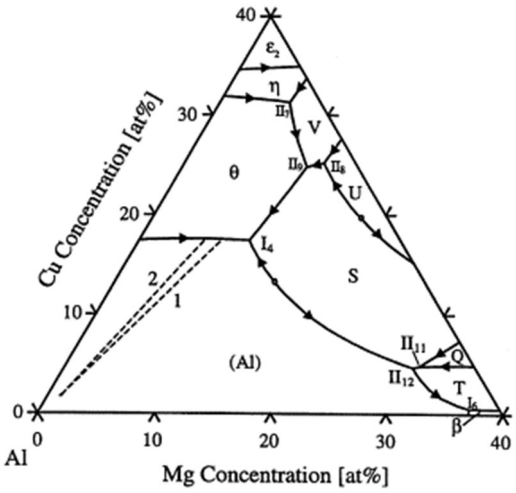

Figure 2-2: A segment of the A-Cu-Mg system at 460 °C. [18]

Vacancy clusters can act as nuclei for the creation of GP zones. Enhanced development of GP zones results in higher strengths during natural ageing. Prior studies have shown the rapid development of cylindrical clusters that have a diameter ranging from 1 to 2 nm and a length between 4 and 8 nm. These clusters are characterized by a high concentration of Cu and Mg. These structures are commonly known as Guinier-Preston-Bagaryatsky (GPB) zones. Shih et al. [19], state that these GPB thereafter change into GPBII zones (S'' phase) by organizing themselves in a tight arrangement. Wang et al. have found that the GPBII zones serve as nuclei for the development of the ordered S'' precipitates during ageing. Continued ageing eventually results in the creation of the near-equilibrium S phase, specifically Al_2CuMg. [15]

The quality of the casting is ensured by the crucial role of fluidity. It pertains to the ability of molten metal to flow until it solidifies. Fluidity is influenced by several elements, such as the composition of the alloy, the process of solidification, the level of melt superheat, the viscosity, the pouring temperature, and the rate of cooling [16],[20]. The addition of alloying elements such as Cu and Si to pure Al reduces its fluidity by increasing the range of temperatures at which it solidifies. Flemings [21] states that melts with a wide solidification range typically have a decreased fluidity. The composition that gives the largest solidification range corresponds to the point of minimum fluidity. The fluidity of the alloy increases as the solidification range decreases, until it reaches the eutectic composition. The fluidity of Al alloys decreases as the Si concentration increases, reaching its lowest point at around 5 to 6 wt.%. This corresponds to the range of maximal solidification when both solid and liquid phases are present simultaneously. Fluidity increases as the Si content further increases, reaching its highest point at 20 wt.% Si. The high latent heat of primary Si increases the time it takes for the liquid state to solidify, which in turn enhances its fluidity. In addition, increasing superheat levels can also improve the fluidity of the material, and the use of grain refiners has been shown to further boost fluidity. [16]

Although Al-Cu-(Mg) based alloys have a poor castingability among Al alloys, they are very strong and have exceptional heat resistance. For instance, after various ageing processes, the yield strength (YS) of commercially available wrought 2024 (Al-Cu-Mg-Mn) alloy ranges from 290 to 455 MPa. After tensile testing at 205 °C and 260 °C, the YS drops to roughly 130 MPa and 60 MPa, respectively. In addition, a reduced sensitivity to hot cracking results in an enhanced castability, which is crucial for both casting and wrought alloy ingots. The hot cracking susceptibility of Al-Cu-(Mg) alloys is reduced by alloying with Si, Ni, Fe, Mn, and Ca; nevertheless, the plasticity is reduced by a higher proportion of brittle intermetallic compounds. [22]

Mg is an essential alloying element in these alloys, and depending on the amount present, they can be categorized as two types of Al-Cu-Mg alloys with either low or high Mg concentrations. This master thesis specifically examines the alloy Al-4Cu-0.3Mg, which has a Mg content of less than 1 wt.% and is renowned for its remarkable strength and hardness. [23]

Hot tearing is a widely studied type of fracture that happens due to stress during the solidification process and must be avoided or reduced in casting. During the solidification process, the solid phase starts, expands, and creates interconnected structures, resulting in specific characteristics such as shape, strength, and ductility. Stress and strain occur as a result of the reduction in size during the solidification process, the pressure exerted by the metal, and the hindered thermal contraction. Insufficient molten metal supply during the later stages of solidification increases the strain on the network structure due to uniform thermal contraction and the shrinkage from solid to liquid, finally resulting in the formation of cracks and fractures in the cast products. Several variables, including the composition of the alloy,

the design and temperature of the mold, and the parameters of the casting process, have been identified as factors that affect hot tearing in casting.[16]

Hot tearing is readily noticeable in complex product designs and in alloys such as Al-Cu and Al-Zn that have broad solidification ranges encompassing temperatures from the point of melting (liquidus) to the point of solidification (solidus). Several measures have been taken to decrease the hot tearing tendency in Al alloys, such as improving the grain structure via grain refinement, adding Si, and ensuring a stable mold temperature. [16]

Grain refinement is a commonly used method in the foundry industry to improve the feeding, fluidity, machinability, and mechanical qualities of materials while also lowering the occurrence of hot tearing. [16]

By increasing the Si concentration, the interconnectivity between primary phases can be disrupted, thereby enhancing the flow of molten metal between the grains. As a result, this decreases the likelihood of hot tearing and lessens the amount of volumetric shrinkage. In addition, the process of refining the grain structure can decrease the total shrinkage that occurs when a material solidifies. This helps reduce stress and strain in the cast products, thus minimizing hot tearing. [16]

Ensuring a constant mold temperature helps reduce temperature fluctuations within the mold, which in turn addresses a uniform and excessive thermal contraction. Consequently, this improves the capacity to withstand hot tearing. [16]

The microstructures and mechanical properties of Al-Cu-Mg alloys can be affected by various factors, including the structure of the ingot, the heat treatment used, and the conditions of subsequent deformation. [24]

Deformation has a double function, improving the material's ability to harden during work and introducing a substantial number of dislocations. Ageing after deformation subsequently mitigates stress caused by deformation, promotes the production and growth of scattered precipitates, and might potentially modify the properties and the sequence of precipitation of these precipitates. [25] [26]

In their study, STYLES and colleagues [27] investigated the correlation between the decomposition sequence of a supersaturated solid solution and the phases found in the Al-Cu-Mg alloy. Their research revealed that the rate of formation of the S phase is significantly higher at higher temperatures in comparison to lower temperatures. LI et al. [28] did a study to investigate the influence of pre-deformation on the microstructure of a high-purity Al-Cu-Mg alloy. According to their investigation, they found that when the level of pre-deformation increases, the density of the S' phase (Al_2CuMg) grew while its size decreases. YIN et al. [29] conducted a study on the development features of S precipitation particles within the grains of a high-strength Al-Cu-Mg alloy.

The addition of Ag to alloys based on the Al-Cu-Mg-Ag system has the ability to improve their performance. These high-performance alloys are being evaluated as potential choices for future utilization in the upcoming generation of supersonic aircraft, which are anticipated to attain speeds ranging from 2.0 to 2.2 Mach. [30]

The addition of Ag to Al-Cu-Mg alloys can result in different changes to their characteristics. Ag additions have the ability to change the formation of ternary phases in Al-Cu-Mg alloys, especially in the section of the four-component system that is rich in Al. [31] This modification in the equilibrium between different phases becomes noteworthy when analyzing the behavior of these alloys with small additions of Ag.[32]

A comparison was made between the Al-Cu-Mg 2022 alloy, which has a high Cu-to-Mg ratio, and the Al-Cu-Mg-Ag 2139 alloy, which contains Ag, both belonging to the 2xxx series

alloys. Upon evaluation of these alloys, it was noted that the 2139 alloy displayed accelerated ageing kinetics and a greater hardness when compared to the 2022 alloy. The 2139 alloy, which includes Ag, exhibited a hardening rate that was twice as rapid as the 2022 alloy without Ag. [33]

Figure 2-2 [33] visually illustrates the comparison in hardness between these two alloys. Precipitation strengthening and grain refinement are the two main methodologies used to enhance the strength and toughness of these alloys. During the standard T6 heat treatment, the primary strengthening phases in Al-Cu-Mg alloys are the S-phase (Al_2CuMg) with a low Cu/Mg ratio and the θ' phase (Al_2Cu) with a high Cu/Mg ratio. [29],[34].

There has been an increasing need for lightweight and strong materials in many sectors, such as aerospace and automotive, in recent times. An emerging option that has garnered significant interests is the advancement of alloys derived from Al-Cu-Mg, supplemented with silicon carbide (SiC) particles. This alloy system has garnered attentions because of its heightened mechanical qualities and enhanced overall performance. This literature review aims to examine the existing research on Al-Cu-Mg-based alloys that incorporate SiC, focusing on the notable discoveries and progress made in this area.

Introducing SiC particles into Al-Cu-Mg-based alloys has been demonstrated to significantly improve their mechanical characteristics. Multiple investigations have recorded enhancements in the tensile strength, hardness, and wear resistance of the alloy when compared to its original form. [35]

SiC particles serve as reinforcing agents within the Al matrix, resulting in an improved tensile strength, hardness, and resistance to wear. The presence of SiC particles effectively impedes the movement of dislocations, thereby increasing the alloy's strength and hardness. Moreover, these SiC particles foster the development of a robust interfacial bond with the surrounding matrix, further enhancing the overall mechanical properties. [35]

Moreover, the addition of SiC particles enhances the dimensional stability of Al-Cu-Mg alloys. SiC has a low coefficient of thermal expansion, which reduces thermal strain and minimizes dimensional changes in the alloy composites. This enhanced dimensional stability is especially beneficial in situations where an exact control over dimensions is essential. [36]

Crystallographic texture and grain size are two crucial microstructural parameters that have a significant impact on the mechanical properties of Al-Cu-Mg alloys. Crystallographic texture pertains to the favored alignment of the crystals within the metal. Varying textures can influence the mobility of dislocations, which are imperfections in the crystal lattice, hence influencing the strength and ductility of the material. The strength and toughness are influenced by the grain size. Smaller particles typically result in a higher strength, but they can also decrease the ability to deform without breaking. Engineers can customize the mechanical properties of Al-Cu-Mg alloys for specific uses by manipulating the crystallographic texture and grain size using processing methods such as hot rolling and annealing. [37]

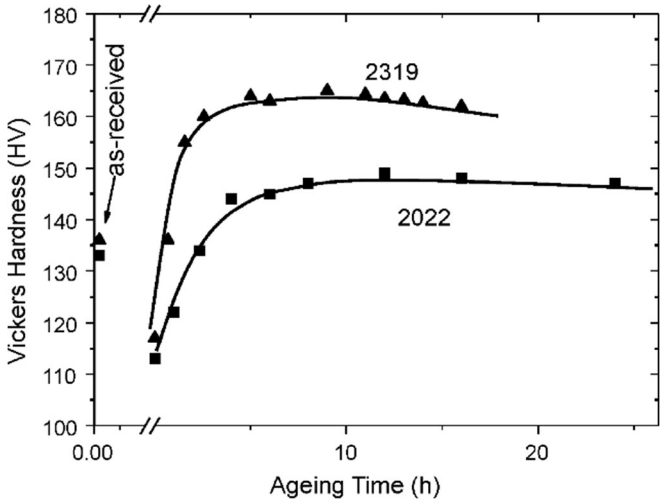

Figure 2-3: Age hardening curves for the 2022 and the 2139. [33]

As stated in the cited paper [38], the 2xxx series alloys demonstrate advantageous mechanical properties. Therefore, the main objective of this thesis is to examine the impact of incorporating SiC into this 2xxx series alloy, specifically in relation to its microstructure after rolling and T6 heat treatment, as well as the manner in which SiC forms precipitates at boundaries. Grigoris E. Kiourtsidis did study on the ageing process of the AA2024 alloy with the addition of SiC.

The process of ageing the 2024 alloy is often recognized as a series of precipitation of different metastable phases: [38]

$$\text{Supersaturated } \alpha\text{-phase} \rightarrow \text{GPI} \rightarrow \text{GPII or } S'' \rightarrow S' \rightarrow S$$

The term "GP (Guinier-Preston) zone" is used to describe a tiny, organized precipitate that develops when Al-Cu-Mg alloys undergo the ageing process. These zones generally comprise clusters that are rich in Cu and/or Mg and are scattered throughout the Al matrix. GP zones are crucial for reinforcing the alloy, leading to a higher hardness and improved mechanical characteristics. [39]

A comprehensive investigation has been carried out on the genesis and maturation of GP zones in Al-Cu-Mg alloys. Researchers have investigated multiple elements that affect the formation and enlargement of these GP zones, such as the temperature and duration of the ageing process, as well as the composition of the alloy. The size, distribution, and density of GP zones have been found to vary based on these criteria, which in turn affects the mechanical properties of the alloy. Researchers have utilized various techniques, including transmission electron microscopy (TEM), atom probe tomography (APT), and X-ray diffraction (XRD), to examine the development and properties of GP zones in Al-Cu-Mg alloys. These approaches provide valuable information about the crystallographic structure, composition, and placement of GP zones in the alloy. [40]

Within the realm of Al based composites, two closely interconnected components exert a substantial influence on their precipitation hardening behavior. Firstly, the dislocation density in these composites is higher compared to that in the unreinforced alloy. The increase can be attributed to the differential thermal contraction that takes place between the ceramic particles and the surrounding matrix during the solution treatment procedure. The coefficient of thermal expansion of SiC particles is significantly lower than that of an Al alloy, with a difference of

roughly tenfold. As a result, thermal stresses occur within the Al matrix, mainly in close proximity to the SiC particles. When the level of these stresses exceeds a specific limit, it causes the material to undergo plastic deformation, which leads to a plastic relaxation and the production of dislocations. The second component pertains to a decrease in the quantity of vacant spaces remaining within the composites after the solution treatment, in contrast to the amount found in the original alloy. The decrease in size is a direct result of the higher dislocation density in the composites, as explained in the previous paragraph. [38]

Papazian's research [41] indicated that the addition of SiC to Al alloys led to a decrease in GP zone formation in all the examined Al alloys. The decrease in the number of retained voids in the composites was related to the solution treatment. Furthermore, it was seen that dislocations acted as areas where vacancies were eliminated. While the overall pattern of precipitation did not change, there were noticeable changes in the rate at which it aged. Janowski and Pletka [42], have found that there is a specific volume of ceramic material that, when below it, the ageing behavior remains unchanged. Nevertheless, once the proportion of ceramic material reaches this key threshold, the ageing process speeds up and becomes noticeable. In addition, the continual incorporation of ceramic materials resulted in the loss of the initial hardening process. This was caused by the inhibition of GP zone formation, which occurred owing to the absence of further vacancies. The primary reason for this absence was the presence of thermal misfit dislocations.

Sannino and Rack [43] executed a study on composites made of AA2009 alloy with 20 vol% SiC particles, examining the effect of different sizes of the reinforcing particles. It was noted that as the size of the particles reduced, there was a steady transition from the dominance of GPI (Guinier-Preston I) zones to GPII (Guinier-Preston II) zones as the main contributor to the strengthening process. The phenomenon can be attributed to the decrease in particle size, which results in an increase in the interfacial area between the Al matrix and SiC particles. Consequently, this increase led to an elevated dislocation density and a concomitant decrease in the quantity of vacancies remaining following the solution treatment. As a result, GPII zones grew more noticeable while GPI zones became less noticeable because of a decrease of the places where GPII zones form (vacancies). Upon reducing the particle size, a corresponding pattern was noted in the rate of precipitation throughout the under-ageing procedure, whereas the maximum hardness and over-ageing remained unaffected.

Grigoris E. Kiourtsidis [38] conducted a study to examine how the AA2024 alloy composites age when they contain different amounts of SiC particles (0%, 8%, 14%, 19%, and 24%). The composites were fabricated using the compocasting technique, in which the AA2024 alloy was agitated and cast while in its partially solidified form. The principle of the compocasting process is a method of producing metal matrix composites where the chemical interaction between the reinforcement material and liquid matrix occurs over time, resulting in the full encapsulation of the reinforcements within the composite slurry. This process is highly effective in creating cast composites with a higher particle content. The ageing procedure took place at a temperature of 177 °C for various durations, spanning from 2 to 200 hours, for both the composites and the unreinforced AA2024 alloy.

During the process of ageing, the precipitation phases that were found in the unreinforced 2024 alloy were Al_2CuMg, while the composites contained Al_2Cu and Mg_2Si. An increase in peak hardness was detected as the volume percentage of SiC particles increased. This increase happened consistently at around 14 hours of ageing for all materials. In addition,

when the SiC particle content increased, the rate at which hardness dropped in the overaged state decreased.

2.2.1 Incorporating of Ag

The additions of Ag is well known to accelerate the age hardening response of Al–Cu–Mg alloys by producing a dense precipitation of Ω phase that nucleates and grows as thin hexagonal-shaped plates on the {111}α planes. [44]

The Al-Cu-Mg-Ag alloy system is renowned for its exceptional mechanical durability at elevated temperatures, characterized by its superior strength, negligible creep rates, and outstanding thermal stability. These characteristics make it a very suitable material for use in aerospace applications. The alloy's favorable characteristics are achieved by the age hardening process, helped by the thermally stable Ω-phase. Because Mg and Ag have a high solubility in Al, they typically remain to be dissolved in the solid solution instead of forming precipitates. Nevertheless, the presence of these substances in a solid solution can have an impact on the characteristics of the surrounding material and determine the specific method of strengthening. The introduction of trace amounts of Ag to an Al-Cu-Mg alloy, which has a high ratio of Cu to Mg, initiates the formation of the Ω-phase. The unique characteristics of this phase can be determined by analyzing its structure via metallographic inspection. It often manifests as thin, hexagonal platelets on the {111} planes. The Ω-phase is not present in Al-Cu-Ag alloys; however, it has been reported in Al-Cu-Mg alloys that do not contain Ag. This indicates that Ag mostly accelerates the formation of the Ω-phase, potentially at the cost of the θ'-phase. **Table 2-1** [45] outlines a comprehensive overview of the major age hardening phases, which are principally determined by the chemical composition. [45],[46]

Table 2-1: Key strengthening phases in Al-Cu-X alloys. [45]

Phase	Structure	Crystal habits	Composition
Ω	orthorhombic	Thin plates on {111}α	~Al_2Cu
Θ′	Tetragonal	Plates on {100}α	Al_2Cu
S′	Orthorhombic	Slat on {210}α	Al_2CuMg
T	FCC	Rectangular plates on {100}α	Al_6CuMg_4

The Ω-phase has the same chemical composition as the θ'-phase, but it also contains higher amounts of Mg and Ag at the α/Ω interface. The production process begins with the appearance of Mg and Ag clusters at 180 °C after 15 seconds, followed by the subsequent gathering of Cu atoms within 30 seconds. The precipitation sequence of the Ω-phase can be summarized as follows:

Supersaturated solid solution (SSSS) → Mg-Ag co-clusters → Ω-Phase [46]

Bakavos and his colleagues [33] conducted a study on the precipitation behavior of two high Cu to Mg ratio 2xxx series alloys, namely 2022 and 2139, during artificial ageing to achieve a T8 temper. The primary distinction in composition between the two alloys is the

addition of 0.3 wt.% Ag in 2139 and a slightly higher Mg content. The presence of Ag in the 2139 alloy results in an accelerated ageing kinetics and a substantial improvement in strength by facilitating the formation of the dominant age hardening precipitates. Precipitation was detected in the Ag-free 2022 alloy, despite the fact that prior reports did not mention the precipitation in 2xxx series alloys with such low quantities of Mg. In both alloys, the S and σ phases were discovered to nucleate heterogeneously as tiny components. However, the size of the phase was decreased in the alloy containing Ag.

Bia, Zhou et al. [44] conducted a study on the microstructures and mechanical properties of Al–Cu–Mg alloys with different amounts of Ag. They used a mix of tensile testing and quantitative TEM research. Their findings demonstrated that an increase in the Ag content from 0.46 to 0.88 wt.% facilitated the formation of the Ω phase, resulting in a significant enhancement of the strength characteristics of the underaged Al–Cu–Mg alloys at different temperatures. The precipitation of Ω phase was increased, while the creation of θ′ phase was reduced. Although subjecting the material to a temperature of 300 °C resulted in a significant reduction in the number density of the Ω phase, the alloy with 0.88 wt.% Ag exhibited a higher number density of plate-shaped precipitates compared to the alloy with 0.46 wt.% Ag. Furthermore, the quantitative TEM results of the examined alloys revealed the disparities in the process of coarsening kinetics of the Ω phase when exposed to a temperature of 300 °C. The Ω phase exhibited a transition from plate thickening to plate lengthening when the Ag content increased at a temperature of 300 °C. In addition, their findings demonstrate that pre-ageing at 165 °C for 2 hours has a beneficial impact on slowing down the rate at which the Ω phase thickens at 300 °C.

The Ω phase demonstrated an exceptional resistance to thickening at high temperatures and played a role in the combination of the strong characteristics and outstanding thermal resistance of Al–Cu–Mg–Ag alloys. [44] Grovenor et al. [47] conducted a Position Sensitive Atom Probe (POSAP) investigation which suggested that the Ω phase had a higher abundance of Mg and Ag, but a lower concentration of Cu compared to the θ phase. Nevertheless, an investigation using APT revealed that the Ω phase, which forms during nucleation and growth, is chemically identical to the θ phase. However, it has an additional layer of Mg-Ag co-segregation at the interface between the α-Al matrix and Ω phases. [44]

In general, Ω precipitates demonstrate an exceptional resistance to coarsening at temperatures of up to 200 °C. [48]

2.2.2 Incorporating of SiC

The use of composite materials is increasing in order to improve the performance of engineering materials.[49] Al metal matrix composites (MMCs) have great potential in aerospace, automotive, and electronic applications because of their high specific strength, wear resistance, and favorable thermal properties. The addition of SiC particles significantly alters the mechanical characteristics of the Al MMCs. Many researchers have investigated the correlation between the SiC reinforcement concentration and the ensuing mechanical properties. [50]

Particle reinforcements are favored over fiber kinds due to their ability to provide a more precise control over microstructure and mechanical properties through the adjustment of reinforcement size and volume fraction. SiC particles are frequently selected as reinforcement

because of their superior wear resistance, exceptional mechanical capabilities at high temperatures, and cost-effectiveness. [49]

The correlation between the SiC phase composition and the strength, hardness, and wear resistance of the Al matrix is widely acknowledged. The presence of SiC particles enhances the load transfer from the matrix, hence restricting the movement of dislocations and increasing the material's strength. Irrespective of the manufacturing methods used, either stirring casting or powder metallurgy, the essential goal remains to achieve a uniform distribution of the reinforcing phase throughout the matrix. The addition of SiC in the casting procedure of an Al-Cu-Mg alloy entails a distinct sequence of steps. [50]

The introduction of SiC particles to the Al-Cu-Mg alloy significantly improves its mechanical properties, including tensile strength, yield strength, and hardness. SiC acts as a reinforcing agent by strengthening the matrix and hindering the migration of dislocations. Al-Cu-Mg alloys, when reinforced with SiC, exhibit an improved wear resistance due to the hardness and extraordinary ability of SiC particles to withstand abrasion. Therefore, these alloys are well-suited for use in applications that require a high resistance to wear, such as automobile components and machine parts. By including SiC particles, the thermal stability of the Al-Cu-Mg alloy can be also improved. This is achieved by eliminating differences in thermal expansion and boosting the alloy's capacity to maintain its dimensions at high temperatures. Additionally, the introduction of SiC during the casting process can aid in the enhancement of grain refinement. SiC particles serve as both nucleation sites, promoting the production of smaller grains, and growth restriction, resulting in a reduced grain growth during solidification. Ultimately, grain refinement can result in improved mechanical properties. The Particle Size Ratio (PSR), which refers to the ratio of particle sizes between the reinforcement and matrix, has a significant impact on the microstructure and mechanical properties of MMC. Particle size reduction is essential for achieving a uniform distribution of the strengthening phase inside the matrix, especially when using powder metallurgy methods. When SiC particles are densely grouped together among the larger Al grains, and when larger SiC particles are present within the Al matrix, this has the ability to generate empty spaces and act as locations where cracks can start. In such situations, the strengthening of particles loses its effectiveness, leading to a decrease in mechanical characteristics. [51]

The authors of patent (US 6972109 B1) [52] outlined a technique for enhancing the tensile characteristics of Al-SiC composites. They claim that reducing the PSR between the matrix and reinforcement (from 8 to 2 µm) resulted in a more uniform distribution of the SiC particles.

El-Kady et al. [49] conducted a study on how the PSR affects the mechanical properties of Al-SiC composites. The lower PSR exhibited a correlation with a reduced porosity and a more uniform dispersion of the reinforcing phase in the matrix. However, enlarging the size of the reinforcing particles may also lead to a decline in mechanical characteristics as a result of the accumulation of excessive stress. The SiC particles are added to the Al-Cu-Mg (2024) alloy in order to enhance its dimensional stability. The combined impact of SiC and ageing precipitates on the dimensional stability of 2024 aluminum alloy is examined during a two-stage ageing procedure. It has been noted that as the amount of SiC increases, the quantity of S′ precipitates decreases. Additionally, the micro-yield strength initially increases and then decreases, whereas the thermal strain (ε_c) first decreases and then increases. At a SiC addition of 10 wt.%, both the micro-yield strength and the thermal strain respectively achieve 191.5 MPa and 0.00243. The increase in dimensional stability of the alloy is caused by the influence of SiC and ageing precipitates on pinning the dislocations, resulting in the consumption of more stored elastic energy. [36]

In addition, the SiC particles are utilized as an additional phase in Al alloys to improve their dimensional stability, thanks to their exceptional hardness and fracture toughness. [36]

Uju et al. [53] showed that SiC particles have a more pronounced impact on enhancing the overall dimensional stability compared to fly ash. Elomari et al. [54] discovered that the coefficient of thermal expansion (CTE) of pure Al can be enhanced with the addition of oxidized SiC reinforcement. They observed that when the average size of the SiC particles decreases, the CTE decreases as well. [36]

Liu et al. [55] created a novel SiC/2024 Al co-continuous composite with a lamellar microstructure. They discovered that the alloy's mechanical properties were enhanced by the presence of minimal defects, a lamellar microstructure, and well-bonded interfaces between the Al matrix and SiC phases. Hence, the addition of SiC phases can improve the microstructure of Al alloys, leading to an increase in dimensional stability. Consequently, both the precipitation particles and the addition of SiC particles contribute to the dimensional stability of the alloy. [36]

2.3 Grain refinement and castability

Crystallization provides a crucial role in understanding the characteristics of cast materials during their manufacturing process. Therefore, when producing various metallic materials, great care is taken to manage the smelting process in order to achieve the appropriate specifications. The conversion from a liquid to a solid state requires a force that prompts the change, usually caused by lowering the temperature. The Gibbs free energy (G) model provides a clear explanation for this occurrence by taking the factors of enthalpy (H), temperature (T), and entropy (S) into account.

$$G = H - T * S \tag{1}$$

Figure 2-4 [56] exhibits the enthalpy curves for the melting phase and the crystal. At a specific temperature, the phase that has a lower Gibbs free energy (G) is considered to be thermodynamically stable. Therefore, at the melting temperature (T_M), both phases exist in a state of thermodynamic equilibrium and possess identical values of the free enthalpy (H).

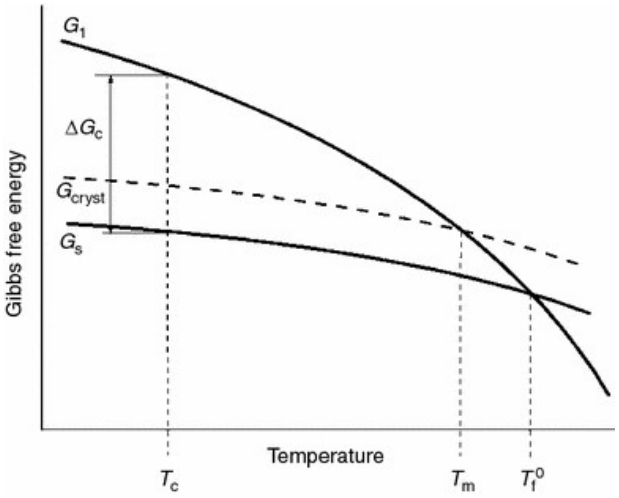

Figure 2-4: The relationship between Gibbs free energy and temperature. [56]

Decreasing the temperature makes the liquid phase metastable, while temperatures beyond the melting point cause the development of clusters that quickly disperse thereafter. Supercooling, denoted as ∆Tc, creates the thermodynamic driving force by causing a change in Gibbs free energy, represented as ∆Gc. The described behavior can be mathematically represented by the following two equations:

$$\Delta Tc = T_M - T \tag{2}$$

$$\Delta Gc = G_l - G_s \tag{3}$$

The variable T represents the current temperature, whereas G_l and G_s represent the Gibbs free energy of the liquid and solid phases, respectively. Clusters form when the temperature drops below the melting point. These clusters have the potential to grow into stable nuclei and expand once they reach a critical radius (r*).

However, this process depends on temperature and only starts when a particular temperature, referred to as T, falls below T_M. [57]

2.3.1 Homogeneous nucleation

In order to achieve homogeneous nucleation from a melt, it is necessary that there are no additional solid compounds or nuclei, such as sulphides or oxides, present in the melt, which should ideally be homogeneous. By considering a nucleus that has a spherical shape and a specific radius (r), it becomes possible to accurately establish both the critical size of the nucleus and the enthalpy of nucleation. The schematic representation of this procedure can be shown in **Figure 2-5.** [58]

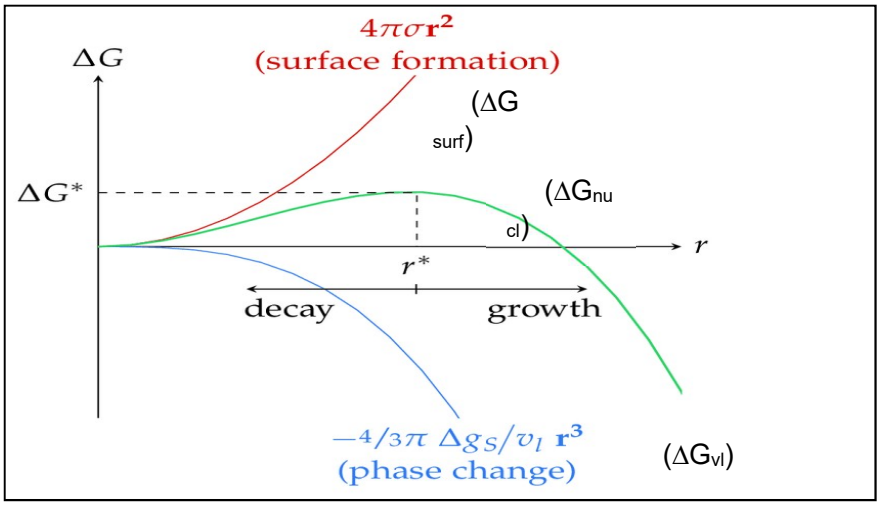

Figure 2-5: Gibbs free energy evolution as a function of particle size. [58]

The total change of Gibbs free energy ($\Delta G_{nucl} = \Delta G^*$) consists of two parts: the proportion of the nucleus that is occupied by volume (ΔG_{vol}) and the proportion that is occupied by the surface (ΔG_{surf}). In this context, σ represents the specific surface energy, while Δg_f symbolizes the driving force, as previously described in the prior chapter. The equation for a spherical nucleus with a radius r can be determined by considering these factors.

$$\Delta G(r) = 4\pi r^2\sigma - \frac{4}{3}\pi r^3 \Delta g f \qquad (4)$$

Homogeneous nucleation is rare in industrially exploited melts due to the presence of particles and surfaces that can act as nucleation sites for solidification. In some cases, they may be deliberately added to alter the morphology and qualities of the material. [57]

2.3.2 Heterogenous nucleation

Figure 2-6 illustrates the relationship between surface free energy and volume free energy with respect to the radius of the nucleus. As the variable r increases, the change in Gibbs free energy (ΔG_v) decreases with r^3, while the change in surface energy (ΔG_s) increases with r^2. Consequently, the total change in Gibbs free energy (ΔG_{total}) first rises with r, but then falls steadily due to the dominant influence of ΔG_v at high r values, eventually reaching a peak. The peak of ΔG_{total} shows the minimum energy needed to start nucleation and transition into a solid state. The critical radius, denoted as r*, is the specific position at which the derivative of the total change in Gibbs free energy with respect to radius $d\Delta G_{total}/dr = 0$. [59] .

The interplay of two contributions to the system's Gibbs function results in the emergence of a second phase. The radius, r, and surface, r^2, of the newly formed phase increase as it forms. Increasing as $4\pi r^2 \gamma$, where γ is the interphase surface energy, is the nucleus' surface energy. The nucleus's volume energy in the new phase is lower than that in the first phase for the same volume as the phase is stable below the transformation temperature. As a result, the volume energy term reduces the system's Gibbs function as r^3. The volume energy of the

nucleus with the radius r is equal to $(4/3)\pi r^3$(DGV), where DGV is the volume energy reduction that occurs when a new phase is created. [60]

As demonstrated in **Figure 2-6**, the nucleation process is initially dominated by surface energy, and a nucleus with radius $r < r^*$ can dissolve ($r \geq 0$) to lower the system's Gibbs energy. Nucleus growth is preferred for $r > r^*$ since it lowers the system's Gibbs function. The critical radius, r*, is the radius at which this transition takes place, and a nucleus inside this radius is a critical nucleus. [60]

Even though we have utilized the term “nuclei” for convenience, it is crucial to use the term with caution, as its meaning varies based on the radius in relation to the critical radius. When the radius exceeds the critical radius, the solidified particles are identified as nuclei. These nuclei can persist in the solution without dissolving back into the solution, allowing them to expand further along the path of nucleation, as the free energy decreases with their growth. Conversely, if the radius of the solidified particles is smaller than the critical radius, they are known as embryos or clusters. In this case, they dissolve back into the solution, as reducing the radius leads to a decrease in free energy. Therefore, r* represents the minimum radius at which a nucleus can exist in the solution and continue growing without dissolving, and it can be calculated as follows: [59]

$$r^* = -2\gamma/\Delta g \tag{5}$$

Equation (5) shows that the critical radius of a nucleus is established by the proportion of the specific surface energy alteration to the specific volume free energy alteration. This implies that the likelihood of nucleation can be managed by adjusting the critical radius, which is dictated by the ratio of the two free energy alterations. The liquid phase of solidified particles can be discerned based on their radius in the diagram shown at the lower portion of **Figure 2-6a.** [59]

The minimum size required for an atom or molecule cluster to initiate the formation of a new phase, such as solidification or precipitation, is referred to as the critical nucleus size. Nucleation theory is centered around the fundamental concept of how new phases emerge from preexisting ones. [61]

Some information on the crucial size can be provided to enhance understanding:

- Thermal variations cause unstable clusters smaller than the critical size to disintegrate.
- The cluster reaches stability at the crucial size and can continue to grow into a new phase. This is because of the fact that the surface energy cost related to the cluster interface is outweighed by the energy obtained via the new phase development.
- Clusters bigger than the critical size are stable and will develop into a new phase. [61]

The following are some of the variables that affect the critical nucleus size:

- The energy connected to the contact between the parent phase and the new phase is known as the surface energy. An increase in the surface energy raises the critical dimension.
- The degree to which the system is "out of equilibrium" and promotes the creation of the new phase is known as undercooling (solidification) or supersaturation

(precipitation). A smaller critical size is produced by higher undercooling or supersaturation.

- The speed at which atoms or molecules can travel and join an expanding cluster is known as the diffusion rate. The critical size may decrease with increasing diffusion rates. [61]

Phase transformation phenomena can be better understood by applying the concept of a crucial nucleus. However, figuring out the crucial nucleus's size has been a long challenge. Thermodynamic calculations of it in the past have failed because it was found that the interface free energy depends on the size. The molecular cluster that is in an unstable equilibrium with the supersaturated phase is known to be the crucial nucleus of a new phase. An unstable equilibrium indicates that there is a chance of this cluster growing and dissolving. To put it another way, the critical sized cluster cannot develop unless molecules are added to it in order to overcome the energy barrier that prevents nucleus formation. According to thermodynamics, the total Gibbs free energy of the crucial nucleus is reduced even when a single molecule is added. However, even with supersaturation, one molecule could not be enough.

While 'nuclei' larger than the critical nucleus become increasingly survivable due to their decreasing Gibbs free energy, the nucleation theory does not specify the size of the clusters that has a nearly 0% disintegration probability, meaning that it is destined to develop unhindered.

The point at which the surface term and the volume term of the Gibbs free energy change (ΔG) balance is chosen to assess the size of such perfectly stable crystal "nuclei." [62]

Therefore, we have explored the comprehensive concept of nucleation, which involves the transformation from a liquid phase to a solid phase during a phase transition. Regarding perovskites, the change in Gibbs free energy should be associated with the solidification of solutes in the solution, which happens when requirements of supersaturation are fulfilled. The degree of supersaturation can be measured as

$$S = C/Cs \tag{6}$$

C represents the concentration of the solute, while Cs represents the maximum amount of solute that can dissolve (C > Cs). Therefore, Δg can be expressed in the following manner:

$$\Delta g = -k_B T \ ln(S)/v \tag{7}$$

The variables in question are v, which represents the molar volume, T, which represents the temperature, and k_B, which represents the Boltzmann constant. Equation (7) contains practical information regarding the parameters that need to be managed in order to enhance nucleation. The increase in Δg is necessary to increase the probability of nucleus formation. Accelerating the supersaturation stage in the spin coating process can be achieved by augmenting the concentration of the fluid. In addition, the intentional removal of solvent through antisolvent dripping during spin coating enhances nucleation, resulting in the rapid formation of many nuclei. This process facilitates the development of dense film structures

without any pinholes. Increasing the temperature is an additional method. The temperatures of the solution, substrate, environment, and antisolvent are crucial variables that significantly influence nucleation and Gibbs free energy. Consequently, meticulous attention must be paid to every component of the nucleation process when carrying out perovskite processing. [59]

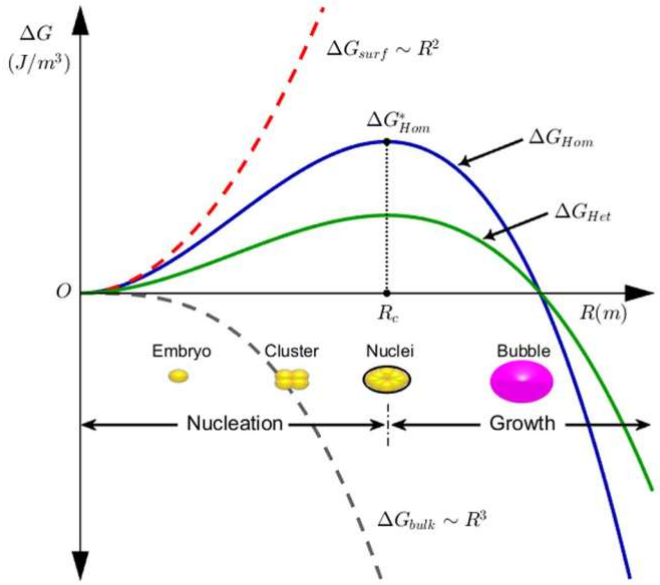

Figure 2-6 : (a) illustrates the variations in Gibbs free energy concerning the particle radius, r. The alterations in Gibbs free energy attributed to surface, volume, homogeneous nucleation, and heterogeneous nucleation are represented as ΔG_s, ΔG_v, ΔG_{hom}, and ΔG_{hetero}, respectively. [63]

2.3.2.1 Additional SiC

SiC particles can serve as heterogeneous nucleation sites, offering a reduced surface energy for the Al phase to initiate nucleation on. [64],[65] This can result in an enhanced nucleation rate and a more refined microstructure characterized by smaller and more abundant grains. The efficacy of SiC as a heterogeneous nucleation site is contingent upon its wetting characteristics with the molten Al. A good wetting promotes an effective interfacial contact, which enhances heterogeneous nucleation. The distribution of SiC particles within the molten substance is also essential for optimizing their impact on the occurrence of nucleation events. SiC particles can impede the motion of the boundary between solid and liquid, resulting in a limited expansion of the crystal, especially in the direction that is perpendicular to the boundary. This can lead to the formation of equiaxed and fine grains. Moreover, the existence of SiC particles can affect the growth morphology of the Al phase. In some cases, it can result in the fragmentation of dendrites or the creation of non-dendritic structures. Furthermore, there are supplementary factors: (i) particle size and morphology: smaller and more angular SiC particles have a greater surface area and enhanced heterogeneous nucleation potential in comparison to bigger or rounder particles. (ii) concentration: increasing the SiC content can amplify the overall impact on heterogeneous nucleation and growth, but it can also result in an agglomeration and a diminished effectiveness. (iii) matrix composition: the precise formulation of the Al-Cu-Mg alloy can impact

the wetting characteristics, the interaction between SiC and the matrix, and the overall influence on the microstructure. SiC content ranging from 0.5 to 1.5 wt.% results in the presence of SiC acting as efficient sites for heterogeneous nucleation. This leads to the formation of a more refined microstructure with smaller grains. However, the smaller number of particles may restrict its ability to significantly affect the crystal development. The addition of SiC in a medium amount (1.5–3 wt. %) has the additional effect on improving heterogeneous nucleation and refining the grain structure. The pinning impact on the crystal formation becomes evident, which has the potential to enhance strength. A high SiC content of more than 3 wt. % exhibits a pronounced pinning effect, which hampers the development of crystals and may result in a decreased ductility. Additionally, there is a heightened susceptibility to agglomeration, a phenomenon in which particles aggregate, leading to a decrease in their efficacy and the potential occurrence of flaws. [65]

2.4 Grain refining with SiC

Grain refinement is crucial in customizing the mechanical characteristics of Al alloys for various uses. This procedure entails diminishing the mean grain size by introducing nucleation sites that promote the creation of new, smaller grains during the solidification process. Its objective is to decrease the size of the primary Al grains and inhibit the growth of elongated dendrites.

Therefore, grain refiners are widely used in the solidification process of many Al alloys. When a large amount of nuclei is produced as a result of significant undercooling or the introduction of nuclei, the molten material solidifies evenly and with a fine dispersion. The neighboring nuclei impede the growth of one another. **Figure 2-7** [66] provides an illustration of the impact of grain refining, serving as an example.

SiC particles are frequently employed as grain refiners in Al alloys. They act as heterogeneous nucleation sites. These sites provide a reduced energy barrier for the solidification of Al atoms compared to the pure molten state. This promotes the development of numerous small grains surrounding the SiC particles, as opposed to a smaller number of bigger ones. This process provides a multitude of advantages for a wide range of alloys, resulting in positive effects on both casting parameters and mechanical qualities. The advantages encompass an enhanced feeding, resulting in a less shrinkage porosity, higher elongation characteristics, an improved fatigue life, and a more even dispersion of secondary intermetallic phases. To do this, one must introduce small amounts of foreign substances into the molten material before casting. These substances act as nucleating agents, facilitating the process of crystallization. It is crucial to emphasize that the additional substance must possess a greater melting point than the alloy to guarantee its solidification takes place prior to cooling. When choosing a grain refiner, it is important to consider the similarity of crystalline phases. This helps to ensure that the crystals created from the melted material can strongly adhere to existing nuclei. The size of the grains in a material decreases as the degree of undercooling of the melt increases. This is because of the fact that the process of undercooling increases the rate at which nucleation occurs, leading to a microstructure that is both fine and uniform. Nevertheless, attaining this optimal situation is theoretically attainable and may not necessarily be achievable in reality, contingent upon the geometry of the manufactured component.

Several advantages are listed below:

Enhanced tensile strength and increased resistance to deformation: increased grain boundaries hinder the movement of dislocations, resulting in an increased resistance to deformation in the material.

Enhanced ductility and toughness: a reduced grain size enables an increased plastic deformation prior to failure, leading to an improved ductility and toughness.

Improved corrosion resistance: a reduced grain size results in a smaller surface area that is susceptible to corrosion.

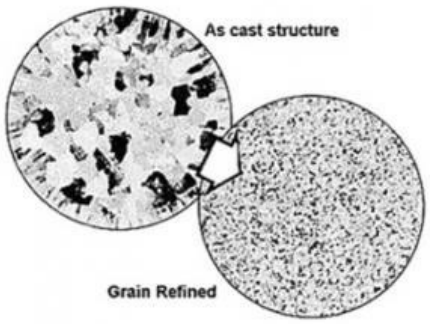

Figure 2-7: Grain refining on the microstructure. [66]

2.5 Heat treatment

Heat treatment refers to a variety of heating and cooling processes used to modify the mechanical properties, metallurgical structure, or residual stress of a metal product. However, when discussing Al alloys, the phase typically refers to processes that are primarily focused on improving the strength and hardness of age hardening wrought and cast alloys. These alloys are generally known as "heat-treatable" alloys, which sets them apart from alloys that cannot be significantly strengthened by the process of heating and cooling. Annealing, a process of heating to enhance ductility and reduce strength, is employed for both types of alloys. The metallurgical reactions involved may differ depending on the specific alloy and the desired level of softening. [67]

The heat treatment method can augment the strength of Al during its production. Artificial ageing is a vital heat treatment for Al and related alloys, especially those containing 2.5 wt.% to 5.0 wt.% Cu. By utilizing artificial ageing that involve manipulating time and temperature, as well as making adjustments to the temperature and duration of the solution treatment, it is possible to significantly increase the hardness of various types of Al. [68]

An experiment was conducted on 2024 T6 Al alloy, which entailed subjecting it to a temperature of 500 °C for a duration of 1 hour, and thereafter undergoing artificial ageing at 190 °C for different periods of time, namely 1, 2, and 5 hours. The most favorable precipitation phase was seen after a period of 5 hours of ageing. [69]

Naveed Afzal and colleagues [70] executed a study on 2024 Al alloy, where they manipulated the ageing period to 2 hours and adjusted the temperature to 105, 135, 165, and 195 °C, respectively. The results indicated that the greatest tensile strength and hardness were attained when the materials were aged at temperatures of 135 °C and 195 °C, respectively. Gowrishankar M. C. and collaborators [71] performed experiments using AA 6061

material. They tested different ageing temperatures, ranging from 100 °C to 200 °C, and varying ageing durations, ranging from 3 to 10 hours. The investigation yielded an evidence of enhanced mechanical characteristics at lower temperatures. Aytekin Polat and his team [72] performed studies on AA 6061 material, where they manipulated the temperature and time of ageing. The solution treatment was done at a temperature of 550 °C for a duration of 2 hours. The process of artificial ageing was conducted at temperatures of 160 °C, 180 °C, and 200 °C, with different durations of 2, 5, 10, 20, 40, 60, and 80 hours, respectively. The results demonstrated that the mechanical characteristics decreased with increasing the ageing temperature, but improved with increasing ageing durations up to peak age.

DAP Reis et al [73] performed trials where they manipulated the solution treatment temperatures to 495 °C, 505 °C, and 515 °C and then subjected the samples to artificial ageing at 190 °C and 208 °C, respectively. The study found that the optimal hardness was obtained by subjecting the material to a solution treatment at a temperature of 505 °C, followed by an artificial ageing process at 208 °C for a duration of 2 hours. MS Khan et al. [74] conducted experiments utilizing Al 2014 material and subjected it to a solution treatment temperature of 502 °C for a duration of 2 hours. The results showed that the hardness increased from 85 HV to 136 HV and after artificial ageing at 180 °C for a duration of 1 hour and further increased to 145 HV when aged at 233 °C for a duration of 1 hour.

Imam et al. [75] successfully attained the highest level of hardness for an Al alloy substrate by subjecting it to a solution treatment at 500 °C, followed by artificial aging at 165 °C for a duration of 1 hour.

Several alloys undergo thermal treatment to exploit phase solubilities, including solution heat treatment, quenching, and ageing. Alloys that have a favorable response to heat treatment are referred to as heat-treatable. These alloys, commonly present in the 2XXX, 6XXX, and 7XXX series, can be fortified by undergoing a regulated process of heating and cooling. Alloys belonging to the 2XXX, 6XXX, and 7XXX series are generally capable of undergoing solution heat treatment. Their strength can be augmented by subjecting them to heating followed by quenching or quick cooling, and it can be further intensified through cold working. The heat treatment can have a substantial impact on the strengthening effect. 2024 Al alloy, when fully annealed and in the O-temper condition, exhibits an ultimate yield strength of around 186 MPa (27 ksi). [76]

Under a specific loading or temperature circumstances, as-cast Al alloys demonstrate a reduced yield strength and hardness. In order to solve these limits, a new generation of wrought alloys has been developed. One example is the Al-Cu-based 2xxx standard system, which is distinguished by its distinctive compositional design and/or thermo-mechanical processing methods. These advancements have been developed specifically to tackle the aforementioned issues. [77] [78]

The prevailing method to enhance the mechanical strength of these alloys commonly entails the use of microalloying components. These components contribute to the simultaneous achievement of precipitation and solution hardening effects. [79]

Al-Cu alloys commonly utilize precipitation hardening as a means to enhance their mechanical properties. [27,28] The heat treatment process consists of three primary stages: solution treatment, quick quenching, and controlled ageing. During the solution treatment, Cu is dissolved and remains inside the Al matrix. The quenching procedure is performed rapidly to uphold the disintegration of Cu. During artificial ageing, certain phases precipitate, resulting in an increased strength and improved mechanical qualities as a result of the change of these phases. The characteristics of this transformation are affected by the conditions present

throughout the heat treatment process. The predominant phase generated by precipitation in Al-Cu alloys is θ (Al_2Cu). [16]

Another essential feature of a precipitation-hardening alloy system is its equilibrium solid solubility, which increases as the temperature increases. This can be observed in phase diagrams, as shown in **Figure 2-8**. [67]

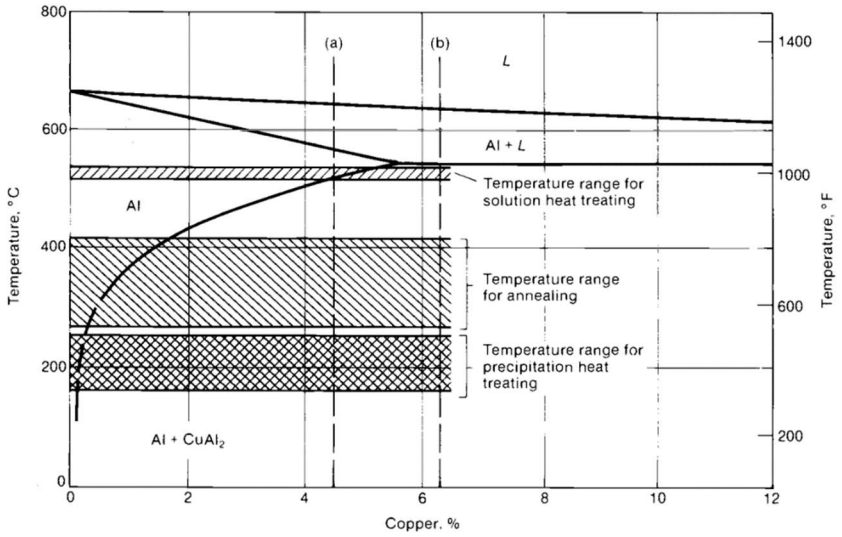

Figure 2-8:Segments of the binary phase diagram for Al-Cu alloy are shown, with marked temperature intervals for annealing, precipitation heat treatment, and solution heat treatment.

To enhance the strength of supersaturated solid solutions through precipitation, it is necessary to create finely dispersed precipitates during ageing treatments, which can be either natural ageing or artificial ageing. The ageing process must occur below both the equilibrium solvus temperature and the Guinier-Preston (GP) zone solvus line, which is a metastable miscibility gap. The existence of an abundance of vacancies allows for a more rapid diffusion and consequent creation of zones, beyond the predictions made by equilibrium diffusion coefficients. During the process of precipitation, the solid solution that was originally saturated produces clusters of solutes, which eventually contribute to the formation of transitional precipitates that are not in a thermodynamic equilibrium. The process of strengthening by precipitation is based on the production of coherent clusters of solute atoms. This means that even though the solute atoms come together to form a cluster, they maintain the same crystal structure as the solvent phase. This leads to a significant strain caused by the disparity in size between the atoms of the solvent and solute. Hence, the presence of these precipitate particles, along with the strain fields in the matrix surrounding them, increases the strength by obstructing and slowing down the motion of dislocations. The coherence or loss of coherence of a precipitate phase is dictated by the level of alignment or misalignment between atomic spacings on the lattice of the matrix and the precipitate. The property changes occur due to the development of microstructural regions that contain a high concentration of solute, which are referred as GP zones. These regions can be examined using TEM and usually appear as spherical areas with a high concentration of solute when the diameters of the atoms of the solvent and solute are identical. In systems like Al-Cu, where there is a notable disparity in the sizes of atoms, GP zones frequently appear as disk-shaped structures. These disks align their

planes with certain low-index planes of the Al matrix lattice. At times, atoms that are dissolved in a substance can take up certain positions within the crystal lattice, resulting in the formation of a region with an organized atomic arrangement known as a GP zone. GP zones generally have widths in the range of tens of angstroms and are characterized by deformed portions of the matrix lattice rather than being separate particles of a new phase with a different lattice structure. They are completely consistent with the Al matrix, causing localized but frequently significant stresses. The mechanical strains, together with the existence of a regionally solute-rich and occasionally ordered lattice, can account for substantial modifications in the mechanical characteristics of the alloy prior to any considerable changes in its microstructure. GP zones are intrinsically unstable and disintegrate when a more stable precipitate is present. This dissolution results in the formation of a zone surrounding stable particles of precipitate that lacks any precipitates (so called precipitates free zone (PFZ)). The ultimate configuration consists of stable precipitates that have a negligible impact on the process of strengthening. [67]

Specifically, the traditional T6 heat treatment has been demonstrated to enhance the mechanical properties of Al-Cu-Mg alloys. [80]

Alloys in T6-type tempers generally attain an optimal strength while maintaining sufficient levels of other qualities and features necessary for engineering applications. [67] However, heat treatment alone has its limitations in terms of achieving enhancement. [80] During the conventional T6 heat treatment process, [81] artificially aged (T6) Al-Cu-based alloys, which are among the conventional Al-based alloys, have gained a significant popularity. These alloys contain small quantities of alloying elements like Mg, Mn, Si, and Sn. These elements have a composition that is either binary, ternary, or quaternary. The coherency, size, interparticle spacing, and distribution of precipitates have a major impact on the strength of Al-Cu-Mg-based alloys at high temperatures. One prior research has shown that the attainment of stable precipitates is strongly linked to the manipulation of the Cu/Mg ratios in the compositional design of Al-Cu-Mg base systems. [77]

The precipitation phase that occurs at approximately 190 °C in alloys with low Cu/Mg ratios is known as the equilibrium S phase (Al_2CuMg). [77],[82],[83]

Nevertheless, before reaching a condition of balanced precipitation, there are usually a number of intermediate changes that occur, specifically the Guinier-Preston-Bagaryatsky (GPB) zone, S″, and S′ phases. These phases form in the following order: SSSS → GPB → S″ → S′ → S. [84] On the other hand, in Al-Cu-Mg alloys with higher Cu/Mg ratios, the precipitation phase that forms at around 190 °C is known as the θ (Al_2Cu) phase. This stage is preceded by three precursors: GPB, θ″, and θ′. The sequence of events is as follows: SSSS → GPB → θ″ → θ′ → θ. [77],[82],[83] Previous studies have shown that the addition of a tiny quantity of a quaternary element, such as Ag, to ternary Al-Cu-Mg alloys speeds up the formation of the required Ω phase on the {111} α planes. [77]

The Ω phase has a chemical composition that is identical to the θ phase. However, it also contains an extra layer of Mg-Ag co-segregation at the interface between the α and Ω phases. It has a notable capacity for precipitation hardening at elevated temperatures, usually about 200 °C. [77]

Several simultaneous research endeavors have examined the impact of the Cu/Mg ratio on both probable precipitation situations and the mechanical properties of Al-Cu-Mg alloys. Liu et al. [85] conducted a study on the influence of the Cu/Mg ratio on two commonly utilized Al alloys, specifically 2519 and 2024, which have high and low Cu/Mg ratios, and an Al–5.10Cu–0.65Mg (wt.%) alloy, called homemade (HM), has a Cu/Mg atomic ratio of 2.96. The

alloys were fabricated using ingredients of exceptional purity. The ingots were fabricated using the direct-chill (D.C.) casting method and subjected to a homogenization process at a temperature of 500 °C for a duration of 72 hours. Subsequently, the ingots were subjected to both hot and cold rolling processes to get sheets with a thickness of 20 mm. Before undergoing the ageing process, the rolled sheets made of 2024, 2519, and HM alloys were subjected to solution heat treatment. This treatment involved heating the sheets to temperatures of 495 °C, 530 °C, and 520 °C, respectively, for a duration of 1 hour in a furnace. Afterward, the sheets were rapidly cooled by quenching them in water until they reached room temperature. The subsequent ageing process was conducted by immersing the material in an oil bath at a temperature of 180 °C for a duration of up to 120 hours. According to the research, decreasing the Cu/Mg ratio results in a higher tensile strength and yield strength of the Al-Cu-Mg alloy. [77],[85] The hardness values of the 2024 alloy, which has a Cu/Mg ratio of about 3.41, and the 2519 alloy, which has a Cu/Mg ratio of about 16.29, were found to be 152 HV and 141 HV, respectively. The research team discovered that the improvement in mechanical properties of the newly designed HM alloy is due to the change in the ratio of Cu/Mg, resulting in the substitution of the θ′ phase with the S phase. [77],[85] Hence, the presence of the S phase may offer benefits in improving the mechanical characteristics of Al-Cu-based alloys.[77]

The presence of the Ω-phase in Al-Cu-Mg-Ag alloys affects both the coarsening resistance and thermal stability, which are influenced by the chemical composition and thermomechanical processes. The T4 heat treatment for a 2XXX alloy involves a process of solution treatment, followed by quenching in water, and then allowing for natural ageing. On the other hand, the T6 heat treatment includes the process of artificial ageing after the quenching stage. **Figure 2-9** presents a schematic depiction of the two probable treatments for the alloy. [86].

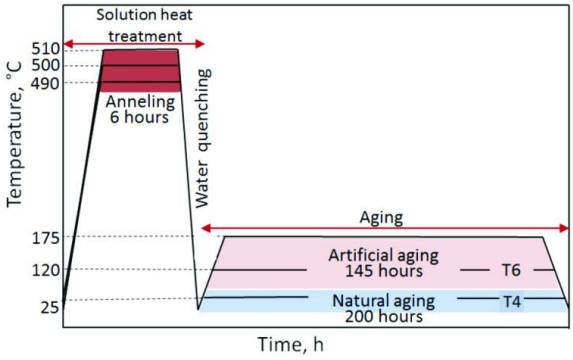

Figure 2-9: Diagram presenting heat treatment of 2XXX-alloy. [86]

The temperature range becomes crucial in this specific group of alloys, particularly when the Cu content reaches 4 wt.%. At this point, the temperature range significantly narrows, which has a notable impact on achieving a uniform microstructure. **Figure 2-10** [87] depicts the correlation between the concentration of Cu and the temperature. High temperatures can cause some parts of the microstructure to partially melt, whereas very low temperatures do not allow for a complete homogeneity. Utilizing artificial peak ageing with this specific alloy can result in an increased strength, although it comes at the cost of a reduced corrosion resistance. [87]

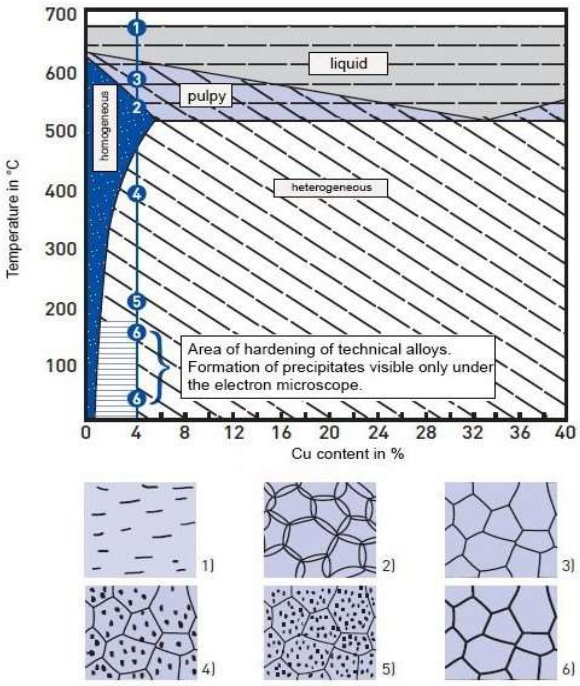

Figure 2-10: The correlation between temperature and microstructure within the Al-Cu system. [87]

2.5.1 Role of alloying elements

2.5.1.1 Cu

Obtaining uniformity in cast Al alloys with the addition of Cu typically requires a longer period of time since the diffusion of Cu in Al is rather slow. [88] The precise diffusion coefficient for Cu in Al is contingent upon various parameters, such as temperature and the specific composition of the Al alloy. At temperatures suitable for cast Al alloys (about 600-700 °C), the diffusion coefficient of Cu in Al often falls within the range of 10^{-13} to 10^{-14} cm²/s. Consequently, the diffusion of Cu atoms over substantial distances inside the Al matrix is a time-consuming process. [89] The rate at which Cu-containing particles dissolve in a casting is primarily affected by the size and structure of Cu-containing phases, such as the equilibrium θ-Al_2Cu. Usually, a time period of 48 hours is recommended to ensure the complete mixing of Cu and Al. However, in fact, the majority of heat-treated casting Al-Cu alloys undergo a solution treatment up to 12 hours or less. [88]

2.5.1.2 Mg

When combined with Cu, Mg is a very useful element for enhancing the age hardening in Al alloys. [88] Small amounts of Mg accelerate and enhance the precipitation hardening. [67] Notable differences in the reaction to age hardening at 150 °C can be observed between alloys containing 0.1 wt. % Mg and those with higher concentrations, such as 0.2–0.3 wt.% Mg, as depicted in **Figure 2-11**. [88]

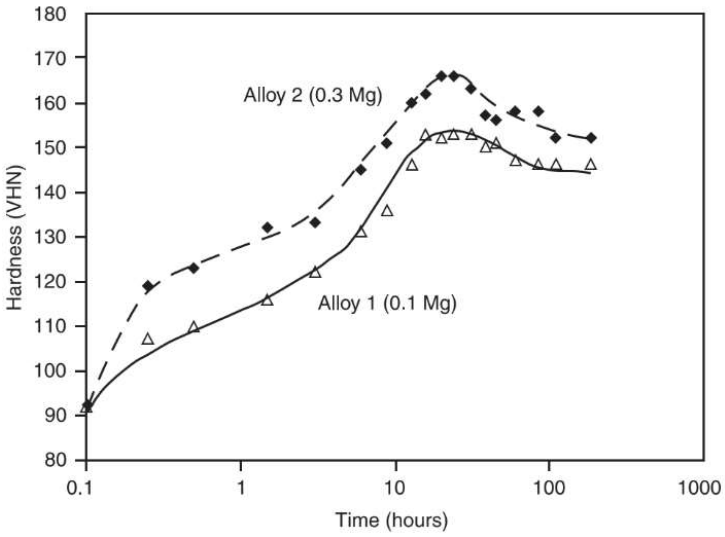

Figure 2-11: A comparison of Al alloys containing either 0.1 wt.% Mg. [88]

The hardness curve depicted in **Figure 2-11** demonstrates that an increase in Mg content from 0.1 wt.% to 0.3 wt.% triggers the onset of rapid initial age hardening. [88]

The addition of Mg in the Al-Cu system has been observed to affect the temperature at which eutectic melting occurs. More precisely, the addition of Mg to the Al-Cu alloy with a composition of 4.4 wt.% Cu decreases the temperature at which the alloy melts. This is because of the fact that the introduction of Mg leads to the production of a ternary eutectic that melts more easily. [90] In addition, the addition of Mg in the Al-Cu-Mg system is linked to the creation of ternary eutectic phases that have lower melting points. This also results in a reduction of the eutectic melting point. [91]

Clearly, Mg has the effect of reducing the eutectic melting point in the Al-Cu alloys. The **Table 2-II** below illustrates the decrease of the temperature ranges used in typical solution treatment for three commonly used Al-Cu-Mg alloys to their respective eutectic melting temperatures. However, the precise reduction is contingent upon the quantity of Mg introduced, although it can be substantial. [67]

Table 2-2: The temperature ranges used in typical solution treatment for three commonly Al-Cu-Mg system. [67]

	Solution-treating temperature		Eutectic melting temperature	
Alloy	°C	°F	°C	°F
2014	496–507	925–945	510	950
2017	496–507	925–945	513	955
2024	488–499	910–930	502	935

Nevertheless, it is crucial to note that the precise impact of Mg on the eutectic melting point can be dependent on the alloy's composition and the existence of other elements. For example, in the case of Al-Cu alloys containing a large amount of Cu, the decrease in temperature related to eutectic melting is more noticeable. [90]

2.5.1.3 Ag

Alloys containing Ag, Li, and Ge components possess the ability to attain a significant strength through the process of heat treatment. [67]

De Geuser et al. employed Small-Angle X-ray Scattering (SAXS) measurements to examine the effects of solution heat treatment on an Al-4Cu-0.3Mg-0.4Ag alloy. The alloy is subjected to temperatures of 200 °C for a maximum of 2 hours, both in its original condition and while being subjected to various loads. In each of the three samples, the clusters experience an initial growth within the first hour until the Ω precipitates are formed. These precipitates then undergo coarsening in the subsequent hours. The precipitates have a size ranging from 2 to 3 nm, with the maximum size seen in the sample without any load. The initial formation of clusters is not significantly affected by the applied stress. [92]

2.5.1.4 SiC

The incorporation of SiC particles into the Al-Cu-Mg alloy results in a substantial enhancement of its mechanical properties, such as tensile strength, yield strength, and hardness. SiC acts as a strengthening agent by enhancing the structural integrity of the material and limiting the mobility of dislocations.

However, the evolution of heat treatment is changed when SiC particles are included into Al alloys. Due to the obstruction of SiC particles during solid solution treatment, the SiCp/Al–Cu–Mg composite has a lower eutectic dissolving rate and coarsening rate of grains than the matrix Al–Cu–Mg alloy. Compared to matrix Al alloy, particle-reinforced aluminum matrix composites (PRAMCs) have a shorter peak aging time. On the other hand, other experts maintain that PRAMC ages more slowly than matrix Al alloy. Additionally, an excessive ageing will weaken the composite. The SiCp/Al–Cu–Mg composites with the fastest ageing kinetics and maximum hardness were discovered by Abarghouie et al [93], at an appropriate solid solution treatment temperature of 495 °C for 1 hour. According to Liu et al [94], after solid solution treatment for 2 hours at 505 °C, the alloy phases of SiCp/2024Al composite were entirely dissolved, and the optimal mechanical characteristics were attained after artificial ageing for 10 hours at 190 °C. PRAMCs may undergo different thermal treatments as a result of variations in preparation and composition. [95]

2.5.2 Strengthening mechanisms

The main method of strengthening Al alloys is precipitation hardening, which is highlighted by the categorization of alloys into hardenable and non-hardenable systems. The hardenable alloy systems, together with their International Alloy Designation System (IADS) codes, consist of Al-Cu and Al-Cu-Mg (2XXX), Al-Mg-Si (6XXX), and Al-Zn-Mg (7XXX). The binary Al-Cu alloy system will be used as an example to explain the concept of precipitation hardening, as shown in **Figure 2-12**. [96]

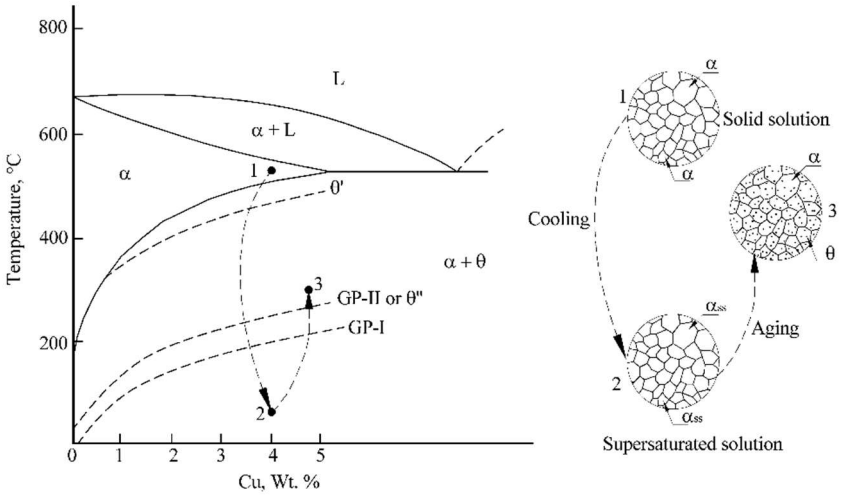

Figure 2-12: Phase diagram of Al-Cu alloy with a high Al content illustrating the processes of solubilization and precipitation. [96]

Figure 2-12 shows that precipitation hardening is achieved by heating the alloy over the solvus temperature. This causes the formation of a homogenous solid solution α, which allows the second phase θ to dissolve and eliminates the separation of different components in the alloy. Once the solubilization temperature is reached, the alloy is rapidly cooled to prevent the passage of atoms towards probable nucleation sites. Afterwards, the SSSS is heated to a temperature that is lower than the solvus temperature. At this temperature, atoms are capable of undergoing short-range diffusion. Due to the instability of the SSSS phase, Cu atoms migrate to various nucleation sites, which helps facilitate a regulated precipitation process. The objective of precipitation hardening in metals is to distribute second-phase particles in order to hinder the migration of dislocations. The degree of hardening is determined by the metallic system, the volume fraction, and size of particles, as well as their interaction with dislocations. The interactions between precipitated particles and dislocations have a considerable impact on the level of hardening. Several methods have been found, such as particle bypassing through Orowan looping, bypass slip, or particle shearing. **Figure 2-13** [96] illustrates the stresses exerted on a movable dislocation in a strained metal that contains a dispersion of second-phase particles. [96]

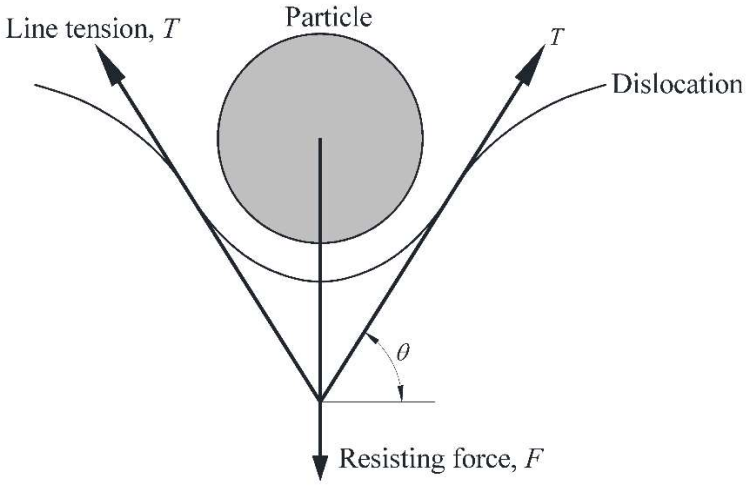

Figure 2-13: Force equilibrium during particle dislocation resistance. [96]

The essential requirements for precipitation hardening are given below:

1. The alloy predominantly or partially persists as a solid solution at high temperatures.

2. The solubility of the secondary components in the crystal reduces as the temperature decreases. Both of these conditions are satisfied for an alloy that has a Cu content of less than 4 wt.%, as observed in the systems analyzed in this investigation. The age-hardening process consists of three primary stages: solution treatment, quenching, and ageing.

(i) The strengthening process begins with a solution treatment. The alloy is heated to a temperature above the solvus temperature and maintained at this temperature until a uniform solid solution is formed. The θ-precipitates in the Al-Cu system undergo a dissolution. It is absolutely crucial to ensure that the individual stages do not melt at any cost during this step. To guarantee a thorough disintegration and homogeneity, it is crucial to avoid very low temperatures. The ideal temperature range is usually limited, frequently covering only 5 to 10 °C.

(ii) The second stage, known as quenching, entails the quick cooling of the workpiece to create a SSSS that is not in an equilibrium state. The rapid cooling process prevents the movement of Cu atoms in the solid solution, which in turn hinders the production of large precipitates. To achieve the highest level of supersaturation, it is necessary to rapidly cool the solution, which is frequently done by using cold water (20 °C).

(iii) The last stage, ageing, involves heating the system to a temperature below the solvus point in order to promote the creation of finely dispersed precipitates. At lower temperatures, the atom diffusion is limited to small distances. This causes an accumulation of surplus Cu atoms at various nucleation sites, where precipitates then develop. Ageing is a natural process that can occur spontaneously at ambient temperature. The transformation from the SSSS to the equilibrium state of the system often occurs through a multi-step process. The precipitation process in the Al-Cu system involves a series of intermediary steps that ultimately lead to the formation of the θ-phase. SSSS transforms into GP-Zones, which further transform into θ' precipitates, and finally into θ precipitates. The Guinier-Preston (GP) zones that form are coherent precipitates enriched in Cu, exhibiting a disk-like morphology and a thickness of only a few atomic layers. Because the diffusion pathways are short, the precipitates are evenly scattered and have a high concentration. The main factor contributing to the strengthening process is the interaction between dislocations and precipitates. As the resistance to the dislocation movement increases, the hardness and strength also increase. [38],[97]

Figure 2-15 illustrates the crucial link between solubility and temperature that is required for precipitation hardening. The text describes the temperature ranges required for both solution treatment and the subsequent strengthening achieved by the production of precipitates in the Al-Cu system. [67]

Precipitation hardening is the phenomenon in which the hardness, yield strength, and ultimate strength of a material increase significantly over time at a constant temperature (referred as the ageing temperature) after being rapidly cooled from a much higher temperature (known as the solution treat temperature). Rapid cooling, also known as quenching, results in SSSS, which triggers the process of precipitation. [98]

The German chemist Alfred Wilm first discovered precipitation hardening in 1906 while studying an alloy with a composition of Al-4Cu-0.6Mg (wt.%). [99] The researcher discovered that the hardness of Al alloys, including minor quantities of Cu, Mg, Si, and Fe, increases gradually after being rapidly cooled to a temperature slightly below the melting point. [98]

Al-Cu alloys, including Cu in the range of 0.2 to 5.6 wt.%, can display two different stable solid states. Cu is completely soluble above the bottom curve depicted in **Figure 2-1**, known as the solvus. If the alloy is held at those temperatures for a sufficient amount of time to allow for the necessary diffusion, the Cu will fully dissolve into the solid solution. [67]

Below the solvus point, the equilibrium state consists of two solid phases: a solid solution called α and an intermetallic compound phase referred as θ (Al_2Cu). When an alloy is heated above the solvus temperature and then cooled below the solvus, it forms a solid solution that is supersaturated. The alloy then tries to reach an equilibrium state with two phases. The formation of the second phase often occurs by solid-state precipitation. After the solution treatment and quick cooling, the hardening process can be accomplished either at room temperature (known as natural ageing) or with an ageing treatment (known as artificial ageing). It is customary for alloys in the 6xxx wrought series, especially the more extensively alloyed variations, the Cu-containing alloys in the 7xxx series, and all alloys in the 2xxx series, to subject a solution treatment followed by quenching. For specific alloys, particularly those in the 2xxx series, the process of natural ageing alone leads to a beneficial precipitation hardening, resulting in useful tempers like the T3 and T4 tempers. These temperaments exhibit high ratios of tensile strength to yield strength, an increased fracture toughness, and a resilience to fatigue. These alloys, when subjected to such tempers, maintain a reasonably high level of atom and vacancy supersaturation due to a rapid quenching. This stimulates the rapid creation of GP zones, resulting in a rapid increase in strength that reaches almost maximum stable values within four or five days. [67]

Age hardening in Al alloys has been a subject of investigation ever since Alfred Wilm first observed it in Al-Cu alloys around one hundred years ago. It is considered a novel method to improve the strength of Al alloys. [70] Ageing at a sufficiently low temperature (usually below around 200 °C) causes precipitation hardening in Al-Cu-Mg alloys to occur in two distinct stages, separated by a plateau. Following the quenching process, there is a significant and rapid increase in hardness at the early stage, accounting for approximately 60% of the maximum level of hardening. The following phase results in the achievement of maximum hardness. The exact reason for the rapid initial hardness is still a subject of discussion. The rapid age hardening of Al–Cu–Mg alloys is believed to occur by several mechanisms, including the creation of Guinier–Preston–Bagaryatsky (GPB) zones, the presence of Cu–Mg co-clusters, and an interaction between dislocations and solutes. During the initial stages of research, the second phase of hardening was commonly attributed to the development of the S´ or S phase. [99]

The existence of a distinct solid formed during a chemical reaction, known as S′′, has been indicated as the main factor responsible for the observed increase in hardness.

In order to understand the processes that cause hardness, it is essential to have a concise understanding of the sequence of precipitation that occurs during ageing. Bagaryatsky suggested the precipitation sequence as follows: SSSS→ GPB Zone → S′′ → S′ → S ($CuMgAl_2$). The S phase has been the subject of various proposed models, but the Perlitz and Westgren (P-W Model) is the most frequently accepted structure. Due to the similarities in their lattice characteristics, it is now understood that there is no distinct differentiation between the S′ and S phases, despite their modest structural variances. The presence of a phase known as S′′ or GPB2, separate from S or GPB, has been a topic of discussion, and multiple crystallographic structures have been documented. [99]

While precipitation can occur spontaneously at room temperature in SSSS after quenching, its effect on mechanical characteristics can be greatly accelerated and improved by ageing at a higher temperature after quenching. Artificial ageing typically occurs within a temperature range of around 200 °F to 400 °F (95 °C – 205 °C). **Figure 2-14** depicts the standard alteration in hardness that occurs as a result of the artificial ageing of Al. [98]

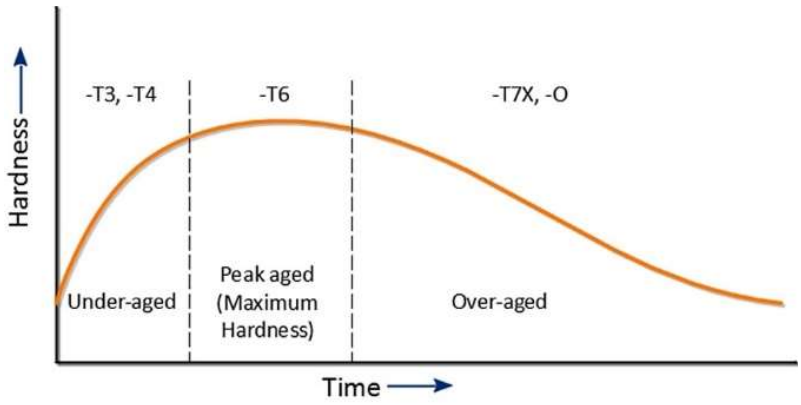

Figure 2-14: The typical change in hardness for artificial ageing of Al. [98]

2.6 Rolling

2.6.1 Hot rolling

The dynamic restoration mechanisms involved in hot deformation are closely linked to the changes in a material's microstructure and texture. The mechanism of dynamic restoration in Al during hot working is widely acknowledged to be fundamentally dynamic recovery (DRV), as evidenced by the strong cross slip propensity and relative rates of dislocation climb resulting from Al's high stacking fault energy (SFE). [100]

Usui et al. [101] observed that dynamic recrystallization (DRX) happens in Al, Al-Si, and Al-Mg alloys during hot rolling after researching the dynamic restoration of Al and its alloys. Additionally, it was shown in their work that high strain rates are beneficial for distinguishing DRX by restricting DRV, in contrast to the effect of strain rates on Cu and Ni. Recently, Yamagata [102] reported that multipeak stress oscillations, typical of DRX in metals, are

detected during the hot compression of high pure Al (99.999 pct) at temperatures between 238 °C and 547 °C and strains up to 2. Additionally, it has been shown that, during hot compression, DRX takes place in both polycrystal and single-crystal Al. [100]

Hot rolling offers a crucial role in the processing and improvement of Al-Cu-Mg alloys, affecting various aspects such as the mechanical properties, microstructure, and texture development of the alloy. Research has investigated the impact of decreasing hot rolling or cold rolling on the development of texture in Al-Cu-Mg alloys. [103],[104]

Hot rolling can induce changes in the texture of a material, which in turn can affect its anisotropic mechanical properties. [104] The methods of XRD, electron backscattered diffraction (EBSD), and TEM have been utilized to examine the changes in texture that occur during hot rolling. [103]

Furthermore, hot rolling has the capability to improve the grain structure of Al-Cu-Mg alloys. The thermomechanical action involved in hot rolling promotes recrystallization and grain refinement, resulting in enhanced mechanical characteristics of the alloy. [104]

Furthermore, subjecting Al-Cu-Mg alloys to heat treatment after hot rolling can enhance their strength and stability. Applying the heat treatment for precipitation hardening can greatly increase the strength of the alloy. The heat treatment is also efficient in regulating grain size, strengthening through dispersion, and enhancing the stability of the microstructure. [105]

Peng Xia and his colleagues conducted a study on the changes in texture in the intermediate layer (1/4 of the total thickness) of hot-rolled Al-Cu-Mg alloy sheets using XRD, EBSD, and TEM. The results indicated a change in texture from the shear texture {001} <110> to the β-fiber textures when the rolling temperature increases from 400 °C to 420 °C. Friction at lower rolling temperatures led to the creation of a robust shear texture through the induction of shear strain. Nevertheless, when the rolling temperature increases, the dominance of shear strains in the intermediate layer was gradually replaced by plane strains, resulting in a significant augmentation in β-fiber textures. In addition, it was noticed that increasing the rolling temperatures resulted in the activation of the non-octahedral {112} <110> slip system, which facilitated the formation of robust Brass textures. When the rolling reduction was decreased to 74%, textures with a low intensity tended to align with the α-fiber, which includes Goss, Brass, P, and L components. On the other hand, when the rolling reduction was increased to 90%, the textures became stronger and progressively shifted towards the β-fiber, which consists of Brass, Copper, and S components. It is worth mentioning that during hot rolling, the S and Copper bands were found to be the preferred locations for the creation of recrystallizing cube grains. The number 87 is enclosed in square brackets. [106]

2.6.2 Cold rolling

The process of cold rolling is crucial in determining the microstructure and mechanical characteristics of the Al-Cu-Mg alloy. [107] As the cold rolling reduction and annealing temperature increase, the alloy's hardness increases due to strain hardening and grain refinement. [107] Cold working operations like rolling or stretching expedite the precipitation process, imparting additional strength and resulting in an improved age hardening response, particularly in Al-Cu alloys with minor Mg additions. [108]

In Al alloys, Goss {110} <001> texture is commonly observed as a characteristic of recrystallization. Nevertheless, Liu et al. [109] discovered that Goss texture may develop

during cold rolling, and the ensuing data demonstrated that the volume percent of Goss texture first increases and subsequently decreases with increasing reduction. As a result, this suggests that the Goss texture is metastable and that, when rolled, it might resemble the β-fiber texture in certain ways. In their review, Leffers et al. [110] hypothesized that the Goss texture in α-fiber likely changed to Brass texture while rolling by rotating 35° about the normal direction (ND). However, direct experimental evidence regarding the Goss texture evolution during cold rolling is currently still lacking. [111]

The energy from stacking faults was crucial in regulating crystal slip, which determines the creation of β-fiber texture while rolling. For example, the rolling textures of the Brass, Copper, and S orientations are similar in terms of the intensity in Al and Al–1.8 wt.% Cu alloys. Nonetheless, our earlier study discovered that the rolled texture of Al–Cu–Mg alloys included a fairly sharp Brass component but very little Copper and S orientations. Consequently, it appears that the alloying elements have an impact on how the texture changes during rolling. [111]

Additionally, during cold rolling, the Goss texture in Al-Cu-Mg alloy changes, a phenomenon that can be analyzed using three-dimensional orientation distribution functions and EBSD. [111]

However, more research is also required to determine how rolling texture creation and slide system performance are related. The solitary {111} <110> slip system's activation is what causes the Al–Cu–Mg alloy to produce a Brass-textured structure. [111]Huang et al. [112] looked into the relationship between texture and microstructure during cold rolling of the AA3104 alloy and discovered that the S grain only had one set of dislocation boundaries, whereas the Copper and Brass grains had two distinct sets. [111]

Using TEM, EBSD, and three-dimensional orientation distribution functions, Qi Zhao et al. [111] examined the evolution of the Goss texture in an Al–Cu–Mg alloy during cold rolling. The findings demonstrated that as the reduction increased from 23.7 to 80%, {111} <110> slip systems were activated, progressively converting Goss textures into Brass textures.

3 Experimental methods

3.1 Casting, heat treatment, rolling, annealing

Several Al alloys were prepared for comparison, including one alloy with 4 wt. % Cu, 0.3 wt.% Mg and 0.7 wt.% Ag, referred to as Al-4Cu-0.3Mg-0.7Ag, and another alloy with the same composition but with the addition of 1 wt.% SiC, indicated as Al-4Cu-0.3Mg-0.7Ag-1SiC. The alloys originated with a casting of Al-4Cu-0.3Mg and were then modified to attain the intended composition. The composition of the various casting ingredients is specified in **Table 3-1**.

Table 3-1: The nominal composition of Al alloys (wt.%).

Alloys	Elements					
	Al (g)	Cu(g)	Mg(g)	Ag(g)	SiC (Al-30SiC) (g)	SiC (Al-20Cu-20SiC) (g)
Al-4Cu-0.3Mg	1914	80	6	-	-	-
Al-4Cu-0.3Mg-1SiC_A	1847.3	80	6	-	66.7	-
Al-4Cu-0.3Mg-1SiC_B	1834	60	6	-	-	100
Al-4Cu-0.3Mg-0.7Ag	1774	80	6	140	-	-
Al-4Cu-0.3Mg-0.7Ag-1SiC_A	1707.3	80	6	140	66.7	-
Al-4Cu-0.3Mg-0.7Ag-1SiC_B	1674	60	6	140	-	100
Al-0.3Mg-1SiC	1847.3	-	6	-	66.7	-

The material used was obtained from the Chair of Casting Research. The basis material used for manufacturing all alloys was commercially pure Al, which may contain tiny quantities of extra elements. The casting procedures were carried out utilizing the casting capabilities of the Chair of Casting Research.

Induction melting was conducted on a variety of alloys to examine the existence of SiC nanoparticles. Two specimens, Al-4Cu-0.3Mg-1SiC and Al-4Cu-0.3Mg-0.7Ag-1SiC, were

created with the addition of SiC nanoparticles. The initial stage involved placing the Al element into the furnace, as depicted in **Figure 3-1**. The furnace temperature was then set to 720 °C. Once the Al had melted, the remaining elements, namely Cu, Mg, and Ag, were introduced in the form of pure Cu, pure Mg and Al-10Ag master alloy, respectively. Finally, the alloy was supplemented with 100 g of SiC nanoparticles (**Figure 3-2**). It is important to mention that two distinct SiC master alloys, namely Al-30SiC and Al-20Cu-20SiC, were utilized, respectively.

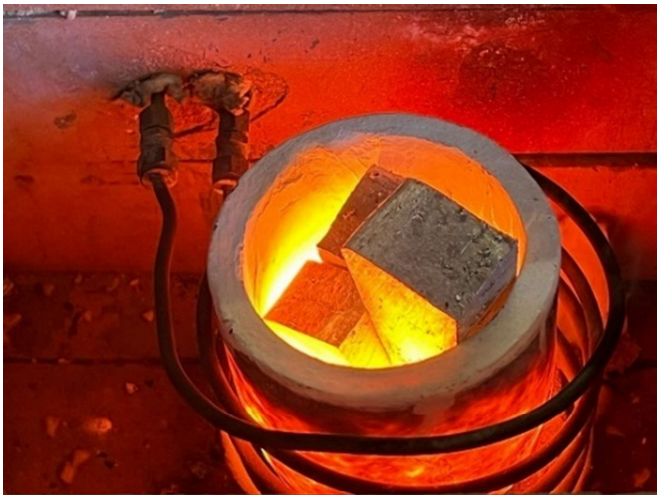

Figure 3-1: Induction melting.

Figure 3-2:The SiC powder in the form of Al-30SiC and Al-20Cu-20SiC.

The initiation of the melting process for the Al-4Cu-0.3Mg-1SiC and Al-4Cu-0.3Mg-0.7Ag-1SiC specimens was prompted by the presence of SiC. Once the alloys were melted and SiC in the form of Al-30SiC and Al-20Cu-20SiC was added at a temperature of 720 °C, the melt was stirred until the SiC nanoparticles were fully dissolved in the alloy. The operation encountered a significant issue wherein the SiC nanoparticles exhibited a limited solubility in the alloy. Instead, they amalgamated with debris and emerged on the surface of the molten substance (**Figure 3-3**).

Figure 3-3: Unsolved SiC in the induction melting.

It was discovered that using induction melting was ineffective in agitating the melting process to incorporate the SiC nanoparticles. The SiC nanoparticles must be introduced into the molten Al alloy while maintaining continuous stirring. The agitation facilitates the uniform distribution of SiC particles throughout the alloy. An alternative method was utilized to fabricate the alloy, employing the Nabertherm crucible furnace, also known as an electrical resistance furnace. This furnace may be observed in **Figure 3-4**. Once the material has been trimmed

and measured, it is then transferred into the crucible to undergo the melting process. The melting temperature for all castings is fixed at 720 °C. In addition, the Al-4Cu-0.3Mg-sample was additionally combined with Al-10Ag, Al-30SiC, and Al-20Cu-20SiC, respectively. Seven specimens are fabricated with steel Diez molds. **Figure 3-5** shows the Diez molds sample after casting.

Figure 3-4: Nabertherm crucible furnace at the Chair of Casting Research.

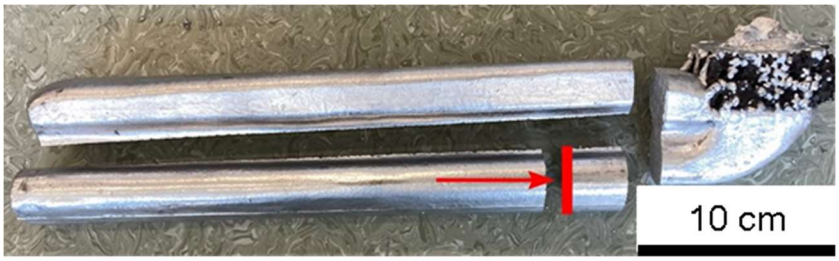

Figure 3-5:The Diez molds sample after casting.

Subsequently, a T4 heat treatment was conducted at a temperature of 540 °C for a period of 6 hours, followed by a rapid cooling in water (20 °C). **Figure 3-6** illustrates the T4 thermal treatment process.

Subsequently, the specimens were subjected to an ageing treatment at a temperature of 180 °C for a duration of 32 hours. The heat treatments were performed using the Nabertherm NA120/85A convection oven, as depicted in **Figure 3-7**.

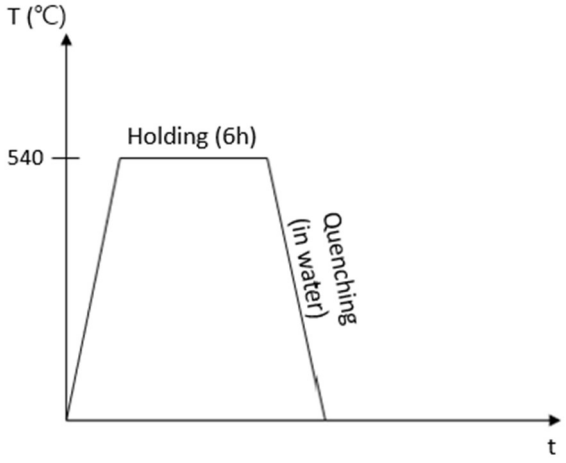

Figure 3-6: T4 Heat treatment.

Figure 3-7: Heat treatment oven.

Furthermore, a T6 heat treatment was conducted at various time intervals, including 30 minutes, 1 hour, 2 hours, 4 hours, 6 hours, 8 hours, 24 hours, and 32 hours (**Figure 3-8**).

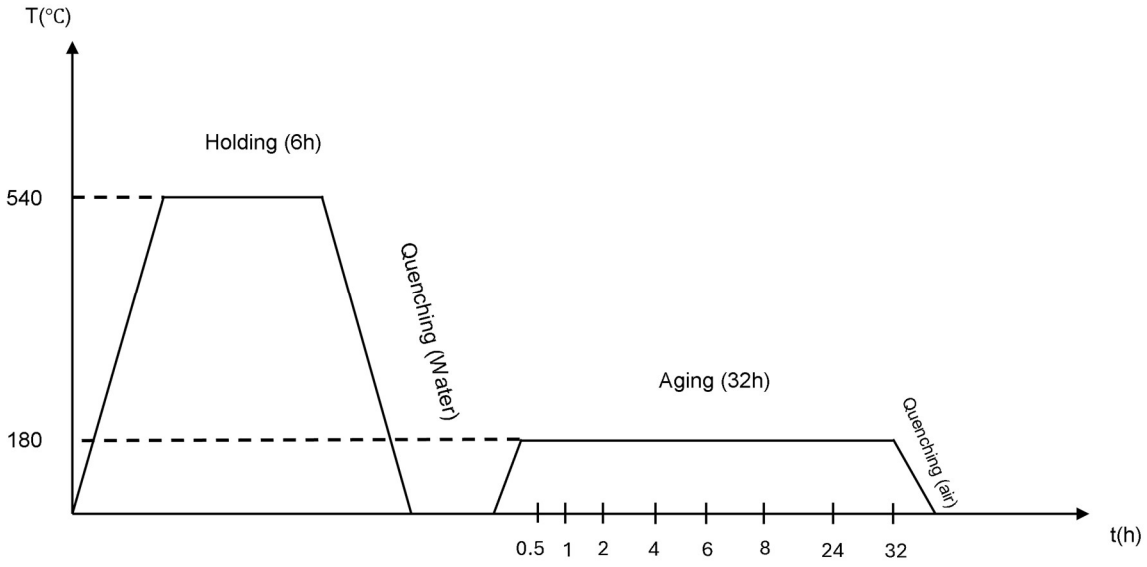

Figure 3-8: Artificial ageing (T6).

Afterwards, samples of the cast material were cut for further testing while in their original cast state. In addition, bigger portions were cut for T4 heat treatment and subsequently immersed in a water bath for quenching. In addition, there alloys (Al-4Cu-0.3Mg, Al-4Cu-0.3Mg-0.7Ag, and Al-4Cu-0.3Mg-0.7Ag-1SiC) underwent rolling processes to achieve different thicknesses, as specified in **Table 3-2**.

Table 3-2: Rolled samples with dimension.

Designation	Thickness [mm]
A	1
B	5

Initially, the Al-4Cu-0.3Mg specimen underwent a cold rolling at room temperature. However, after numerous rolling cycles, the specimen developed a crack. During the further rolling of the Al-4Cu-0.3Mg-0.7-1SiC specimen, it experienced more pressure and force. However, this also resulted in the formation of a fracture, as depicted in **Figure 3-9**.

Figure 3-9: Crack after cold rolling.

The T4 rolled materials, including Al-4Cu-0.3Mg, Al-4Cu-0.3Mg-0.7Ag, and Al-4Cu-0.3Mg-0.7Ag-1SiC, were therefore subjected to hot rolling using a rolling machine at a temperature of 340 °C. This process is illustrated in **Figure 3-10** and **Figure 3-11**.

Figure 3-10: Rolling machine.

Figure 3-11: Heat treatment oven before hot rolling

Initially, the specimens were rolled to a thickness of 5 mm, as depicted in **Figure 3-12**. Subsequently, they were sliced into very small sizes in order to prepare EBSD samples.

Figure 3-12: The 5 mm specimens after 340 °C rolling

The specimens, first rolled to a thickness of 5 mm, were further rolled to a thickness of 1 mm, as depicted in **Figure 3-13**.

Figure 3-13: The 1 mm specimens after 340 °C rolling

The specimens Al-4Cu-0.3Mg, Al-4Cu-0.3Mg-0.7Ag, and Al-4Cu-0.3Mg-0.7Ag-1SiC, which were hot rolled up to 1 mm, underwent annealing at a temperature of 350 °C for time intervals of 1 h, 2 h, 3 h, and 4 h in order to compare their hardness. The annealing process utilized the identical oven employed for T4 heat treatment, as depicted in **Figure 3–7**.

3.2 Hardness measurement

The hardness measurement is conducted in the Chair of Metal Forming at Montanuniversität Leoben. The EMCO Test M1C 010 machine, equipped with a pyramid-shaped diamond indenter and a square pedestal, is used for this task. The peak angle between two opposed sides of the pyramid is 1360, as depicted in **Figure 3–14**. The hardness examination was performed using the Vickers method, which measures the diagonals of the imprint made by the indenter. The requirements for conducting the test are listed as follows: (i) the surface must be flat and parallel, (ii) the test material must have a thickness that is at least 10 times more than the depth of the indentation, and (iii) the space between indentations should be at least 6 times more than the length of the diagonal. These standards are enforced to avoid any misinterpretation of hardness data caused by changes in the post-indentation deformation of the surrounding material.

Figure 3-14: The Vickers machine at the Chair of Metal Forming.

3.3 Microstructure characterization methods

This chapter presents a brief summary of the microstructure characterization methods utilized in this thesis. To observe the microstructure of the specimens, it is necessary to apply an etching process to all of them. In order to carry out etching, several stages must be undertaken, including grinding and polishing.

Thus, the process of specimen preparation involved the utilization of stages such as sectioning, mounting, coarse grinding, fine grinding, polishing, etching, and examination. The six specimens were completed and trimmed in order to be ground. Grinding eliminates the presence of saw marks and achieves a smooth and clean surface on the specimen. The objective of the grinding process is to achieve a surface that has a minimal damage, allowing for the removal of any remaining imperfections during the polishing stage in the most efficient manner.

3.3.1 Optical microscope

Prior to the investigation of the samples using the optical microscope, they were initially subjected to grinding using abrasive paper of various grades, namely P220, P800, and P1200. Afterwards, the surface will be polished using a diamond suspension with a particle size of 3 µm, followed by polishing with an alkaline silica suspension with a particle size of 20 nm. The stages are executed manually at the Chair of Casting Research using an ATM Saphir 350 machine, as depicted in **Figure 3-15**.

Figure 3-15: Grinding machine ATM Saphir 350.

In order to observe the microstructure using an optical microscope, electrolytic Barker etching was performed by using a solution consisting of 35 ml of hydrofluoric acid (HF), 13 g of boric acid (H_3BO_3), and 800 ml of water (H_2O). The technique is carried out at the Österreichischen Gießereiinstitut (ÖGI) using the ATM Kristall 620, etc., as shown in **Figure 3-16**. The ground and polished specimen is placed in the solution with the etching side submerged, and it is attached as the anode using a metallic connection. Every sample is subjected to etching for a period of 2 minutes. After undergoing this procedure, the microstructure becomes discernible when seen under an optical microscope in a polarized light mode. This is because of the fact that the etching process creates a contrast that allows for differentiation.

Figure 3-16: Barker etching (ATM Kristall 620).

Optical microscopes often have a limited range of focus at high magnifications, highlighting the need for meticulous sample preparation to ensure accurate observation of microstructures. Their resolution is normally limited to the visible light wavelength range, which is approximately up to 0.3 µm. This range is adequate for most investigations of microstructures in their original or post-heat treatment states. The Chair of Casting Research conducted microstructural investigations using a Carl Zeiss Axio Imager. A1m microscope, which has a maximum resolution of about 0.5 µm. In addition, the incorporation of a Nikon DS-Fi1 camera enabled the examination and assessment of microstructures on a fixed computer using the NIS-Elements BR 3.0 program. In order to evaluate etched microstructures and measure grain size, samples were analyzed using a polarized light mode and the reflected light TC technique. **Figure 3-17** illustrates the arrangement of the microscope.

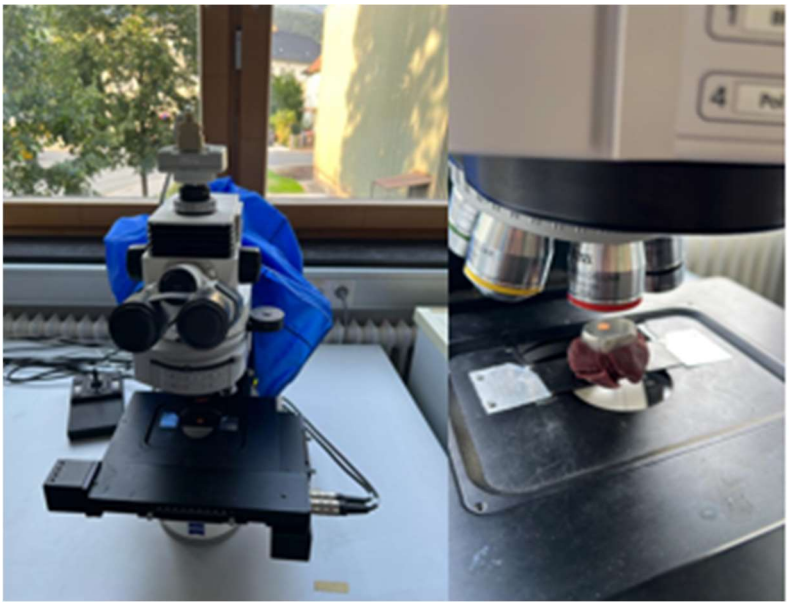

Figure 3-17: Optical microscope.

There are both analog and digital methods available for determining the grain sizes of an Al alloy. The grain sizes in this study are evaluated using the linear intercept approach. In addition to utilizing the NIS Elements BR 3.0 application, the Origin software is also utilized. This technique involves placing measurement lines of a predetermined length on the sample and counting the number of times they connect with grain boundaries. The line's length is subsequently divided by the number of grains it intersects to determine the average grain size along that line. In order to accommodate possible differences in the alignment of grains throughout the process of solidification, three lines are drawn horizontally. Afterwards, a mean value and standard deviation are determined.

3.3.2 SEM (EBSD)

Due to the limited resolution of the light microscope, SEM is used to observe and assess grains in the submicrometric range. SEM analysis requires an extensive surface area preparation for obtaining suitable samples. The initial steps entail the process of grinding and polishing, which is similar to the techniques used in light microscopy. However, in order to perform EBSD, it is necessary to subject the sample to vibration polishing for at least 32 hours using the ATM Saphir Vibro machine, as shown in **Figure 3-18**.

Figure 3-18: Vibration polishing (ATM Saphir Vibro).

After undergoing vibration polishing, the samples were broken and then cleaned in ethanol with the help of ultrasonic agitation for about 20 minutes. Ultimately, they were attached to the sample holder by means of silver paste. The objective of the cleaning process is to eradicate any remnants of polishing agents and mounting compounds from the surface of the specimen. The equipment used for this technique at the Chair of Casting Research is shown in **Figure 3-19**. The intermediate step is essential since even slight contamination might greatly affect sample analysis using SEM.

Figure 3-19: Ultrasonic Cleaner.

SEM functions by utilizing a concentrated and powerful electron beam to produce multiple signals on the surface of the sample. The beam's diminutive dimensions allow for the scanning of the area under scrutiny. There is a relationship between the length of time that a measurement is taken and the size of the region that is being scanned. The interactions between the beam and the sample provide a comprehensive data about the studied part, encompassing its shape, chemical composition, crystal structure, and grain orientation. Usually, this information is presented on a computer monitor in a two-dimensional format. It is possible to attain resolutions of up to 30,000 times, and it is also possible to make point measurements of chemical composition.

SEM analysis of a sample includes the use of energy dispersive X-ray spectroscopy (EDS) for chemical analysis. This method not only identifies the chemical elements present and their quantities, but also detects the spatial arrangement of these elements within the sample. The approach is based on X-ray microanalysis, which relies on the emission of characteristic X-ray radiation by each chemical element. This radiation is then captured by the EDS detector. By employing this method, it becomes feasible to determine the composition of distinct phases, particles, and contaminants present in the sample. The magnitude of the peaks in an EDS spectrum is directly correlated with the concentrations of the relevant elements in the sample. Moreover, the location of the peaks changes depending on the electron energy used, resulting in variations in characteristic lines depending on the investigative technique performed.

The SEM employed in this investigation is a JOEL JSM-7200F, located at the Department of Metallurgy, as shown in **Figure 3-20**. This equipment is equipped with a backscatter electron detector and a secondary electron detector to capture images. In addition, an Oxford detector was used to do EBSD measurements. Afterwards, the collected data was evaluated using the AZtec software suite.

Figure 3-20: SEM machine.

4 Result

The specimens described were subjected to various testing methods as outlined in the previous chapter (chapter 3). The goal is to determine the effects of alloying components, deformation, and annealing on the mechanical characteristics, namely hardness. The introductory section commences by investigating the impact of alloying elements on the size of grains and the formation of phases. Next, the second part explores the impact of rolling (specifically hot rolling) and annealing on the microstructure. The initial investigations primarily concentrate on the morphology and chemical composition of the sample using (SEM).

4.1 Influence of Cu

The initial phase of this study examines the impact of the alloying element Cu on the grain size. In addition to using the optical microscope for determining grain size, further analyses are carried out. **Figure 4-1** depicts the microstructures acquired following the casting process and subsequent Barker etching. The Al-0.3Mg-1SiC microstructures exhibit significant equiaxed grains. The presence of more than 4 wt.% of Cu leads to the development of tiny grains with equal dimensions.

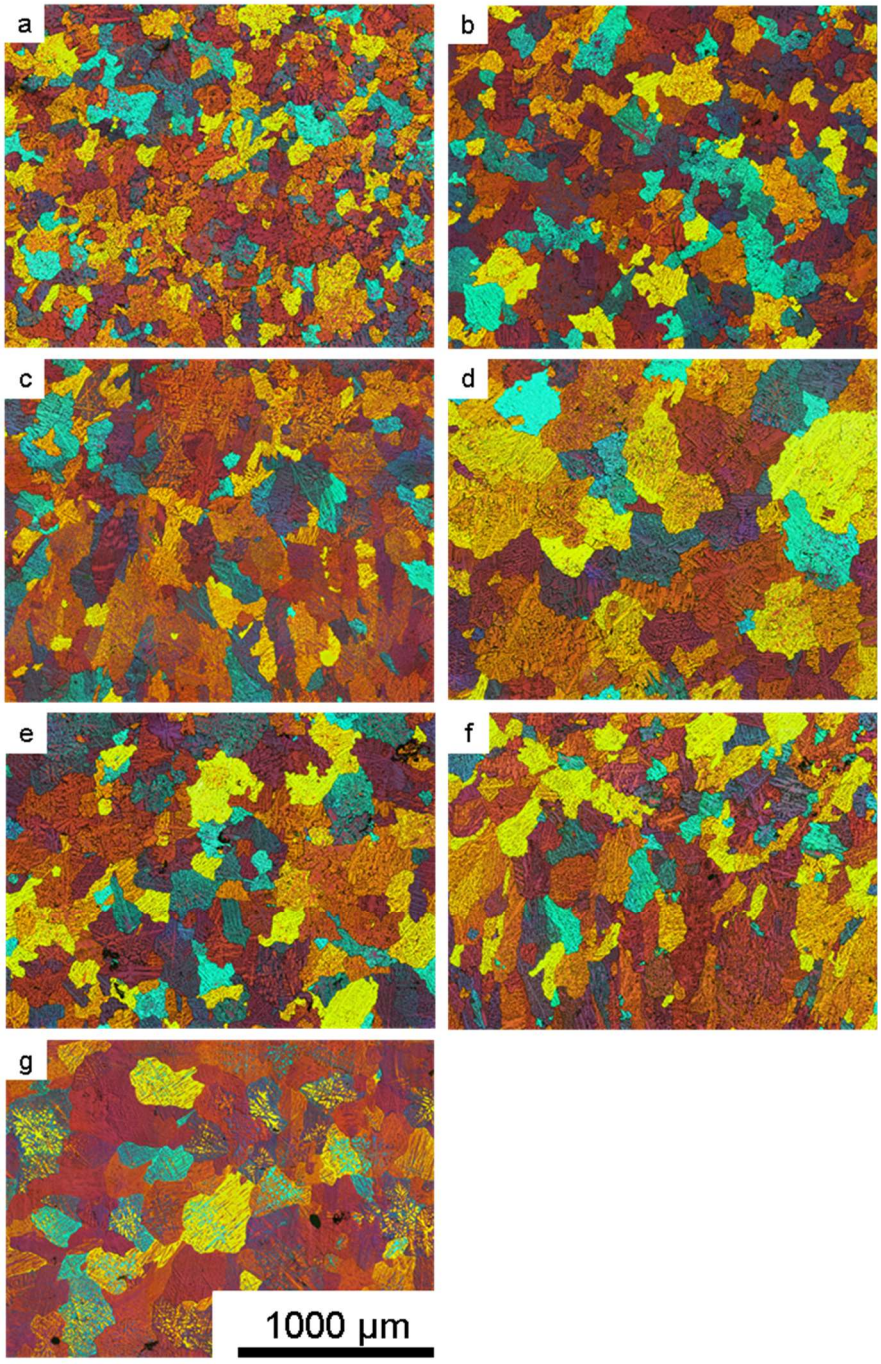

Figure 4-1: Microstructure of the specimens after casting and etching: a) Al-4Cu-0.3Mg, b) Al-4Cu-0.3Mg-1SiC (66.7g SiC), c) Al-4Cu-0.3Mg-1SiC (100g SiC), d) Al-4Cu-0.3Mg-0.7Ag, e) Al-4Cu-0,3Mg-0.7Ag-SiC (66.7g SiC), f) Al-4Cu-0.3Mg-0.7Ag-SiC (100g SiC), g) Al-0.3Mg-1SiC.

Upon submitting the material to a heat treatment at a temperature of 540 °C for a length of 6 hours, the microstructure may be viewed in **Figure 4-2**.

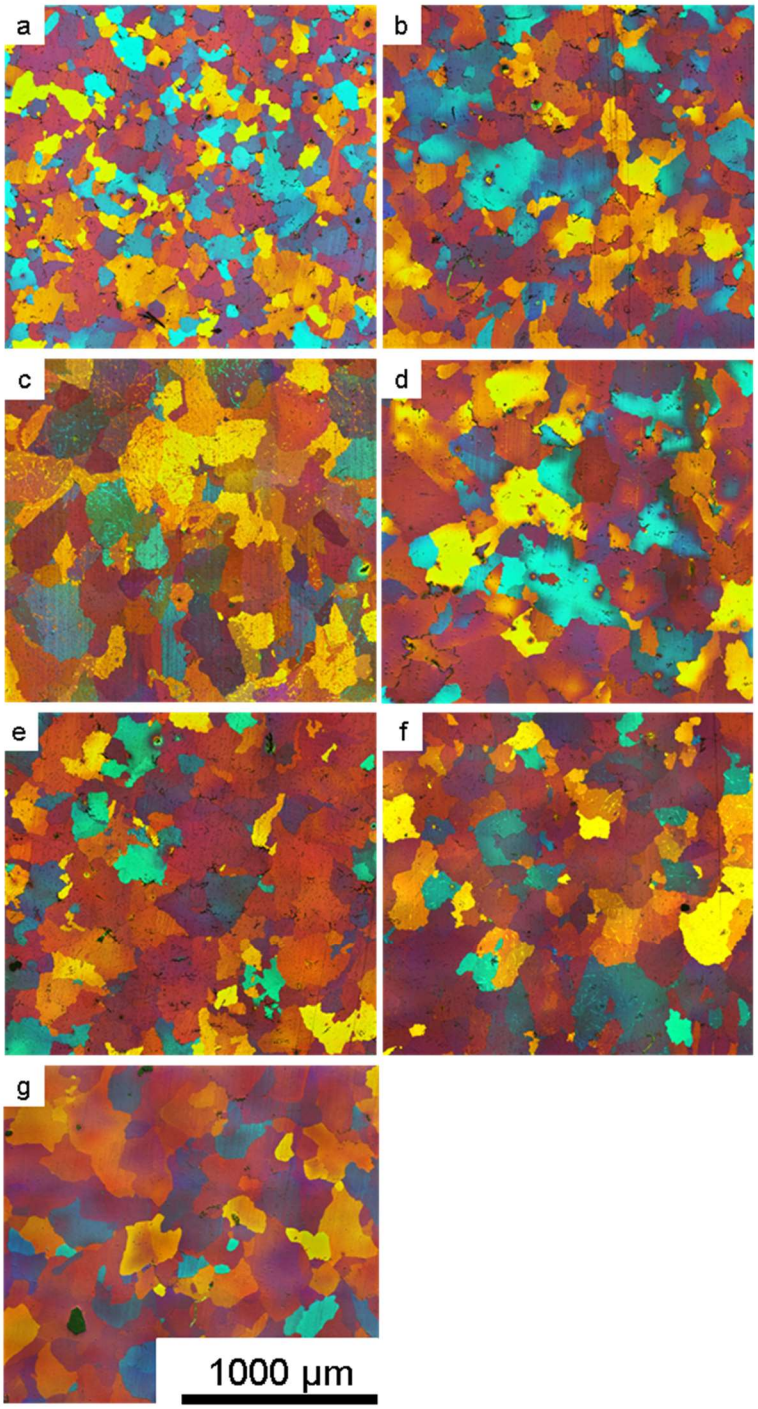

Figure 4-2: Microstructure of the specimens after T4 heat treatment: a) Al-4Cu-0.3Mg, b) Al-4Cu-0.3Mg-1SiC (66.7g SiC), c) Al-4Cu-0.3Mg-1SiC (100g SiC), d) Al-4Cu-0.3Mg-0.7Ag, e) Al-4Cu-0.3Mg-0.7Ag-SiC (66.7g SiC), f) Al-4Cu-0.3Mg-0.7Ag-SiC (100g SiC), g) Al-0.3Mg-1SiC.

4.1.1 Grain size

The measured grain size is depicted in **Figure 4-3**, illustrating a coarse grain size in the alloy without Cu. The disparities in grain size between the two alloys can have substantial ramifications on the characteristics and effectiveness of the materials.

a

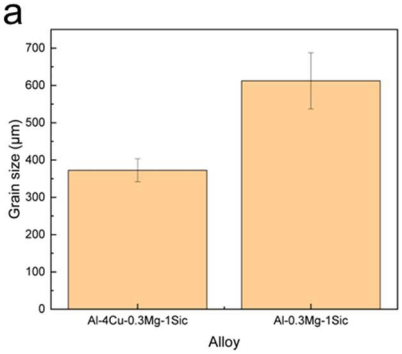

b

Alloy [-]	Grain size [µm]
Al-4Cu-0.3Mg-1SiC (0.667 wt.% SiC)	372±30
Al-0.3Mg-1SiC	612±75

Figure 4-3: Grain size distribution with Cu and without Cu a) diagram b) table with mean and standard deviation.

By contrast, the average grain size of the Al-4Cu-0.3Mg-1SiC sample following T4 solution treatment is less than that in as casting condition. The Al-4Cu-0.3Mg-1SiC sample exhibits a little decrease in grain size. After undergoing solution treatment, the soluble components were dissolved within the Al matrix. Generally, increased grain sizes can result in a decreased ductility in materials. The alloy possessing a greater grain size may exhibit a less ductility in comparison to the alloy possessing a smaller grain size.

a

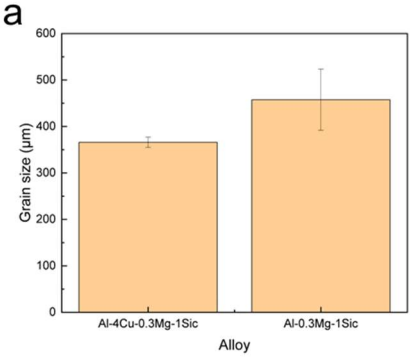

b

Alloy [-]	Grain size [µm]
Al-4Cu-0.3Mg-1SiC (0.667 wt% SiC)	365±11
Al-0.3Mg-1SiC	457±65

Figure 4-4:Grain size distribution after T4 with Cu and without Cu a) diagram b) table with mean and standard deviation

4.1.2 Hardness

Figure 4-5 depicts the Vickers hardness of the Al-4Cu-0.3Mg-1SiC alloy in relation to the measured value of the Al-0.3Mg-1SiC alloy. The absence of Cu diminishes the hardness. The alloy with a smaller grain size (Al-4Cu-0.3Mg-1SiC) may demonstrate a superior strength and toughness compared to the alloy with a larger grain size (Al-0.3Mg-1SiC). This is because of the fact that in the alloy without Cu, the initial GP zone does not form during the solution

treatment, prior to the precipitation of the Al_2Cu (the θ phase responsible for precipitation hardening). Subsequently, the θ-phase was unable to initiate and expand. Due to its tendency to move towards a central point in the lattice and create an intermediate phase, Cu plays a significant role in the formation of GP zones. The content of Cu also influences the formation of these GP zones.

a

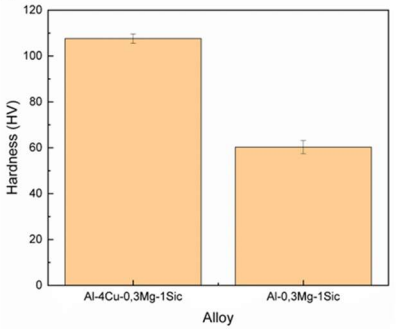

b

Alloy [-]	Hardness [HV]
Al-4Cu-0.3Mg-1SiC (0.667 wt.% SiC)	107.6±2.01
Al-0.3Mg-1SiC	60.28±2.91

Figure 4-5: Hardness after T4 with Cu and without Cu a) diagram b) table with mean and standard deviation.

The alloys undergo T6 heat treatment, which involves ageing at a temperature of 180 °C. **Figure 4-6** displays the hardness curves of these alloys. The absence of Cu results in an earlier appearance of the initial peak in hardness. The addition of Cu significantly increases the hardness of the alloy, making it twice as hard as the alloy without Cu. Indeed, the alloy without Cu did not exhibit any notable precipitation hardening as a result of the absence of the Al_2Cu precipitate.

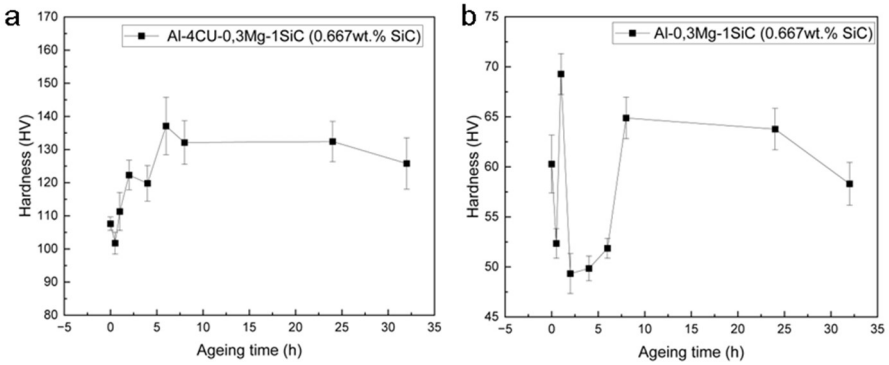

Figure 4-6: The effect of Cu on hardness after T6: a) with Cu b) without Cu.

4.2 Influence of Ag

The impact of the alloying element Ag on grain size is being examined closely. In addition to determine grain size by using the optical microscope, further investigations are performed. The microstructures obtained after casting and Barker etching are shown in **Figure 4-1**. The microstructures of the Al-4Cu-0.3Mg-0.7Ag-1SiC alloy exhibit large-sized grains.

4.2.1 Grain Size

The assessment of grain size was performed on 7 samples in their original as cast state. The grain size determination findings are displayed in **Figure 4-7** and **Figure 4-8**.

This is essential because the absence of grain-refining methods allows for a direct analysis of the impact of the elements. In addition, the use of automated grain size estimation in the SEM, as used in subsequent studies on rolled samples, was not possible in this case due to the large grain size.

Observations indicate that the Al-4Cu-0.3Mg alloy has a lower average grain size. In this scenario, the introduction of Ag leads to a notable augmentation in grain size. The addition of Ag promotes the expansion of the material's grain, potentially counteracting the strengthening effect of solid solution strengthening and leading to a decrease in hardness. This could happen through various means, such as:

Ag, when present at high temperatures, can influence the recrystallization process, leading to the formation of larger grains after heat treatment.

During processing, Ag atoms have the tendency to segregate to grain boundaries, which can lead to a weakening of the grains and an increase in their sensitivity to grain expansion. The occurrence is referred as solute segregation.

a

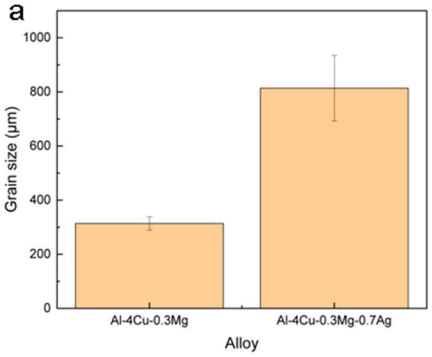

b

Alloy [-]	Grain size [µm]
Al-4Cu-0.3Mg	312±24
Al-4Cu-0.3Mg-0.7Ag	813±121

Figure 4-7: Grain size distribution for with Ag and without Ag after casting with: a) diagram b) table with mean and standard deviation.

Coarsening occurs as a consequence of subjecting the material to a heat treatment process at a temperature of 540 °C for a duration of 6 hours. However, the degree of standard deviation reported in the Al-4Cu-0.3Mg-0.7Ag alloys is comparatively lower than that observed in other alloys.

a

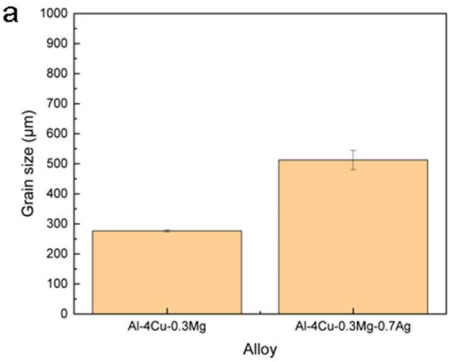

b

Alloy [-]	Grain size [µm]
Al-4Cu-0.3Mg	276±3
Al-4Cu-0.3Mg-0.7Ag	512±32

Figure 4-8: Grain size distribution for with Ag and without Ag after T4 with: a) diagram b) table with mean and standard deviation.

4.2.2 Hardness

The Vickers method was employed to conduct the hardness assessment. After being subjected to solution treatment (T4), the samples were rapidly quenched in water. The measurement outcome is depicted in **Figure 4-9**. The presence of 0.7 wt.% Ag does not increase the hardness greatly.

a

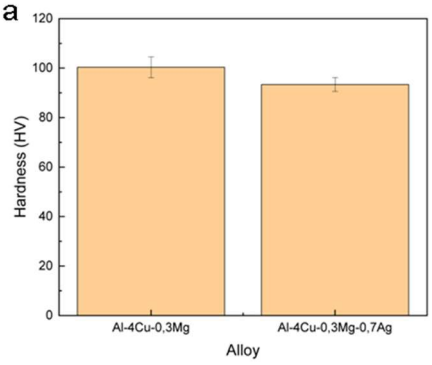

b

Alloy [-]	Hardness [HV]
Al-4Cu-0.3Mg	100.34±4.23
Al-4Cu-0.3Mg-0.7Ag	93.35±2.78

Figure 4-9: Vickers hardness for with Ag and without Ag after T4: a) diagram b) table with mean and standard deviation.

4.3 Influence of SiC

The impact of the SiC nanoparticle on grain size is being examined closely. In addition to determine grain size by using the optical microscope, other analyses are also performed. The microstructures obtained after casting and Barker etching are shown in **Figure 4-1**. The addition of SiC to the Al-4Cu-0.3Mg-0.7Ag alloy results in the formation of smaller grain structures.

4.3.1 Grain size

The assessment of grain size was performed on two samples: one is in its as-cast state and the other is in its T4 state. The grain size determination findings are displayed in **Figure 4-10** and **Figure 4-11**.

Observations indicate that the alloy Al-4Cu-0.3Mg-0.7Ag has a rather large average grain size. The addition of 0.667 wt.% and 1 wt.% SiC in the Al composite results in a process of refining.

a

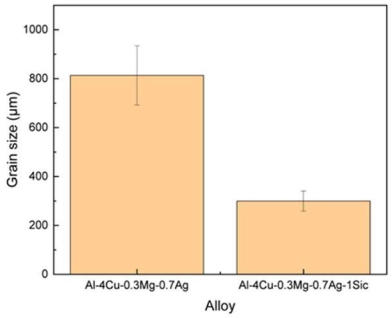

b

Alloy [-]	Grain size [µm]
Al-4Cu-0.3Mg-0.7Ag	813±121
Al-4Cu-0.3Mg-0.7Ag-1SiC (1 wt.%g SiC)	299±41

Figure 4-10:Grain size distribution for with SiC and without SiC after casting with: a) diagram b) table with mean and standard deviation.

a

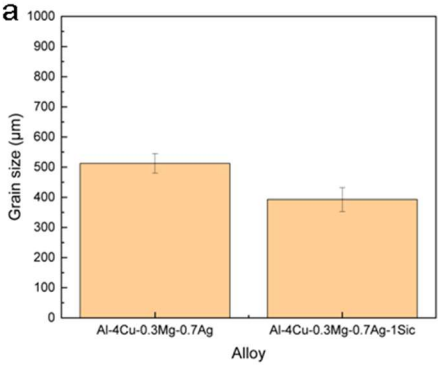

b

Alloy [-]	Grain size [µm]
Al-4Cu-0.3Mg-0.7Ag	512±32
Al-4Cu-0.3Mg-0.7Ag-1Sic (1 wt.% Sic)	392±39

Figure 4-11: Grain size distribution for with SiC and without SiC after T4 with: a) diagram b) table with mean and standard deviation.

4.3.2 Hardness

The Vickers method was employed to conduct the hardness assessment. Following the solution treatment (T4), the samples were rapidly quenched in water. The measurement's outcome is displayed in **Figure 4-12**, indicating a pattern in which the hardness of the alloys increases as the SiC percentage increases. Significantly, the addition of 0.667 wt.% and 1 wt.% SiC in Al-4Cu-0.3Mg led to a higher hardness value compared to the case with the absence of SiC.

a

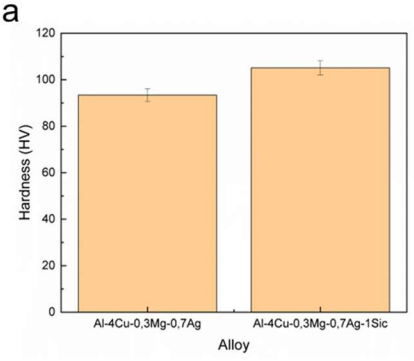

b

Alloy [-]	Hardness [HV]
Al-4Cu-0.3Mg-0.7Ag	93.35 ±2.78
Al-4Cu-0.3Mg-0.7Ag-1SiC	105.1±3.01

Figure 4-12: Vickers hardness for with SiC and without SiC after T4: a) diagram b) table with mean and standard deviation.

The samples were quenched in air after undergoing T6 heat treatment. The measurement outcome is depicted in **Figure 4-13**. An empirical evidence demonstrates that the addition of Ag and SiC leads to a notable enhancement in hardness. On the other hand, the alloy that does not contain Ag exhibits the lowest level of hardness. In the Al-Cu alloy system, precipitation hardening occurs in three stages: solution treatment, quenching, and ageing treatment. To achieve optimal hardness in this system, it is necessary to initiate the formation of the θ Al_2Cu phase and allow it to grow. **Figure 4-6** demonstrates that the absence of Al_2Cu leads to a decrease in hardness in the presence of Cu. The ageing process is not progressing normally. **Figure 4-13** demonstrates that the ageing process of the system is carried out in the typical manner, resulting in the formation of a supersaturated solvent solid with 2 GP zones. From the photos below, it is evident that there is a specific zone where the hardness increases. This zone reaches its greatest hardness in the metastable phase, characterized by a combination of theta prime θ′ and double prime θ′′. Following the metastable phase (θ′′, θ′), the hardness diminishes due to the production of θ, a process referred as over ageing. The precipitates in this region is no longer coherent with the Al matrix and the grain size will become larger. Furthermore, it is possible to observe a tetragonal crystal structure. Additionally, the GP-zone can be represented as follows:

$$SSS \rightarrow GP1 \rightarrow GP2\ (\theta'') \rightarrow \theta' \rightarrow \theta$$

The addition of SiC particles as a reinforcing element considerably influences the ageing behavior of Al-Cu alloys, enhancing their mechanical properties. Age hardening is the specific process responsible for imparting strength to Al-Cu alloys. During the ageing process, Cu atoms gradually disperse from a SSSS to form strengthening phases, such as $CuAl_2$ (also known as the θ phase). The nucleation sites for the precipitation of the $CuAl_2$ phase are provided by inerting SiC particles. As depicted in **Figure 4-13**, this may be due to the fact that the presence of SiC facilitates the preferential locations for the assembly of Cu and Al atoms into precipitates. Accelerated precipitation kinetics may lead to a reduction in the required ageing time for the Al-Cu-SiC composite to achieve its maximum hardness. Unlike the Al-Cu alloy without reinforcement, the addition of SiC particles promotes the formation of smaller and more uniformly distributed $CuAl_2$ precipitates. Finer precipitates typically yield stronger findings as they are more effective in impeding dislocation movement.

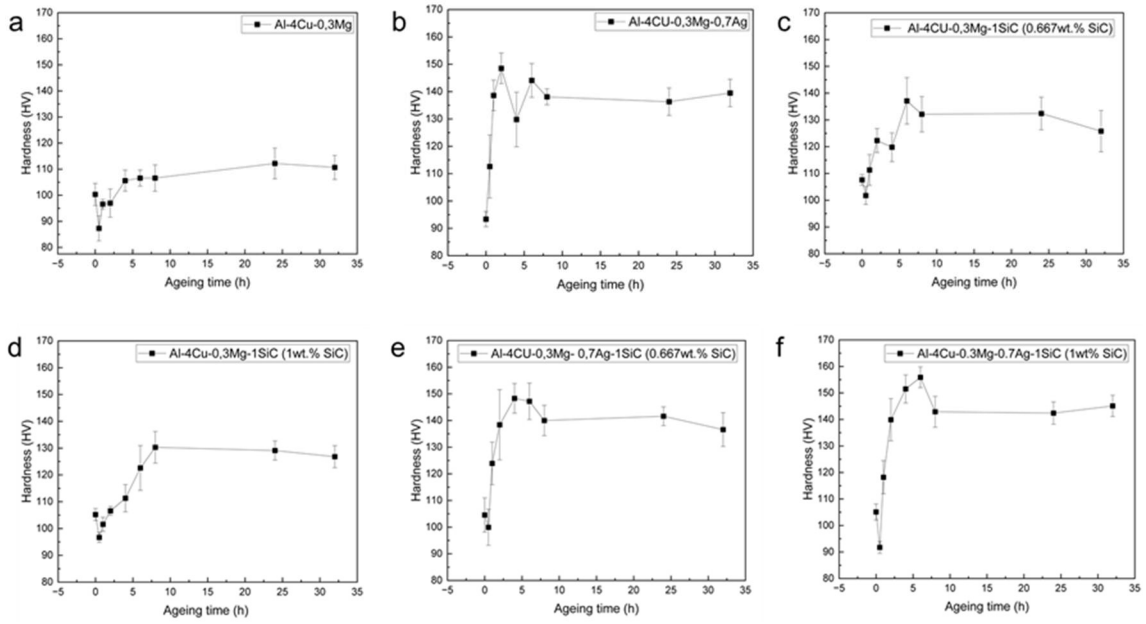

Figure 4-13: Ageing hardness curves after T6 heat treatment.

4.4 Influence of hot rolling

The second aim of this study focuses on investigating the effects of hot rolling on the microstructure and precipitates created after a T4 heat treatment. Three alloys (Al-4Cu-0.3Mg, Al-4Cu-0.3Mg-0.7Ag, and Al-4Cu-0.3Mg-0.7Ag-1SiC) were subjected to rolling. Following the rolling process, the grain size of the specimens cannot be evaluated using an optical microscope. Consequently, EBSD has been utilized for this study. The microstructure achieved following hot rolling is depicted in **Figure 4-14**. The observable precipitates exhibit a consistent size distribution. Specifically, **Figure 4-14** illustrates that the alloy containing SiC displays precipitates with a more uniform distribution and a higher number density.

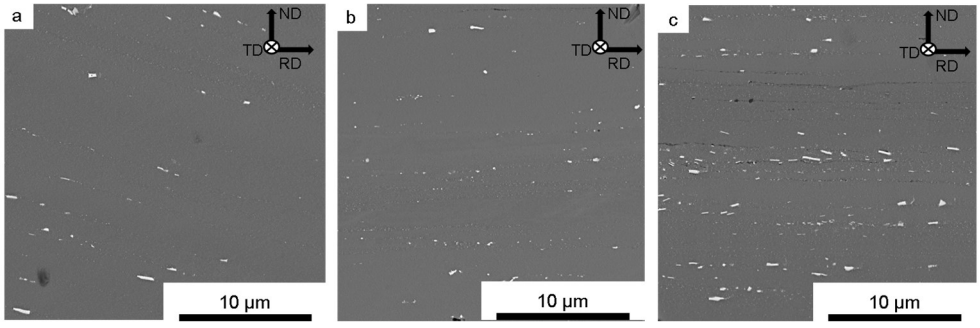

Figure 4-14: Microstructure 1 mm samples after rolling: a) Al-4Cu-0.3Mg b) Al-4Cu-0.3Mg -0.7Ag c) Al-4Cu-0.3Mg -0.7Ag-1SiC.

Hot rolling involves subjecting the material to plastic deformation, resulting in the refining grain structure. Generally, materials that experience more deformation, like the 1 mm sample, will have a finer grain structure compared to materials that experience less deformation, like

the 5 mm sample. Smaller grains typically lead to a greater hardness because they enhance the strengthening effects at the boundaries between grains.

4.4.1 EBSD analysis

The specimens, namely Al-4Cu-0.3Mg, Al-4Cu-0.3Mg-0.7Ag, and Al-4Cu-0.3Mg-0.7Ag-1SiC, underwent hot rolling processes resulting in thicknesses of 5 mm and 1 mm. The SEM has been used to investigate the microstructure and texture of these specimens, which have a smaller grain size compared to their as-cast state before rolling.

EBSD investigation provided texture distribution maps for hot-rolled sheets of Al-Cu-Mg alloys, as shown in **Figure 4-15**.

The 5 mm samples exhibit an elongated microstructure along the rolling direction (RD), as evidenced by the SEM images. Nevertheless, following the ultimate reduction to a thickness of 1 mm, a refined arrangement with a relatively uniform alignment becomes apparent.

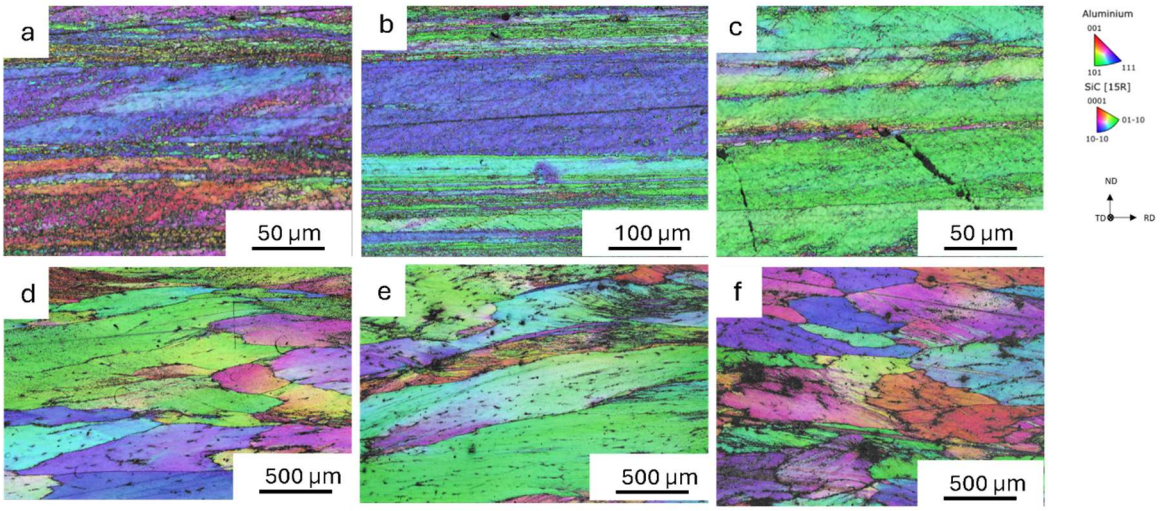

Figure 4-15: IPF maps of the 1 mm and 5 mm specimens (a) and (d) Al-4Cu-0.3Mg, (b) and (e) Al-4Cu-0.3Mg-0.7Ag, (c) and (f) Al-4Cu-0.3Mg-0.7Ag-1SiC.

According to the EBSD pictures and hardness curves, the alloy that has been rolled to a thickness of 5 mm and contains SiC exhibits a much higher hardness compared to other alloys that have been rolled to a thickness of 1 mm. It pertains to the increased hardness exhibited by the material, which is accompanied by alterations in the microstructure and texture along RD, as observed in the EBSD images.

By employing inverse pole figure (IPF) analysis, it is possible to examine rolled samples and gain valuable information about crystal orientation and texture. Within this particular environment, individual crystals display a homogeneous color, indicating a persistent alignment. Although there is a little tendency for the crystals to align in a certain direction after the first rolling pass, they nevertheless maintain large and consistent grain sizes. Within the local area, one may detect the presence of large elongated grains and very fine microstructures in the close proximity to each other.

The thorough analysis of the sample textures (pole figure (PF)), shown in **Figure 4-16** and **Figure 4-17**, strengthens the previously observed patterns. The grain orientation in samples with a thickness of 1 mm is primarily aligned along the <111> direction. The only specimen with a deviating grain orientation in the <101> direction is the 1 mm sample of Al-4Cu-0.3Mg-0.7Ag. This variation can be ascribed to either the possible recrystallization or the unique deformation mechanisms that take place during the hot rolling process. Similarly, the 5 mm specimens also show a propensity for the <111> orientation.

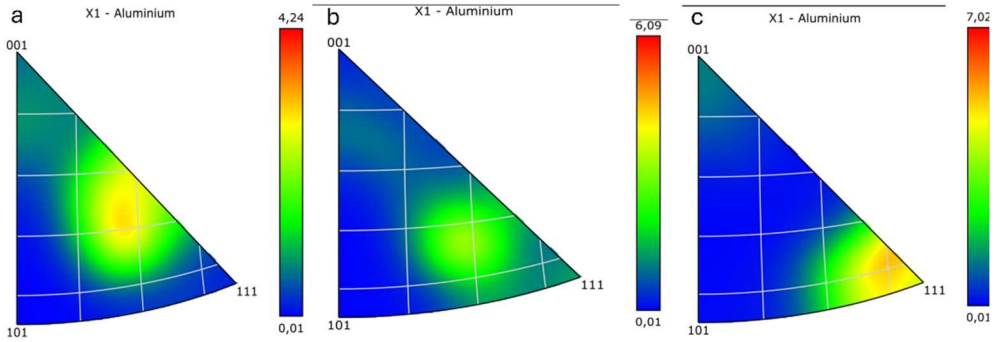

Figure 4-16: Texture analysis (PF) of 1 mm hot rolled samples: a) Al-4Cu-0.3Mg, b) Al-4Cu-0.3Mg-0.7Ag, c) Al-4Cu-0.3Mg-0.7Ag-1SiC.

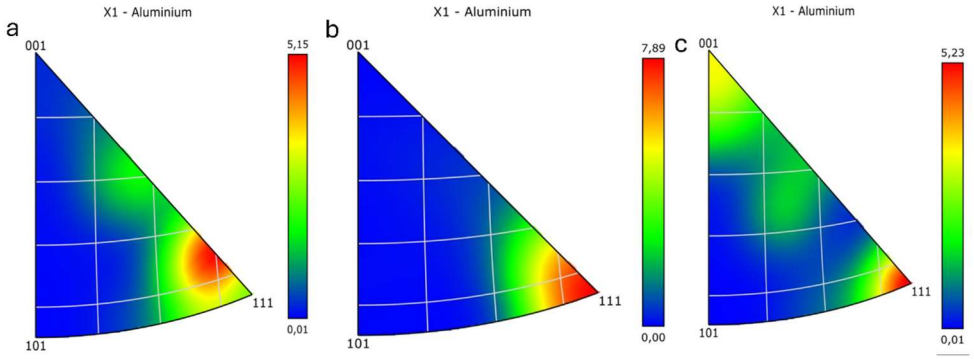

Figure 4-17: Texture analysis (PF) of 5 mm hot rolling specimens: a) Al-4Cu-0.3Mg, b) Al-4Cu-0.3Mg-0.7Ag, c) Al-4Cu-0.3Mg-0.7Ag-1SiC.

4.4.2 Grain size distribution

Figures 4-18 and **4-19** depict the graphical evaluation of the determined grain sizes of the Al phase using EBSD in a SEM. Multiple ranges were considered for each sample.

According to the result of grain size distribution, the samples with 5 mm can show the greater variation compared with 1 mm, therefore it can be seen that the finer grain size, which leads to a higher hardness.

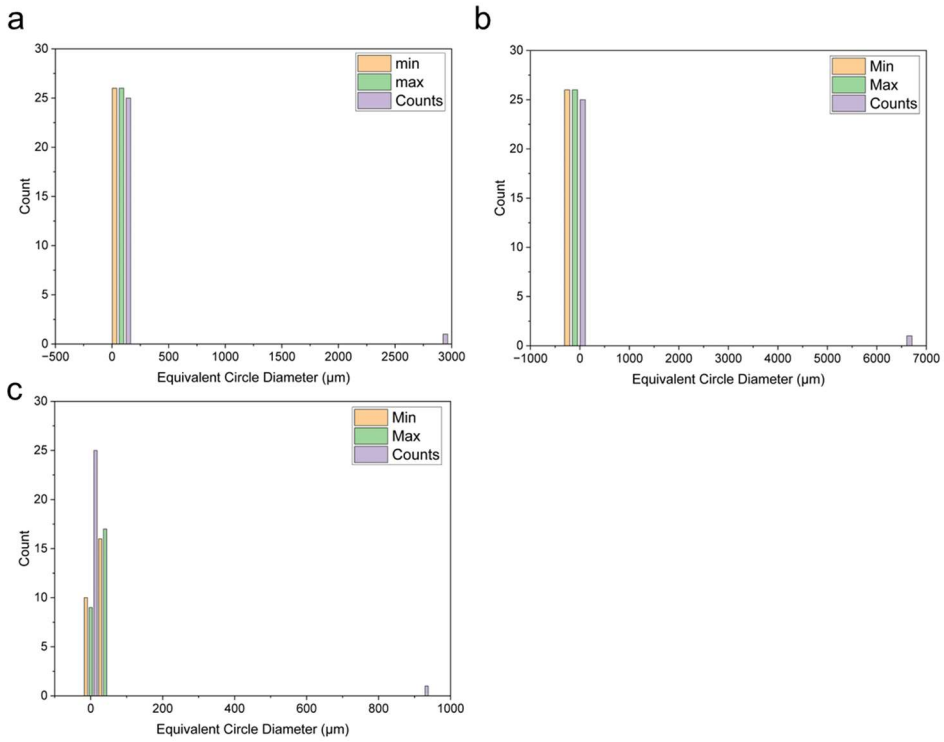

Figure 4-18: Grain size distribution of the samples after 1 mm rolling: a) Al-4Cu-0.3Mg, b) Al-4Cu-0.3Mg-0.7Ag, c) Al-4Cu-0.3Mg-0.7Ag-1SiC.

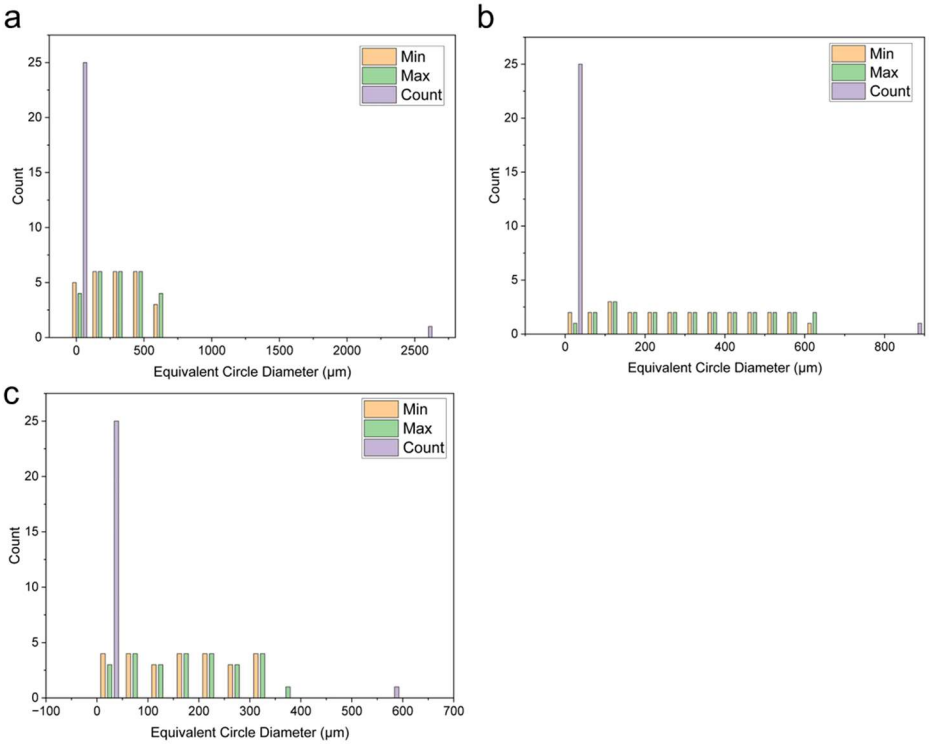

Figure 4-19: Grain size distribution of the samples after 5 mm rolling: a) Al-4Cu-0.3Mg, b) Al-4Cu-0.3Mg-0.7Ag, c) Al-4Cu-0.3Mg-0.7Ag-1SiC.

4.4.3 SEM EDS analysis

This study employs EDS analysis to observe the elements and enables a quantitative examination of their distribution within the defined area. Nevertheless, it is important to mention that this approach does not yield quantitative measurements for the composition. **Figure 4-20** displays the EDS maps of the Al-4Cu-0.3Mg sample with a thickness of 1 mm, as well as the distribution of elements during the hot rolling of the alloy. The spectrum analysis of the entire region indicates that it consists of 74 at.% Al, 16.81 at.% Cu, 4.70 at.% Fe, and 0.55 at.% Ni.

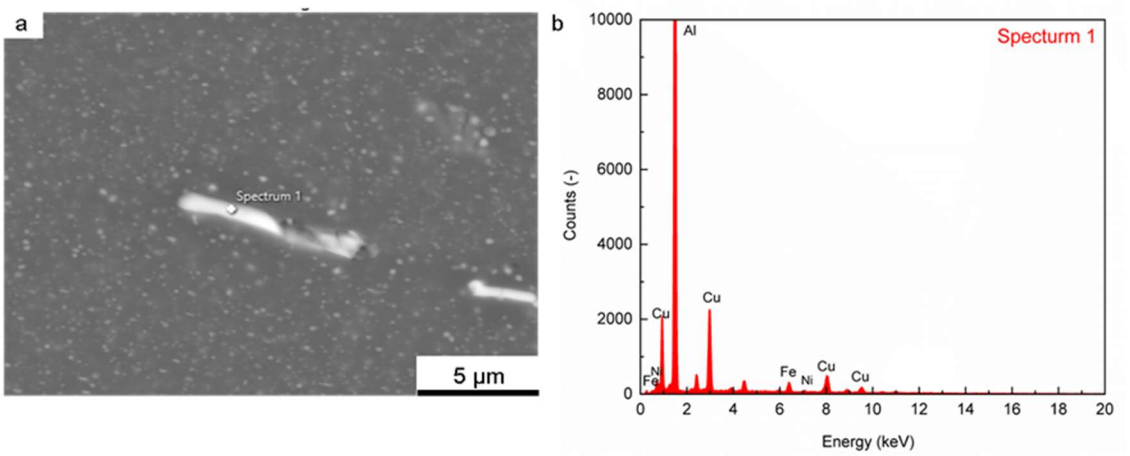

Figure 4-20: (a) SEM image, (b) EDS spectrum taken from the whole region.

Figure 4-21 shows EDS maps of the Al-4Cu-0.3Mg-0.7Ag-1SiC sample with a thickness of 1 mm. The maps illustrate the distribution of elements in the alloy after undergoing hot rolling. The first spectrum for the entire region shows that 59.06 at. % of the composition is Al, 9.58 at. % is Fe, and 31.35 at. % is Cu. The second spectrum for the entire region shows that 53.80 at. % is Al, 0.27 at. % is Si, 11.01 at. % is Fe, 0.38 at. % is Ni, and 34.54 at. % is Cu. The spectrum 3 corresponds to the composition of 69.95 at. % Al, 7.06 at. % Fe, 0.38 at. % Ni, and 22.61 at. % Cu. **Figure 4-21e** clearly illustrates that SiC is situated adjacent to the grain boundaries.

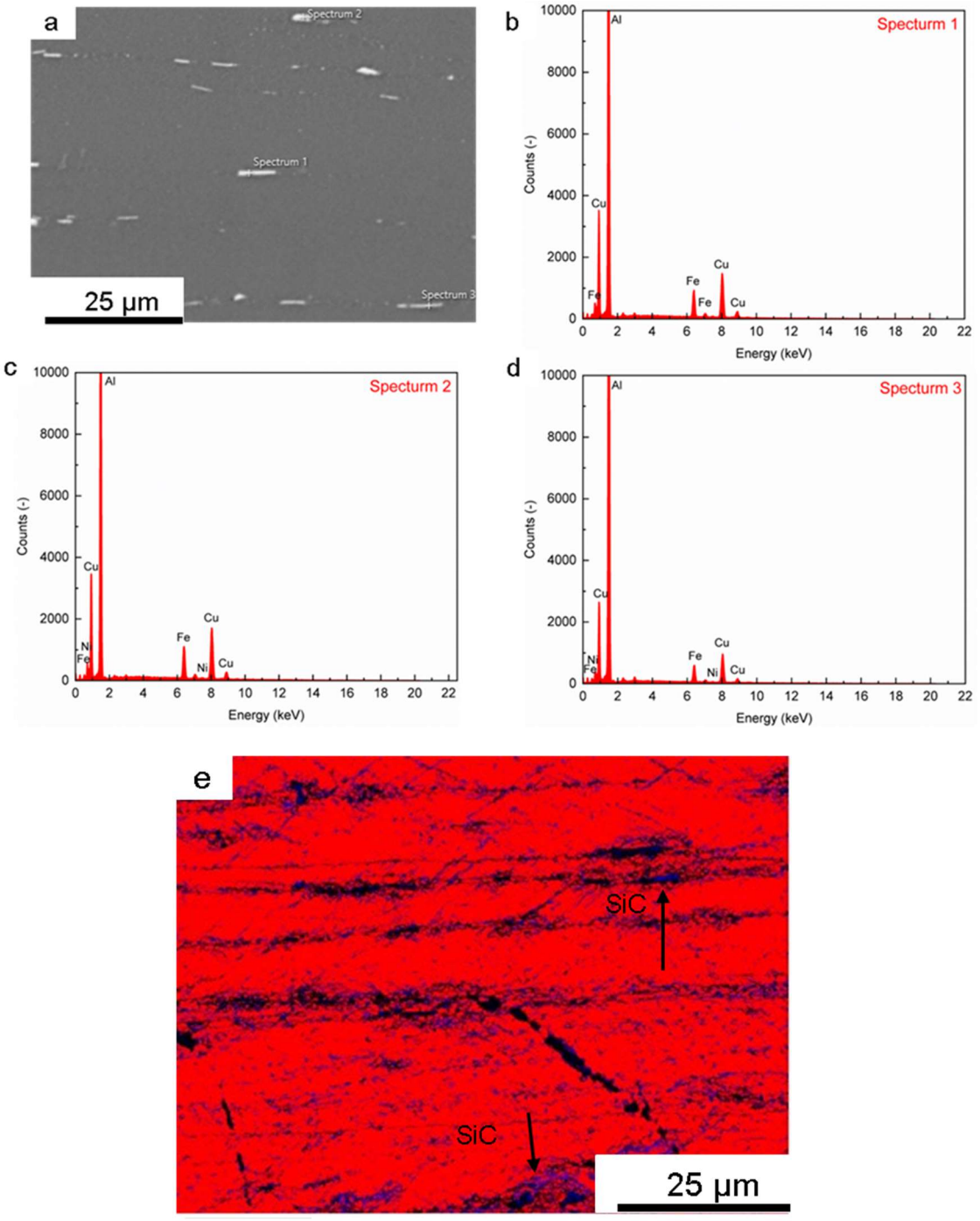

Figure 4-21: (a) SEM image, (b) EDS spectrum1 taken from the whole region, (c) EDS spectrum 2, (d) EDS spectrum 3, *(e) distribution of SiC along grain boundaries.*

Figure 4-22 displays the EDS phase maps (red: Al, blue: SiC) of the Al-4Cu-0.3Mg-0.7Ag-1SiC sample with a thickness of 5 mm, together with the dispersion of the SiC particles following the hot rolling.

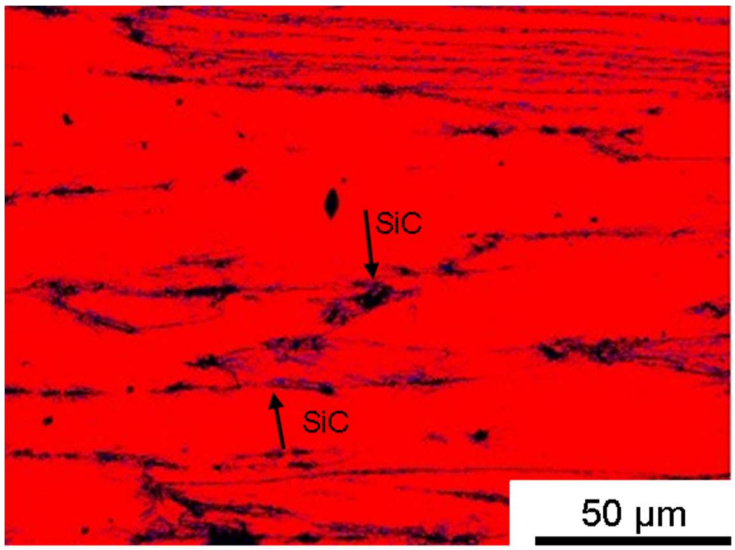

Figure 4-22: Distribution of SiC after hot rolling up to 5 mm.

4.4.4 Hardness

Initially, the rolled samples undergo analysis using Vickers hardness testing, and the hardness result is depicted in **Figure 4-23**.

According to the findings of this experiment, the unrolled samples exhibit a high level of hardness. However, the hardness reduces after rolling them to 5 mm and 1 mm, respectively. This result indicates that the 1 mm sample exhibits a greater level of hardness compared to the 5 mm sample. The reason for this is that in samples with a thickness of 1 mm, there is a smaller grain size which results in a higher level of hardness. Furthermore, the subsequent paragraph also provides a concise explanation on the factors that contribute to the reduction in hardness.

Hot rolling induces a certain level of recovery and maybe recrystallization, depending on the initial grain size and rolling temperature (in this case, 340 °C).

Reorganization of dislocations inside the grains leads to a minor reduction in the dislocation density, which is a consequence of the recovery process. Work hardening induces the formation of dislocations, which contributes to the increase in hardness of materials. Nevertheless, the process of recovery can partially counteract this effect and result in a reduction in material hardness. The presence or absence of precipitates after cooling will be determined by the cooling rate at which the material cools down following hot rolling. If the material remains to be dissolved, it will have a softer texture compared to its original pre-rolled state.

The addition of Ag (0.7 wt.%) in the Al-4Cu-0.3Mg alloy is unlikely to have a substantial effect on the previously described softening behavior. Nevertheless, the impact of Ag on hardness is contingent upon its interaction with Cu during the cooling process.

Ag may have a negligible impact on the overall hardness if it forms a precipitate or remains in a solid solution.

Ag may alter the co-precipitation process of $CuAl_2$ precipitate during cooling, potentially leading to slightly altered characteristics of the precipitate, which could have an effect on its hardness.

The presence of 1 wt.% SiC particles in the Al-Cu-Mg-0.7Ag-1SiC alloy does not directly cause softening during the hot rolling. However, it can impact the overall hardness in the subsequent manners:

The 1 wt.% SiC particles may not significantly increase the overall hardness of the composite, despite the exceptional hardness of these particles. The decrease in hardness may be attributed to the influence of SiC particles on grain boundaries during hot rolling, which finally results in a complete recrystallization.

Hot rolling at 340 °C can partially dissolve existing $CuAl_2$ precipitates. Considering the gradual cooling process carried out at ambient temperature, there is a possibility of re-precipitation of $CuAl_2$. Unlike the initial pre-rolled state, this re-precipitation process may not occur on a large scale or produce precipitates with the same size and distribution. This could potentially result in a decrease in hardness.

a

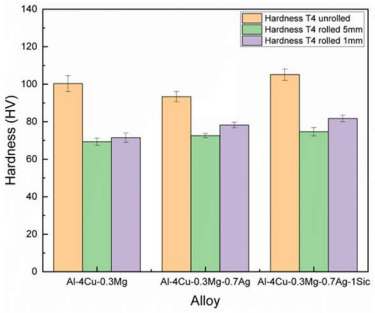

b

Alloys	Hardness (HV)		
	T4	T4 (5mm)	T4 (1mm)
Al-4Cu-0,3Mg	100.34±4.23	69,28±2,03	71,47±2,41
Al-4Cu-0,3Mg-0,7Ag	93.35±2.78	72,59±1,10	78,21±1,50
Al-4Cu-0,3Mg-0,7Ag-1SiC (1 wt.% SiC)	105.1±3.01	74,64±2,22	81,70±1,67

Figure 4-23: a) The diagram of the comparison of the T4 unrolled with the T4 rolled samples, b) table with mean and standard deviation.

4.5 Influence of annealing at 350 °C

The rolled specimens with a thickness of 1 mm were subjected to annealing at a temperature of 350 °C for different durations (1 hour, 2 hours, 3 hours, 4 hours). Subsequently, the hardness was quantified, as depicted in **Figure 4-24**. The dispersion and arrangement of reinforcing phases, such as SiC particles, inside the Al matrix may exhibit a non-uniformity across the material. The total hardness of the alloy can be affected by variations in the distribution of these strengthening phases. The 1 mm sample is likely to exhibit a more homogeneous dispersion of reinforcing phases, resulting in an increased overall hardness. Furthermore, the subsequent paragraph contains an additional clarification.

The process of annealing at a temperature of 350 °C causes the alloys to become softer by allowing dislocations to reorient and regain their original structure.

The presence of Ag in the Al-4Cu-0.3Mg-0.7Ag alloy is likely to contribute to the initial increase in hardness (after 1 hour) due to precipitation hardening. Ag atoms have the ability

to detach from their solution and create small particles that hinder the movement of dislocations, thus increasing the hardness of the material.

The SiC particles in the Al-4Cu-0.3Mg-0.7Ag-1SiC alloy may exhibit a slower precipitation rate in the rearrangement process during annealing. Nevertheless, when subjected to extended annealing durations (2, 3, and 4 hours), the likelihood of effectively capturing dislocations increases, leading to the presence of the peak hardness.

Overall, the primary reason for the early hardness advantage of the Al-4Cu-0.3Mg-0.7Ag alloy is likely to due to the precipitation hardening involving Ag. Nevertheless, when subjected to extended annealing periods, the Al-4Cu-0.3Mg-0.7Ag-1SiC alloy demonstrates an enhanced hardness as a result of the synergistic effects of precipitation hardening and immobilization caused by SiC particles.

a

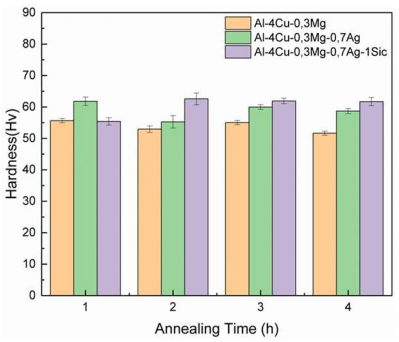

b

Alloys	Hardness [HV]			
	1h	2h	3h	4h
Al-4Cu-0,3Mg	55,63±0,66	52,93±1,04	55,03±0,63	51,64±0,65
Al-4Cu-0,3Mg-0,7Ag	61,81±1,31	55,27±1,97	59,97±0,79	58,69±0,81
Al-4Cu-0,3Mg-0,7Ag-1SiC (1 wt.% SiC)	55,41±1,20	62,55±1,88	61,93±0,86	61,71±1,30

Figure 4-24: a) The diagram of the comparison of annealing samples, b) table with mean and standard deviation.

5 Discussion

5.1 The impact of SiC

Initially, the assessment of grain sizes using the linear intercept approach revealed that the presence of SiC nanoparticles in the Al alloys resulted in a smaller average grain size compared to the Al alloys without SiC. The presence of columnar grains in the edge of the microstructures may be attributed to a rapid cooling rate. The solidification initiates at the periphery and progresses towards the center.

The presence of Cu in the Al-4Cu-0.3Mg alloy affects the measured grain sizes and hardness. When comparing with the samples with 66 g and 100 g of SiC, it was seen that the samples with 100 g SiC has a higher hardness. However, it should be noted that increasing the SiC concentration may not necessarily affect the mechanical properties. By increasing the proportion of SiC, the hardness can be enhanced through dispersion strengthening and Orowan strengthening mechanisms. This results in the particles being positioned closer together, leading to a more effective pinning effect on dislocations. Dislocations can only bypass the SiC particles by bending around them. This bending process necessitates a greater amount of energy, so intensifying the material's ability to resist deformation and hence enhance its hardness. As previously stated, a significant SiC concentration might pose challenges in processing and fabricating Al alloy due to difficulties like inadequate wetting and heightened tool wear. Additionally, the phenomenon of agglomeration can occur, where SiC particles tend to aggregate at large volume fractions. This aggregation diminishes their ability to operate as dispersed strengtheners and has the potential to create areas of weakness in the material. Excessive amounts of SiC can result in the formation of a material that is extremely hard but also prone to brittleness. This can be unfavorable in certain situations where a certain level of ductility is still necessary. Hence, there exists an optimized proportion of SiC that maximizes hardness while simultaneously preserving other favorable attributes such as workability and toughness. The optimized proportion of SiC is contingent upon the precise composition of the Al alloy, the intended use, and the selected processing technique.

5.2 The impact of heat treatment

The Al-4Cu-0.3Mg alloys' grain sizes and hardness were significantly affected by a T4 solution treatment.

The alloys' hardness is enhanced through T4 solution treatment and natural ageing. The increase in hardness primarily results from the nucleation and growth of GP zones. The alloy undergoes a solution treatment at a temperature of 540 °C. The elevated temperature causes the majority of the Cu and Mg present in the alloy to dissolve into the Al matrix. The process of solution treatment is then accompanied by a quick quenching procedure. The quick quenching process hinders the reorganization of the dissolved Cu and Mg atoms into their original equilibrium phases. However, they are confined within a highly concentrated solid solution inside the Al matrix. After the quenching and subsequent storage at room temperature, known as natural ageing, the SSSS does not retain total stability. Cu and Mg atoms undergo precipitation from the solution and aggregate into tiny clusters known as Guinier-Preston (GP) zones. These zones exhibit high concentrations of Cu and Mg, but lack a clearly defined crystal lattice. The existence of these GP zones in the Al matrix impedes the displacement of dislocations (imperfections in the crystal lattice). Dislocations facilitate the deformation of the metal, so restricting their mobility results in an increase in the material's

hardness. This is the primary cause of the heightened hardness following T4 solution treatment. T4 solution treatment generally requires a shorter or no ageing period compared to T6 treatment, leading to the formation of smaller and less densely distributed GP zones. This leads to a decreased level of hardness in comparison to T6 treatment. Essentially, the development and expansion of GP zones during the natural ageing following T4 solution treatment is the primary mechanism responsible for the enhanced hardness observed in Al-Cu-Mg alloys.

Upon examination in its original state, it was seen that the Al-4Cu-0.3Mg-0.7Ag alloy had large grain sizes. The greater grain size observed may be mainly attributed to the solidification process. In addition to this, other factors such as casting temperature and the presence of impurities can also influence the grain size and lead to a large grain size.

When comparing the hardness of T4 specimens to T6 specimens, first the hardness decreases, then it increases until reaching the peak hardness. After that, the hardness decreases during the over-ageing process. On the basis of the Al-Cu diagram and TTT diagram, along with the microstructure evolution at peak aged conditions, the peak hardness can result from the formation of finer precipitates. However, with over-ageing, precipitates with a fine distribution transforms into those with a coarser distribution. Therefore, the hardness begins to decrease.

The alloys including Ag and SiC exhibit a higher hardness than the reference alloy (Al-4Cu-0.3Mg) according to the hardness curves. Additionally, the removal of Cu in the alloy leads to a decrease in hardness. Consequently, it is anticipated that the mechanical properties of the Al-Cu-Mg based alloy can be enhanced by including Ag and SiC.

5.3 The impact of rolling

This study utilized hot rolling to process the specimens of Al-4Cu-0.3Mg, Al-4Cu-0.3Mg-0.7Ag, and Al-4Cu-0.3Mg-0.7Ag-1SiC. The results indicate that the hardness of Al-4Cu-0.3Mg-0.7Ag-1SiC, with the addition of Ag and SiC, is higher than the reference material. However, the hardness decreases during rolling, reaching a minimum at 5 mm and 1 mm, as depicted in **Figure 5-1**.

Hot rolling at a temperature of 340 °C can induce material softening, resulting in a decrease in hardness compared to the state before rolling. This phenomenon of softening is a result of various metallurgical processes, including the rearranging of the crystal lattice within the metal, known as recovery. Dislocations, which are structural defects within the crystal lattice, can undergo a partial annihilation or repositioning, resulting in a decrease in their total concentration and the internal strain. As a result, the material's strength and hardness decrease, and the deformed grains are completely replaced by new, strain-free grains during recrystallization. The newly formed grain structure is generally less rigid than the previous one, leading to a decrease in hardness.

The addition of Mg into an Al alloy containing 4 wt.% Cu (Al-4Cu) can result in the formation of a new S-phase, in addition to the existing θ phase. This can be detected using differential scanning calorimetry (DSC). In addition, the existence of Mg causes a minor delay in the creation of first clusters of atoms (GP zones) during the early stages of the ageing process. It has been found by Heinl Leon [113] in the three alloys that the Al-4Cu-0.3Mg-0.7Ag alloy has the highest number density and the lowest Porod radius.

The coexistence of Ag and Mg in the alloy further accelerates the production of the GP zones, causing them to occur at an earlier stage. Nevertheless, the development of the

clusters occurs at a later stage in comparison to the Al-4Cu alloy. Both Mg and Ag have an impact on the creation of the GP zones. The presence of Ag together with Mg in the alloy again shifts the formation of the GP zones to an earlier stage. However, the formation of the clusters takes place somewhat later compared to the Al-4Cu alloy. It indicates that both Mg and Ag have an influence on the formation of the GP zones.

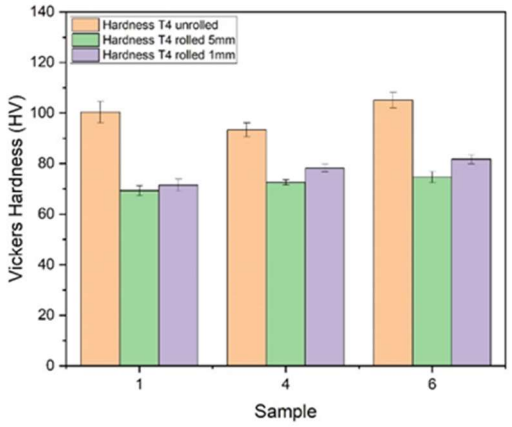

Figure 5-1: The comparison of the hardness among T4-unrolled, T4-5 mm and T4-1 mm hot rolled at 340 °C.

5.4 The impact of annealing

The alloys Al-4Cu-0.3Mg and Al-4Cu-0.3Mg-0.7Ag exhibit a great hardness after hot rolling. However, this hardness decreases after the annealing process due to following possible causes, such as changes in the microstructure, precipitation processes, and the development of dislocations within the material. Alloying elements, such as Cu, Mg, and Ag, in the Al alloy can cause the development of precipitates when annealing occurs.

Precipitation hardening is a method of increasing strength, where the total hardness can be affected by the size, distribution, and composition of the precipitates. The annealing process undoubtedly induces alterations in the precipitate structure, leading to a reduction in hardness. During the annealing, the size of the grains in the material tends to increase as a result of either recrystallization or grain growth. Typically, larger grains are correlated with a reduced hardness.

The use of SiC implies the potential for precipitation hardening. During the process of annealing, the alloy can experience a deliberate formation of small particles, which can serve as barriers to the movement of dislocations, resulting in an enhanced level of hardness. The presence of Cu, Mg, Ag, and SiC in the material results in the utilization of several methods to enhance its strength, such as solid solution strengthening, precipitation strengthening, and dispersion strengthening.

In conclusion, it is likely that the hardness of the Al-4Cu-0.3Mg-0.7Ag alloy is due to precipitation hardening. With increasing annealing duration, the Al-4Cu-0.3Mg-0.7Ag-1SiC alloy exhibits an enhanced hardness as a result of both precipitation hardening and pinning effect caused by SiC particles.

6 Summary and outlook

This study investigates the impact of several conditions on the properties of Al-Cu-Mg based alloys. The criteria comprise the existence of specific elements (Cu, Mg, Ag, and SiC). The samples utilized in this study are in their original as cast state, subsequent to undergoing T4 treatment, T6 treatment, hot rolling, and annealing treatment. The impact of these factors on the microstructure and hardness in the T4 (540 °C for 6 hours), T6 (180 °C), hot rolling (340 °C), and annealing at 350 °C conditions were investigated by using both an optical microscope and SEM as well as hardness measurement.

The main conclusions can be drawn as follow:

Effect of alloying elements

In order to elucidate the impact of various alloying elements on grain size, a method known as the linear intercept method was initially employed.

The process consisted of engraving Al-Cu alloys in two conditions: in their original as cast state and after undergoing a T4 solution treatment. Furthermore, the hardness was also measured in these two conditions. It was found that the addition of 4 wt.% Cu had a substantial impact on both grain size and hardness. According to the hardness curves after T6, it is evident that the alloy without Cu is unable to produce the Al_2Cu phase, also known as the θ phase, which is responsible for precipitation hardening. Furthermore, it can be demonstrated that the T4 solution treatment can result in a decrease of the grain size. However, this alloy without Cu still possesses the lowest level of hardness. As the concentration of Cu increases, the size and aggregation of the metal's precipitates also increase. This phenomenon occurs due to the presence of Cu, which facilitates the mobility of these particles within the metal.

The addition of Ag was often expected to result in improved mechanical properties. However, in this thesis, in contrast to expectations, the alloy with Ag exhibited a lower hardness and a larger grain size compared to the alloy without Ag, both in as casting condition and after T4 solution treatment. Furthermore, the grain size increases after T4 solution treatment. In this scenario, it should be noted that the addition of Ag does not necessarily result in an increase in hardness. The specific mechanisms at play are determined by the material system and processing conditions. The incorporation of Ag results in a significant increase in the grain size. The presence of Ag facilitates the enlargement of the material's grain, potentially counterbalancing the reinforcement effect of solid solution strengthening and resulting in a reduction in hardness. This can occur through many mechanisms, such as the impact on the recrystallization and the tendency of Ag to accumulate at grain boundaries, which can result in the weakening of the grains and thereby a reduction in hardness.

Effect of SiC

SiC is a type of nanoparticles that are incorporated into Al alloys in order to enhance their mechanical properties. In this sense, two distinct weight percentages of SiC, namely 0.667 wt.% and 1 wt.% were employed. The study revealed that SiC with a concentration of 1 wt.% exhibited a higher hardness. The Al-Cu-Mg alloys possess favorable characteristics for aerospace applications; however, their inadequate hardness and strength, together with their vulnerability to corrosion, restrict their utilization in this industry. The mechanical properties of Al-Cu-Mg alloys can be enhanced through heat treatment, namely by employing the T6

treatment. Consequently, the T6 treatment was conducted on the following alloys: Al-4Cu-0.3Mg, Al-4Cu-0.3Mg-0.667SiC, Al-4Cu-0.3Mg-1SiC, Al-4Cu-0.3Mg-0.7Ag, Al-4Cu-0.3Mg-0.7Ag-0.667SiC, Al-4Cu-0.3Mg-0.7Ag-1SiC, and Al-0.3Mg-0.667SiC. An empirical research clearly shows that the addition of Ag and SiC significantly improves hardness. Conversely, the alloy without Cu demonstrates the lowest hardness. Precipitation hardening in the Al-Cu alloy system involves three distinct stages: solution treatment, quenching, and ageing. In order to obtain the highest level of hardness in this system, it is important to commence the creation of the θ phase and provide conditions for its growth. The presence of SiC nanoparticles as a reinforcing component significantly impacts the ageing characteristics of Al-Cu alloys, resulting in improved mechanical properties.

Influence of hot rolling

The impact of hot rolling on the microstructure and hardness is primarily evaluated using SEM and hardness measurement. Subsequently, the samples with the thicknesses of 5 mm and 1 mm are analyzed. The hot-rolled specimens are thoroughly examined in their rolled state at a temperature of 340 °C. In this investigation, the addition of Ag did not result in an increase in hardness compared to the alloy without Ag. Conversely, the use of SiC leads to an augmentation in particle size and an increase in hardness. It was found that the hardness decreases after hot rolling, and the 1 mm sample containing SiC exhibits a higher hardness compared to the 5 mm sample. The texture during hot rolling follows the <111> direction. Adding Ag and SiC to Al-Cu-Mg-based alloys during hot rolling and annealing is aimed to improve their mechanical properties and overall performance. However, in this particular case, Ag exhibits a distinct behavior. SiC acts as a dispersion-strengthening agent. During the rolling process, the Al matrix undergoes a deformation and is subsequently reinforced. The presence of SiC particles additionally impedes the motion of dislocations, resulting in a more robust rolled product in comparison to Al alloys that are not reinforced. Increasing the SiC concentration can have advantages, but it also leads to more challenges in rolling and a higher risk of surface flaws. Instead, decreasing the SiC concentration may be desirable in order to promote smooth rolling and achieve a high-quality surface. Achieving an optimal SiC concentration is of utmost importance in terms of rolling.

Influence of annealing

The hardness of rolled specimens, each having a thickness of 1 mm, was assessed following annealing at a temperature of 350 °C for varying periods of time. The arrangement of reinforcing phases, such as SiC particles, can impact the overall hardness of the alloy. The 1 mm sample is expected to have a more uniform distribution, resulting in an overall increase in hardness. The presence of Ag in the Al-4Cu-0.3Mg-0.7Ag alloy enhances the initial hardness by promoting precipitation hardening.

Some outlooks are listed below:

The addition of Ag into Al-Cu-Mg alloy results in the formation of a more thermally resistant precipitate (Ω-phase), which enhances its suitability for broader applications at elevated temperatures. Nevertheless, Ag is costly; hence, it is imperative to minimize its usage in order to achieve cost-effectiveness. Thus, it is necessary to have a database including a wide range of alloy compositions. Additional research is required to investigate the durability of the precipitates under elevated temperatures and prolonged exposure durations.

By increasing the SiC content in this alloy, we can determine the threshold at which SiC becomes ineffective. In this case, achieving an optimal SiC concentration is of utmost importance.

By varying the thickness of the rolling and comparing the resulting hardness, rolling parameters can be further optimized.

Apart from hardness, the effect of annealing on other mechanical properties (tensile properties, impact toughness, fracture toughness, fatigue properties), the corrosion resistance and wear resistance should be taken into consideration.

Finally, following up the present work, a more detailed investigation on precipitation kinetics is still needed by using DSC, TEM, APT, SAXS and XRD to elucidate how the physical properties of a sample change as a function of temperature and time.

7 Literature

[1] A.L. Page (1986), Methods of Soil Analysis: Part 2½ Chemical and Microbiological Properties. Second edition, Madison, WI, American Society of Agronomy Soil Science Society of America. doi:10.2134/agronmonogr9.2.2ed

[2] F. Habashi (2011), BAYER ' S PROCESS FOR ALUMINA PRODUCTION A HISTORICAL PERSPECTIVE.

[3] Prof. Helmut Antrekowitsch (Feb. 2020), LV Primärmetallurgie und Recycling von Nichteisenmetallen I, Montanuniversity

[4] Kloeckner Metals, A GUIDE TO THE MOST POPULAR, ALL-PURPOSE ALUMINUM ALLOYS. https://www.kloecknermetals.com/blog/a-guide-to-the-most-popular-all-purpose-aluminum-alloys/, Accessed: 12.08.2023

[5] F. Liu, Z. Liu, P. Jia, S. Bai, P. Yan and Y. Hu (2020), Dynamic dissolution and texture evolution of an Al–Cu–Mg–Ag alloy during hot rolling. Journal of Alloys and Compounds 827, pp. 154254. doi:10.1016/j.jallcom.2020.154254

[6] S. Zhang, W. Zeng, W. Yang, C. Shi and H. Wang (2014), Ageing response of a Al–Cu–Li 2198 alloy. Materials & Design 63, pp. 368–374. doi:10.1016/j.matdes.2014.04.063

[7] The metal casting institute, Aluminum Alloys. https://metalcastinginstitute.com/aluminum-alloys/, Accessed: 12.08.2023

[8] S. Beroual, Z. Boumerzoug, P. Paillard and Y. Borjon-Piron (2019), Effects of heat treatment and addition of small amounts of Cu and Mg on the microstructure and mechanical properties of Al-Si-Cu and Al-Si-Mg cast alloys. Journal of Alloys and Compounds 784, pp. 1026–1035. doi:10.1016/j.jallcom.2018.12.365

[9] Y. Sun, W. Gong, J. Feng, G. Lu, R. Zhu and Y. Li (2022), A Review of the Friction Stir Welding of Dissimilar Materials between Aluminum Alloys and Copper. Metals 12, 4, pp. 675. doi:10.3390/met12040675

[10] Boris Wilthan, NIST alloy data (2020).

[11] F. Tariq, N. Naz, R.A. Baloch and Faisal (2012), Characterization of Material Properties of 2xxx Series Al-Alloys by Non Destructive Testing Techniques. J Nondestruct Eval 31, 1, pp. 17–33. doi:10.1007/s10921-011-0117-5

[12] T. CHEN, X. LI, H. GUO and Y. HAO (2015), Microstructure and crystal growth direction of Al–Cu alloy. Transactions of Nonferrous Metals Society of China 25, 5, pp. 1399–1409. doi:10.1016/S1003-6326(15)63739-6

[13] O. Mokhtari, M.-S. Kim, H. Nishikawa, F. Kawashiro, S. Itoh, T. Maeda, T. Hirose and T. Eto (2014), Investigation of Formation and Growth Behavior of Cu/Al Intermetallic Compounds during Isothermal Aging. Transactions of The Japan Institute of Electronics Packaging 7, 1, pp. 1–7. doi:10.5104/jiepeng.7.1

[14] V. Fuß (1934), Metallographie des Aluminiums und Seiner Legierungen. Berlin, Heidelberg, Springer Berlin / Heidelberg.

[15] Roy Morgenstern (2019), Anodische Oxidation von kupferhaltigen Aluminiumlegierungen.

[16] B.K. Kang and I. Sohn (2018), Effects of Cu and Si Contents on the Fluidity, Hot Tearing, and Mechanical Properties of Al-Cu-Si Alloys. Metall Mater Trans A 49, 10, pp. 5137–5145. doi:10.1007/s11661-018-4786-x

[17] F.d. Forschungsinstitut der Schweizerischen Aluminium Ag, D. Altenpohl and S.A. Schweizerische Aluminium AG (2013), Aluminium und Aluminiumlegierungen. Berlin, Heidelberg, Springer Berlin / Heidelberg.

[18] F.-Y. Xie, T. Kraft, Y. Zuo, C.-H. Moon and Y. Chang (1999), Microstructure and microsegregation in Al-rich Al–Cu–Mg alloys. Acta Materialia 47, 2, pp. 489–500. doi:10.1016/S1359-6454(98)00372-3

[19] H.-C. Shih, N.-J. Ho and J.C. Huang (1996), Precipitation behaviors in Al-Cu-Mg and 2024 aluminum alloys, Springer; Springer-Verlag. Metall Mater Trans A 27, 9, pp. 2479–2494. doi:10.1007/BF02652342

[20] K.R. Ravi, R.M. Pillai, K.R. Amaranathan, B.C. Pai and M. Chakraborty (2008), Fluidity of aluminum alloys and composites: A review. Journal of Alloys and Compounds 456, 1, pp. 201–210. doi:10.1016/j.jallcom.2007.02.038

[21] M.C. Flemings (1974), Solidification Processing McGraw-Hill: Casting Processing. New York

[22] S.M. Amer, M.V. Glavatskikh, R.Y. Barkov, A.Y. Churyumov, I.S. Loginova, M.G. Khomutov and A.V. Pozdniakov (2023), Comprehensive Analysis of Microstructure and Hot Deformation Behavior of Al-Cu-Y-Mg-Cr-Zr-Ti-Fe-Si Alloy. Metals 13, 11, pp. 1853. doi:10.3390/met13111853

[23] A.W. Shah, S.-H. Ha, J.A. Siddique, B.-H. Kim, Y.-O. Yoon, H.-K. Lim and S.K. Kim (2023), Microstructure Evolution and Mechanical Properties of Al-Cu-Mg Alloys with Si Addition. Materials (Basel, Switzerland) 16, 7. doi:10.3390/ma16072783

[24] H.Z. Li, Y.J. Ou, H.J. Liao, X.P. Liang and J. Jiang (2014), Microstructural Evolution of High Purity Al-Cu-Mg Alloy during Homogenization. MSF 788, pp. 208–214. doi:10.4028/www.scientific.net/MSF.788.208

[25] (2017), Effect of snake rolling on strength, toughness and microstructure of Al-Cu-Mg alloy plate.

[26] M. Mirzaei, M.R. Roshan and S.A. Jenabali Jahromi (2015), Microstructure and mechanical properties relation in cold rolled Al 2024 alloy determined by X-ray line profile analysis. Materials Science and Engineering: A 620, pp. 44–49. doi:10.1016/j.msea.2014.09.110

[27] M.J. Styles, R. Marceau, T.J. Bastow, H. Brand, M.A. Gibson and C.R. Hutchinson (2015), The competition between metastable and equilibrium S (Al2CuMg) phase during the

decomposition of AlCuMg alloys. Acta Materialia 98, pp. 64–80. doi:10.1016/j.actamat.2015.07.011

[28] H. LI, R. LIU, X. LIANG, M. DENG, H. LIAO and L. HUANG (2016), Effect of pre-deformation on microstructures and mechanical properties of high purity Al–Cu–Mg alloy. Transactions of Nonferrous Metals Society of China 26, 6, pp. 1482–1490. doi:10.1016/S1003-6326(16)64253-X

[29] Z. HU, C. FAN, D. ZHENG, W. LIU and X. CHEN (2019), Microstructure evolution of Al–Cu–Mg alloy during rapid cold punching and recrystallization annealing. Transactions of Nonferrous Metals Society of China 29, 9, pp. 1816–1823. doi:10.1016/S1003-6326(19)65089-2

[30] H.W. Liu, Y.G. Zhang, J.B. Zhang, B.H. Zhu, F. Wang, Z.H. Li, X.W. Li and B.Q. Xiong (2011), DSC and TEM Study of Al-Cu-Mg-Ag Alloy Ageing at Low and Elevated Temperature. AMR 295-297, pp. 1225–1229. doi:10.4028/www.scientific.net/AMR.295-297.1225

[31] J.H. AULD, J.T. VIETZ and I.J. POLMEAR (1966), T-phase Precipitation induced by the Addition of Silver to an Aluminium–Copper–Magnesium Alloy. Nature 209, 5024, pp. 703–704. doi:10.1038/209703a0

[32] V. Raghavan (2010), Ag-Al-Cu-Mg (Silver-Aluminum-Copper-Magnesium). J. Phase Equilib. Diffus. 31, 3, pp. 297–299. doi:10.1007/s11669-010-9686-8

[33] D. Bakavos, P.B. Prangnell, B. Bes and F. Eberl (2008), The effect of silver on microstructural evolution in two 2xxx series Al-alloys with a high Cu:Mg ratio during ageing to a T8 temper. Materials Science and Engineering: A 491, 1, pp. 214–223. doi:10.1016/j.msea.2008.03.014

[34] C.J. Xiang-peng (2018), Deformation-induced Ω Phase Precipitation Strengthening of AlCuMg Alloy with High Cu/Mg Atomic Ratio. Journal of Hunan University

[35] Q. An, X. Cong, P. Shen and Q. Jiang (2019), Roles of alloying elements in wetting of SiC by Al. Journal of Alloys and Compounds 784, pp. 1212–1220. doi:10.1016/j.jallcom.2019.01.138

[36] Y.F. Song, X.F. Ding, X.J. Zhao, L.R. Xiao and C.X. Yu (2018), The effect of SiC addition on the dimensional stability of Al-Cu-Mg alloy. Journal of Alloys and Compounds 750, pp. 111–116. doi:10.1016/j.jallcom.2018.03.257

[37] X. Su, Y. Lei, Y. Chen, H. Qu, Z. Qi, G. Zheng, X. Liu, H. Xiang and G. Chen (2024), Precipitating thermally reinforcement phase in aluminum alloys for enhanced strength at 400 °C. Journal of Materials Science & Technology 172, pp. 71–82. doi:10.1016/j.jmst.2023.06.038

[38] G.E. Kiourtsidis, S.M. Skolianos and G.A. Litsardakis (2004), Aging response of aluminium alloy 2024/silicon carbide particles (SiCp) composites, Elsevier. Materials Science and Engineering: A 382, 1-2, pp. 351–361. doi:10.1016/j.msea.2004.05.021

[39] Y. Liu, F. Teng, F.H. Cao, Z.X. Yin, Y. Jiang, S.B. Wang and P.K. Shen (2019), Defective GP-zones and their evolution in an Al-Cu-Mg alloy during high-temperature aging. Journal of Alloys and Compounds 774, pp. 988–996. doi:10.1016/j.jallcom.2018.10.061

[40] L. Kovarik and M.J. Mills (2012), Ab initio analysis of Guinier–Preston–Bagaryatsky zone nucleation in Al–Cu–Mg alloys. Acta Materialia 60, 9, pp. 3861–3872. doi:10.1016/j.actamat.2012.03.044

[41] J.M. Papazian (1988), Effects of SiC whiskers and particles on precipitation in aluminum matrix composites, Springer; Springer-Verlag. Metall Trans A 19, 12, pp. 2945–2953. doi:10.1007/BF02647721

[42] G.M. Janowski and B.J. Pletka (1995), The effect of particle size and volume fraction on the aging behavior of a liquid-phase sintered SiC/aluminum composite, Springer; Springer-Verlag. Metall Mater Trans A 26, 11, pp. 3027–3035. doi:10.1007/BF02669659

[43] A.P. Sannino and H.J. Rack (1995), Effect of reinforcement size on age hardening of PM 2009 Al-SiC 20 vol% participate composites, Springer; Kluwer Academic Publishers. JOURNAL OF MATERIALS SCIENCE 30, 17, pp. 4316–4322. doi:10.1007/BF00361511

[44] S. Bai, X. Zhou, Z. Liu, P. Xia, M. Liu and S. Zeng (2014), Effects of Ag variations on the microstructures and mechanical properties of Al–Cu–Mg alloys at elevated temperatures. Materials Science and Engineering: A 611, pp. 69–76. doi:10.1016/j.msea.2014.05.065

[45] L. Eschbach (1997), Entwicklung von sprühkompaktierten AlCuMgAg-Legierungen mit hoher Warmfestigkeit und Zähigkeit. ETH Zurich

[46] S. Bai, H. Xu, Z. Liu, X. Yi, J. Zhao and J. Wang (2019), On the role of the solute partitioning and chemistry in initial precipitation of Ω plates. Materials Science and Engineering: A 766, pp. 138339. doi:10.1016/j.msea.2019.138339

[47] C.R. GROVENOR, B.A. SHOLLOCK and K.M. KNOWLES (1989), POSITION SENSITIVE ATOM PROBE STUDIES OF THE COMPOSITION OF Ω AND θ' PRECIPITATES IN Al-Cu-Mg-Ag ALLOYS. J. Phys. Colloques 50, C8, C8-377-C8-380. doi:10.1051/jphyscol:1989864

[48] Y. Zhou, Z. Liu, S. Bai, P. Ying and L. Lin (2017), Effect of Ag additions on the lengthening rate of Ω plates and formation of σ phase in Al-Cu-Mg alloys during thermal exposure. Materials Characterization 123, pp. 1–8. doi:10.1016/j.matchar.2016.11.008

[49] O. El-Kady and A. Fathy (2014), Effect of SiC particle size on the physical and mechanical properties of extruded Al matrix nanocomposites. Materials & Design 54, pp. 348–353. doi:10.1016/j.matdes.2013.08.049

[50] T. Ye, Y. Xu and J. Ren (2019), Effects of SiC particle size on mechanical properties of SiC particle reinforced aluminum metal matrix composite. Materials Science and Engineering: A 753, pp. 146–155. doi:10.1016/j.msea.2019.03.037

[51] A. Wąsik, B. Leszczyńska-Madej and M. Madej (2017), THE INFLUENCE OF SiC PARTICLE SIZE ON MECHANICAL PROPERTIES OF ALUMINIUM MATRIX COMPOSITES. mafe 43, 1, pp. 41. doi:10.7494/mafe.2017.43.1.41

[52] Spowart J., Maruyama B., Miracle D, Method for improving tensile properties of AlSiC composites, Unit- ed States Patent. US 6972109 B1 .

[53] W.A. Uju and I. Oguocha (2009), Thermal cycling behaviour of stir cast Al–Mg alloy reinforced with fly ash. Materials Science and Engineering: A 526, 1-2, pp. 100–105. doi:10.1016/j.msea.2009.07.055

[54] S. ELOMARI, R. BOUKHILI, C. SAN MARCHI, A. MORTENSEN and D. LLOYD (1997), Thermal expansion responses of pressure infiltrated SiC/Al metal-matrix composites. JOURNAL OF MATERIALS SCIENCE 32, 8, pp. 2131–2140. doi:10.1023/A:1018535108269

[55] Q. Liu, F. Ye, Y. Gao, S. Liu, H. Yang and Z. Zhou (2014), Fabrication of a new SiC/2024Al co-continuous composite with lamellar microstructure and high mechanical properties. Journal of Alloys and Compounds 585, pp. 146–153. doi:10.1016/j.jallcom.2013.09.140

[56] J.E.K. Schawe (2015), The Gibbs free energy difference between a supercooled melt and the crystalline phase of polymers. J Therm Anal Calorim 120, 2, pp. 1417–1425. doi:10.1007/s10973-015-4453-z

[57] G. Schulze (2004), Die Metallurgie des Schweißens: Eisenwerkstoffe - Nichteisenmetallische Werkstoffe. Dritte, neu bearbeitete und erweiterte Auflage, Berlin, Heidelberg, Springer Berlin Heidelberg. doi:10.1007/3-540-35051-9_4

[58] D. Heinze, Physically-Based Models for Two-Phase Flow Phenomena in Steam Injectors A One-Dimensional Simulation Approach (KIT Scientific Reports ; 7704) (2015).

[59] P. Barua and I. Hwang (2023), Bulk Perovskite Crystal Properties Determined by Heterogeneous Nucleation and Growth. Materials (Basel, Switzerland) 16, 5. doi:10.3390/ma16052110

[60] Ashby and Jones, Engineering Materials 2: Critical Nucleus. https://www.princeton.edu/~maelabs/mae324/glos324/criticalnucleus.htm#:~:text=r%20%3C%20r*%20can%20reduce%20the,radius%20is%20a%20critical%20nucleus.

[61] Wikipedia, Nucleation. https://en.wikipedia.org/wiki/Nucleation

[62] C.N. Nanev (2020), Evaluation of the critical nucleus size without using interface free energy. Journal of Crystal Growth 535, pp. 125521. doi:10.1016/j.jcrysgro.2020.125521

[63] A. Taqieddin, M.R. Allshouse and A.N. Alshawabkeh (2018), Review-Mathematical Formulations of Electrochemically Gas-Evolving Systems. Journal of the Electrochemical Society 165, 13, E694-E711. doi:10.1149/2.0791813jes

[64] V.Y. Goldstein and V.Y. Novikov (2023), Heterogeneous Nucleation During Solidification, Springer; Springer US. Met Sci Heat Treat 64, 9-10, pp. 491–494. doi:10.1007/s11041-023-00840-2

[65] F. Akhlaghi, A. Lajevardi and H.M. Maghanaki (2004), Effects of casting temperature on the microstructure and wear resistance of compocast A356/SiCp composites: a comparison between SS and SL routes. Journal of Materials Processing Technology 155-156, pp. 1874–1880. doi:10.1016/j.jmatprotec.2004.04.328

[66] Daeho Industries Ltd., Aluminum Mast Alloys & Grain Refiner [online]. http://www.daeholtd.co.kr/?page_id=1834&lang=en&ckattempt=1 [Zugriff am: 19. Aug.

[67] ASM International Handbook Committee (1991), Heat treating of aluminium alloy. 4. Auflage, ASM International, ASM Handbook. doi:10.1361/asmhba0001205

[68] I.M. Astika (2019), Hardness improvement of aluminum alloy 2024 t3 after artificial aging treatment. IOP Conf. Ser.: Mater. Sci. Eng. 539, pp. 12004. doi:10.1088/1757-899X/539/1/012004

[69] Ekhlas Ahmed (2013), The Effect Of Heat Treatments On Mechanical Properties Of Aluminum Alloy Aa 2024-T6. The Iraqi Journal For Mechanical And Material Engineering

[70] N. Afzal, T. Shah and R. Ahmad (2013), Microstructural Features and Mechanical Properties of Artificially Aged AA2024, Springer Science and Business Media LLC. Strength Mater 45, 6, pp. 684–692. doi:10.1007/s11223-013-9504-8

[71] Gowrishankar M. C., Shravan, Rakesh, Rahul, Achutha Kini, S. S. Sharma (2014), Effect of Artificial Aging on Strength and Wear Behaviour of Solutionized Aluminium 6061 Alloy. Proceedings of the 3rd World Conference on Applied Sciences, Engineering and Technology.

[72] A. Polat, M. Avsar and F. Ozturk (2015), Effects of the artificial-aging temperature and time on the mechanical properties and springback behavior of AA6061, Institute of Metals and Technology. Mater. Tehnol. 49, 4, pp. 487–493. doi:10.17222/mit.2013.154

[73] D.A. Reis, A.A. Couto, N.I. Domingues Jr., A.C. Hirschmann, S. Zepka and C. de Moura Neto (2012), Effect of Artificial Aging on the Mechanical Properties of an Aerospace Aluminum Alloy 2024, Trans Tech Publications Ltd. DDF 326-328, pp. 193–198. doi:10.4028/www.scientific.net/DDF.326-328.193

[74] M. S. Khan, A. Salam, N. Ikram (2015), Effect of Cold Work on the Age Hardening Behaviour of Al 2014 Al alloy. Technical Journal, University of Engineering and Technology (UET) Taxila.

[75] M. F. I. A. Imam, M. S. Rahman, M. Z. H. Khan (2015), INFLUENCE OF HEAT TREATMENT ON FATIGUE AND FRACTURE BEHAVIOR OF ALUMINIUM ALLOY. Journal Of Engineering Science And, School Of Engineering, Taylor’s University.

[76] J.R. Davis and Davis & Associates Aluminum and Aluminum Alloys, William W.Scoot, Director of Technical Publications.

[77] T.T. Alshammari, H.F. Alharbi, M.S. Soliman and M.F. Ijaz (2020), Effects of Mg Content on the Microstructural and Mechanical Properties of Al-4Cu-xMg-0.3Ag Alloys, Multidisciplinary Digital Publishing Institute. Crystals 10, 10, pp. 895. doi:10.3390/cryst10100895

[78] R.S. Mishra (uuuu-uuuu), Friction stir welding of 2XXX aluminum alloys including Al--Li alloys a volume in the welding and friction stir processing book series, Elsevier.

[79] A.M. Al-Obaisi, E.A. El-Danaf, A.E. Ragab and M.S. Soliman (2016), Precipitation Hardening and Statistical Modeling of the Aging Parameters and Alloy Compositions in Al-Cu-Mg-Ag Alloys. J. of Materi Eng and Perform 25, 6, pp. 2432–2444. doi:10.1007/s11665-016-2076-6

[80] R. Su, Y. Jia, J. Xiao, G. Li, Y. Qu and R. Li (2023), Effect of secondary aging on microstructure and properties of cast Al-Cu-Mg alloy. China Foundry 20, 1, pp. 71–77. doi:10.1007/s41230-023-1049-2

[81] 伍翠兰·,周斌,牛凤姣,段石云,巩向鹏,陈江华 and WU Cuilan·, ZHOU Bin, NIU Fengjiao, DUAN Shiyun, GONG Xiangpeng, CHEN Jianghua (2018), 高Cu/Mg比AlCuMg合金的形变诱导Ω相析出强化. 湖南大学学报(自然科学版)英文版 45, 6, pp. 1–10.

[82] T. Ouissi, G. Collaveri, P. Sciau, J.-M. Olivier and M. Brunet (2019), Comparison of Aluminum Alloys from Aircraft of Four Nations Involved in the WWII Conflict Using Multiscale Analyses and Archival Study. Heritage 2, 4, pp. 2784–2801. doi:10.3390/heritage2040172

[83] S. Li, J. Zhang, J. Yang, Y. Deng and X. Zhang (2014), Influence of Mg Contents on Aging Precipitation Behavior of Al–3.5Cu–xMg Alloy. Acta Metall. Sin. (Engl. Lett.) 27, 1, pp. 107–114. doi:10.1007/s40195-014-0033-7

[84] S.C. Wang and M.J. Starink (2007), Two types of S phase precipitates in Al–Cu–Mg alloys. Acta Materialia 55, 3, pp. 933–941. doi:10.1016/j.actamat.2006.09.015

[85] J.Z. Liu, S.S. Yang, S.B. Wang, J.H. Chen and C.L. Wu (2014), The influence of Cu/Mg atomic ratios on precipitation scenarios and mechanical properties of Al–Cu–Mg alloys. Journal of Alloys and Compounds 613, pp. 139–142. doi:10.1016/j.jallcom.2014.06.045

[86] M.-N. Grażyna, K. Gancarczyk, A. Nowotnik, K. Dychtoń and G. Boczkal (2020), Microstructure and Properties of As-Cast and Heat-Treated 2017A Aluminium Alloy Obtained from Scrap Recycling. Materials (Basel, Switzerland) 14, 1. doi:10.3390/ma14010089

[87] Wärmebehandlung von Aluminiumlegierungen [online]. https://docplayer.org/47446107-Merkblatt-aluminium-zentrale-w-7-waermebehandlung-von-aluminiumlegierungen.html

[88] R. Lumley (2011), Fundamentals of Aluminium Metallurgy Woodhead Publishing Series in Metals and Surface Engineering, Woodhead Publishing.

[89] Robert E. Laughlin et al. (2004), ASM Handbook Metallography and Microstructures.

[90] V.A. Brodov, A.V. Zhil'tsov, Y.V. Levinskii and G.N. Romanov (1992), Volumetric deformation of Al-4.4% Cu and Al-4.4% Cu-0.5% Mg compacts during sintering. Powder Metall Met Ceram 31, 2, pp. 108–111. doi:10.1007/bf00794042

[91] J. Shen, U.F.H. Suhuddin, M.E.B. Cardillo and J.F. dos Santos (2014), Eutectic structures in friction spot welding joint of aluminum alloy to copper. Applied Physics Letters 104, 19. doi:10.1063/1.4876238

[92] F. de Geuser, F. Bley and A. Deschamps (2010), Early stages of Omega phase precipitation in Al-Cu-Mg-Ag observed in situ with and without applied stress by small angle X-ray scattering. International Conference on Aluminium Alloys (ICAA 12),

[93] S. Mousavi Abarghouie and S.S. Reihani (2010), Aging behavior of a 2024 Al alloy-SiCp composite. Materials & Design 31, 5, pp. 2368–2374. doi:10.1016/j.matdes.2009.11.063

[94] G.F. Liu, T.J. Chen and Z.J. Wang (2021), Effects of solid solution treatment on microstructure and mechanical properties of SiCp/2024 Al composite: A comparison with 2024 Al alloy. Materials Science and Engineering: A 817, pp. 141413. doi:10.1016/j.msea.2021.141413

[95] Z.-H. Gao, H.-J. Gao, Y.-D. Zhang and Q. Wu (2023), Experiment and mechanism investigation on the effect of heat treatment on residual stress and mechanical properties of SiCp/Al–Cu–Mg composites. Materials Science and Engineering: A 884, pp. 145555. doi:10.1016/j.msea.2023.145555

[96] R.R. Ambriz and D. Jaramillo (2014), Mechanical Behavior of Precipitation Hardened Aluminum Alloys Welds, in: W.A. Monteiro (Ed.), Light Metal Alloys Applications, InTech. doi:10.5772/58418

[97] (1997), Entwicklung von sprühkompaktierten AlCuMgAg-Legierungen mit hoher Warmfestigkeit und Zähigkeit.

[98] P. D. Scott MacKenzie (2021), Heat treatment of aluminum VI – Artificial aging.

[99] S.C. Wang, M.J. Starink and N. Gao (2006), Precipitation hardening in Al–Cu–Mg alloys revisited. Scripta Materialia 54, 2, pp. 287–291. doi:10.1016/j.scriptamat.2005.09.010

[100] B. Ren and J.G. Morris (1995), Microstructure and texture evolution of Al during hot and cold rolling, Springer; Springer-Verlag. Metall Mater Trans A 26, 1, pp. 31–40. doi:10.1007/BF02669792

[101] E. Usui, T. Inaba and N. Shinano (1986), Dynamic Restoration of Aluminium and its Alloys During Hot Rolling, De Gruyter. International Journal of Materials Research 77, 10, pp. 684–693. doi:10.1515/ijmr-1986-771009

[102] H.Yamagata (1992), Scripta Metall.

[103] Q. Zhao, Z. Liu, S. Li, T. Huang, P. Xia and L. Lu (2017), Evolution of the Brass texture in an Al-Cu-Mg alloy during hot rolling. Journal of Alloys and Compounds 691, pp. 786–799. doi:10.1016/j.jallcom.2016.08.322

[104] S. Guo, Z. Liu, S. Bai, L. Ou, J. Zhang, G. He and J. Zhao (2022), Effect of rolling temperature on mechanical properties and corrosion resistance of Al-Cu-Mg-Ag alloy. Journal of Alloys and Compounds 897, pp. 163168. doi:10.1016/j.jallcom.2021.163168

[105] S. Ma and X. Wang (2022), The effects of hot rolling and heat treatment on the microstructure and mechanical properties of an Al-Cu-Mg-Sc alloy reinforced with in situ TiB2 particulates. Journal of Materials Research 37, 21, pp. 3680–3694. doi:10.1557/s43578-022-00741-9

[106] P. Xia, Z. Liu, W. Wu, Q. Zhao, L. Lu and S. Bai (2018), Texture Evolution in an Al-Cu-Mg Alloy During Hot Rolling. J. of Materi Eng and Perform 27, 7, pp. 3255–3267. doi:10.1007/s11665-018-3427-2

[107] F. Liu, Z. Liu and G. He (2022), Effect of cold rolling on microstructure and hardness of annealed Al–Cu–Mg alloy. Archives of Civil and Mechanical Engineering 22, 2, pp. 64. doi:10.1007/s43452-021-00372-7

[108] I.S. Zuiko and R. Kaibyshev (2020), Ageing response of cold-rolled Al–Cu–Mg alloy. Materials Science and Engineering: A 781, pp. 139148. doi:10.1016/j.msea.2020.139148

[109] W.C. Liu and J.G. Morris (2004), Quantitative analysis of texture evolution in cold-rolled, continuous-cast AA 5xxx-series aluminum alloys, Springer; Springer-Verlag. Metall Mater Trans A 35, 1, pp. 265–277. doi:10.1007/s11661-004-0127-3

[110] T. Leffers and R.K. Ray (2009), The brass-type texture and its deviation from the copper-type texture. Progress in Materials Science 54, 3, pp. 351–396. doi:10.1016/j.pmatsci.2008.09.002

[111] Q. Zhao, Z. Liu, Y. Hu, S. Li and S. Bai (2020), Evolution of Goss texture in an Al–Cu–Mg alloy during cold rolling. Archives of Civil and Mechanical Engineering 20, 1. doi:10.1007/s43452-020-00023-3

[112] Y.C. Huang, Y. Liu, Q. Li, X. Liu and C.G. Yang (2016), Relevance between microstructure and texture during cold rolling of AA3104 aluminum alloy. Journal of Alloys and Compounds 673, pp. 383–389. doi:10.1016/j.jallcom.2016.02.226

[113] L. Heinl (2023), Influence of alloying elements (Cu, Mg, Ag) and hot rolling on the solidification microstructure, precipitation microstructure and hardness of an Al-Cu-Mg-Ag alloy. Leoben

8 List of figures

9 List of table